DESIGN CONSIDERATIONS FOR REFRIGERATION CYCLES

by

MATTHIAS HARTMUT RAUCK

A thesis submitted in partial fulfillment of

the requirements for the degree of

MASTER OF SCIENCE

(Chemical Engineering)

at the

UNIVERSITY OF WISCONSIN-MADISON

1992

ABSTRACT

Refrigeration equipment consumes worldwide a major part of the annual electrical energy production. The US domestic refrigerator industry is interested in methods which improve refrigerator performance in order to meet US government energy standards. It is necessary to find suitable replacements for refrigerants which are now known to deplete the ozone layer or which contribute to the greenhouse effect. A possible solution may be the use of non-azeotropic refrigerant mixtures (NARMs) instead of the common chlorofluorcarbons (CFCs).

The isobaric phase change for a NARM does not occur isothermally as for pure refrigerants, but over a temperature range. This behavior offers a potential improvement of the coefficient of performance (COP) in a refrigeration cycle. Two models are developed to investigate the potential improvements of the COP in an ideal refrigeration cycle. These models allow the refrigerant to change temperature throughout the heat transfer process. The models account for irreversibilities due to heat transfer rate limitations from the refrigeration cycle to external fluids. The COP obtained offers a realistic design goal for the refrigeration system. Design guidelines which lead to the maximum possible COP for such a system are established.

A standard vapor compression cycle is then investigated with another simulation model. NARMs consisting of real refrigerants are used to evaluate the performance of the cycle and these results are compared to the results from the previous developed ideal cycle.

ACKNOWLEDGMENT

Special thanks go to my academic advisors Professor Sanford A. Klein and Professor William A. Beckman. I am thankful to Sandy for finding an interesting and suitable research project for me as I decided, after my first semester, to go for a Master of Science in Chemical Engineering. He and Bill believed in me, made the project possible and supported me whenever I needed help or motivation. Osama A. Ibrahim deserves a 'special' thank you. He offered a great deal of help in tackling my first problems before he left the Solar Energy Laboratory.

My time in the SEL was enjoyable and intense at all times. I am going to miss the stimulating environment: the seminars, the discussions with other students all over the globe, my own office on campus and all the social events. The Chemical Engineering Department, which was very challenging for me, 'provided' me also with a lot of work, but also with even more friends. When do I see Louis, Stephan, Jon, Christine, Brian, Dan, Jörg, Svein, Gerold, Øystein, Jürgen, Nate, Jeff, Bob, Paul,.... and Bob, Frank, Rahmat, Rajesh and the fun guys from the Nottingham Coop, again ?

I want to thank my brother Thomas and his wife Cilly for visiting me, sharing some american experiences and taking care of all these nasty things like going through all the formalities with the University of Hannover and a lot more.

My stay in Madison was made possible by the German Academic Exchange Service (DAAD) and the Institut für Thermodynamik at the University of Hannover in Germany. I am grateful to Professor H. D. Baehr and Dipl. Ing. Dipl. Ing.(MS) Frank-Detlef Drake for putting their personnel effort into this program. Frank also spent 1 1/2 years in Madison at the Solar Energy Laboratory. He knew how great the study in Madison is and initiated the program. Thanks a lot, Frank, for making this great study abroad experience possible.

Last, but not least, I want to thank Klaus. We became great buddies during our stay in America. He was a wonderful friend and listener when the time in Madison, with all the ups and downs, got a little bit rougher for me.

Finally I dedicate this 'work' to my father Wolfgang who always believed in me and who is probably now looking down from far far above to me.

My time was a great experience and I will always keep good memories of Madison and, of course, I will be back.

TABLE OF CONTENTS

LIST OF TABLES

LIST OF FIGURES

NOMENCLATURE

ROMAN LETTER SYMBOLS

Symbol	Definition	SI-Units
$\dot{C}$	heat capacitance rate (mass flow rate - specific heat product)	[kW/K]
c_p	specific heat capacity at constant pressure	[kJ/kgK]
COP	Coefficient of Performance	
CSD	Carnahan-Starling-DeSantis equation of state	
EES	Engineering Equation Solver	
f	fraction, mole fraction	
GTD	gliding temperature difference	[K]
h	specific enthalpy	[kJ/kg]
$\dot{m}$	mass flow rate	[kg/s]
NTU	number of transfer units	
p	pressure	[N/m^2]
$\dot{Q}$	heat transfer rate	[kW]
S	entropy	[kJ/K]

$\dot{S}$	entropy transfer rate	[kW/K]
T	temperature	[K]
ΔT	temperature difference defined in Equation (1.8)	[K]
$\Delta T'$	temperature difference defined in Equation (3.33)	[K]
UA	Heat Exchanger Conductance	[kW/K]
$\dot{W}$	Power	[W]
x	quality	
y	parameter for the CSD equation of state defined in Equation (4.6)	

GREEK LETTER SYMBOLS

Symbol	Definition
β	parameter for the calculation of the COP defined in Equation (3.27)
Δ	difference
ε	heat exchanger effectiveness
η	polytropic compressor efficiency
λ	parameter for the calculation of the COP defined in Equation (3.29)
λ'	parameter for the calculation of the COP defined in Equation (3.35)
Ω	potential improvement of the COP defined in Equation (3.30)
ψ	deviation of the optimum temperature deviation defined in equation (4.7)

SUBSCRIPTS

Symbol	Definition
C	compressor
cond	condenser
evap	evaporator
ext	external stream
H	high, referring to external stream condition in high temperature heat exchange
h	high, referring to refrigerant condition in high heat exchanger, liquid
hx	heat exchanger
i	cycle
in	inlet
L	low, referring to external stream condition in low temperature heat exchanger
l	low, referring to refrigerant condition in low heat exchanger; liquid
lm	logarithm mean
mean	mean
min	minimum
max	maximum
n	number of individual Carnot cycles
opt	optimum
out	outlet
refr	refrigerant

sh	superheat
T	turbine
total	total
v	vapor
x	local condition in the heat exchangers
1	one Carnot cycle
10	ten Carnot cycles in sequence
∞	COP calculated from Analytical Simulation Model

SUPERSCRIPTS

Symbol	Definition
*	partially optimized COP from analytical simulation model

CHAPTER
ONE

INTRODUCTION

1.1 BACKGROUND AND SCOPE OF STUDY

Various economic and ecological reasons make it necessary to look more in detail at the potential performance improvements of refrigeration systems. More energy efficient systems have to be developed because of stricter energy standards issued all over the world. American refrigerator manufacturers are being forced by the government and by environmental and economic interests to produce more energy efficient systems and to eliminate chlorofluorcarbons (CFCs) [1].

More energy efficient systems are needed to curb the greenhouse effect. The greenhouse effect is caused by an increase of carbon dioxide (CO_2) and other gases in the atmosphere in addition to refrigerants. These substances prevent radiation emitted or reflected from the earth to leave the atmosphere and hence the atmospheric temperature may increase. CO_2 is released in all energy producing processes based on fossil fuel.

Consequently a decrease of the energy consumption and of the use of these refrigerants is desired.

Substitutes for CFCs must be used. It is now well known that the ozone layer protecting the earth from excessive ultraviolet radiation is already dangerously depleted primarily by CFCs. CFCs, the main culprit that causes ozone destruction, work their way slowly to the stratosphere, break apart, and release ozone destroying chlorine. In many parts of the world, especially in the southern hemisphere, the uv radiation is already above physical tolerable amounts. Especially the fully halogenated chlorofluorcarbons like R11, R12, R113, R114 have a high ozone depleting potential. Two of the most commonly used refrigerants, R11 and R12, are the major of ozone destruction. These chemicals are used in small refrigeration systems, automobile air conditioning and as a agent to blow plastic foam. These refrigerants have been used in refrigeration systems for decades due to their desired characteristics like low toxicity, non-flammability and their non-aggressive behavior against other design materials.

The purpose of this work is it to determine the optimum refrigeration cycle for a vapor compression cycle. The maximum possible coefficient of performance (COP), which may be used as a realistic design goal, will be identified. Design guidelines are found for this cycle , which is first considered to be ideal with no irreversibilities. These guidelines are then applied and checked for real vapor compression cycles using pure refrigerants and mixtures.

The circumstances for which performance improvements may be obtained using non-azeotropic refrigerant mixtures (NARMs) as the refrigerant will be identified. For a NARM, the phase change does not occur isothermal as for pure refrigerants. This temperature change is due to a composition change which accompanies the phase change

processes occurring in a refrigeration cycle. This property and other may be used to mix suitable refrigerants for different applications.

1.2 LITERATURE SEARCH

Many studies on alternative refrigerants have been published in the last few years. The use of NARMs as a refrigerant is considered by many authors, e.g., [8,9,10,11,12]. Atwood [8] reports that there is still insufficient experience with NARMs and that refrigeration systems applying a NARM may require significant changes. It is most likely that these changes result in refrigeration systems which are more costly than the conventional in mass manufactured applications.

Kruse et al. [13] investigated a two-evaporator refrigeration system similar to a household refrigerator. Theoretical and experimental investigations have been carried out for the refrigerant mixtures R22/R114 and R13B1/R-114 and compared to R12. Kruse calculated an increase of 18% and 20% of the COP of the mixtures R22/R114 and R13B1/R-114 respectively. The corresponding experiments leaded to improvements of 13% (R22/R114) and 15% (R13B1/R-114) compared to R12.

Domanski and McLinden [14] worked on refrigeration cycle simulations models for the performance rating of refrigerants and their mixtures. Their model Cycle11 is able to predict the COP for refrigerants and their mixtures in a vapor compression cycle. McLinden and Radermacher [15] describe methods for comparing the performance of pure and mixed refrigerants in a vapor compression cycle. They computed the COPs for the mixtures R22/R114 and R22/R11 and reported that COP improvements may be

obtained for mixtures where the temperature change of the refrigerant mixture matches with the temperature change of the heat sink or source.

Klein [16] pointed out that the Carnot COP for a refrigeration cycle does not provide a realistic upper limit for design considerations. He derived another expression for the COP of a simple internal reversible refrigeration cycle. This COP considers heat transfer mechanism from and to the cycle which are a necessarily an irreversible process and the analysis assumes that the heat transfer occurs isothermally.

1.3 REVIEW OF THE VAPOR COMPRESSION AND THE CARNOT REFRIGERATION CYCLE

1.3.1 VAPOR COMPRESSION REFRIGERATION CYCLE

A review of the standard vapor compression cycle is presented [2,3]. Later in this work, the use of a NARM will be investigated. The different components and the thermodynamic basics are described and explained.

Figure 1.1 shows the schematic of a vapor compression refrigeration cycle operating between a low temperature T_l and at a higher temperature T_h. An accompanying temperature-entropy and pressure-enthalpy diagram are presented in the Figures 1.2 and 1.3. The refrigerant is continuously circulating through this cycle and its different states are described beginning at the inlet of the evaporator.

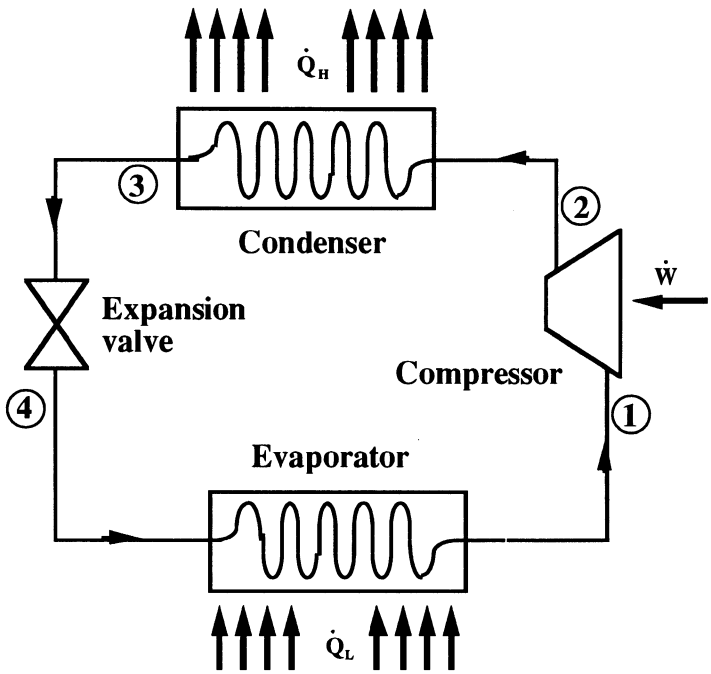

Figure 1.1 Vapor compression refrigeration cycle

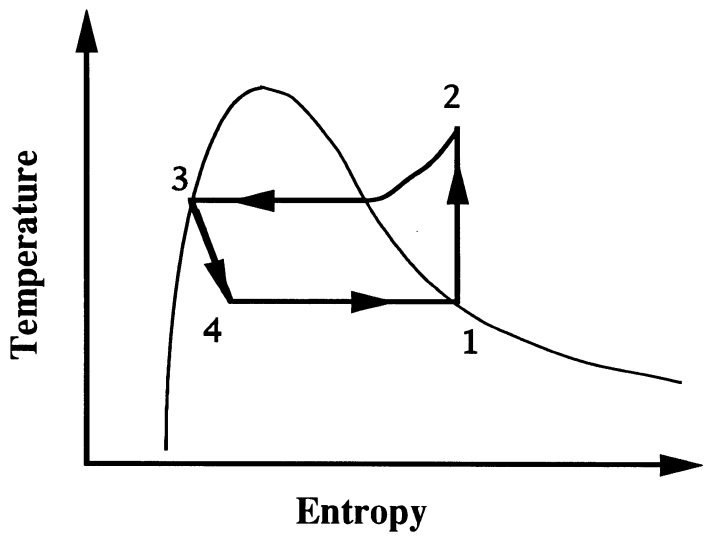

Figure 1.2 Temperature-Entropy diagram for a vapor compression cycle

The refrigerant enters the evaporator as a two phase liquid-vapor mixture at low quality at state 4. It changes to vapor and leaves the evaporator at state 1 with a quality of x=1 or in a slightly superheated state. Heat transfer in the evaporator occurs from an external cold region at lower temperature as the refrigerant to the refrigerant. For a pure fluid, the pressure and temperature remain approximately constant throughout the phase change, but the temperature of the refrigerant rises the a superheated region. The refrigerant is then compressed from state 1 to state 2, where it leaves the compressor as superheated vapor at a higher pressure and temperature.

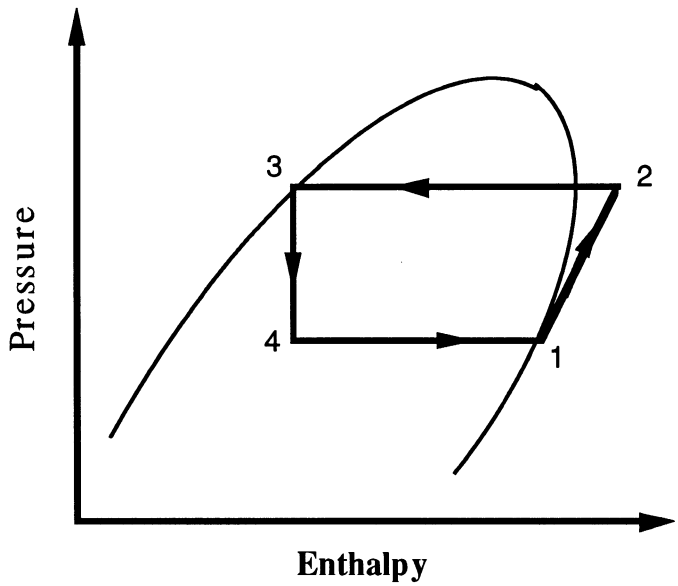

Figure 1.3 Pressure-Enthalpy diagram for a vapor compression cycle

The refrigerant passes from the compressor into the condenser, where it changes at constant pressure to saturated liquid at a quality of x=1. The phase change in the condenser occurs, as in the evaporator, isothermal and almost isobar. The refrigerant, now at state 3, returns then into state 4 of the inlet of the evaporator by expanding

adiabatically through a expansion valve. This throttling process during which the refrigerants expands from the condenser pressure to the evaporator pressure, takes place at approximately constant enthalpy. In practice, irreversibilities occurs due to heat losses during compression and expansion (non-adiabatic), pressure drops in the evaporator and condenser, and additional heat- and pressure losses in the remaining lines.

As the refrigerant passes through the evaporator, heat transfer from the refrigerated space into the cycle results in the vaporization of the refrigerant. This is the refrigeration capacity or the cooling load and determined by the product of enthalpy difference across the evaporator and the mass flow rate of the refrigerant.

$$\dot{Q}_L = \dot{m}_{ref} \cdot (h_1 - h_4) \tag{1.1}$$

The power requirement for the cycle is given by the product of the mass flow rate of the refrigerant and the enthalpy difference between evaporator outlet and condenser inlet.

$$\dot{W} = \dot{m}_{ref} \cdot (h_2 - h_1) \tag{1.2}$$

The rate of heat transfer from the condenser to the surroundings is given by

$$\dot{Q}_H = \dot{m}_{ref} \cdot (h_2 - h_3) \tag{1.3}$$

The throttling is assumed to be isenthalpic, but it is irreversible and there is an accompanying entropy increase.

$$h_3 = h_4 \tag{1.4}$$

The coefficient of performance (COP), is defined as the cooling load or cooling capacity divided by the power supplied to the cycle. The COP may take values between zero and infinite.

$$COP = \frac{\dot{Q}_L}{\dot{W}} = \frac{h_1 - h_4}{h_2 - h_1} \tag{1.5}$$

1.3.2 CARNOT REFRIGERATION CYCLE

The Carnot refrigeration cycle has no internal irreversibilities. Instead of the expansion valve, as in the vapor compression cycle, an expander is applied to the system, so that the energy which was dissipated in the expansion valve can now be gained as a power output. Figures 1.4 illustrates the schematic of the Carnot cycle.

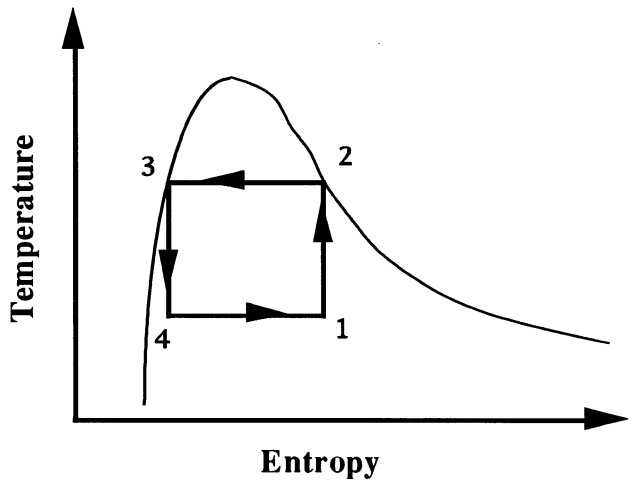

Figure 1.4 Temperature-Entropy diagram for a Carnot cycle

The coefficient of performance for the Carnot cycle is determined by [2]

$$COP = \frac{T_1}{T_2 - T_1} \qquad \text{with } T_4 = T_1 \text{ and } T_2 = T_3 \tag{1.6}$$

where T_2 is the temperature at which heat is rejected from the cycle to an isothermal heat sink and T_1 is the temperature at which heat is added to the cycle from an isothermal heat source.

1.4 LIMITATIONS OF THE CARNOT COP AS A REALISTIC DESIGN GOAL FOR REFRIGERATION SYSTEMS

The Carnot COP does not consider heat transfer mechanisms, which are necessarily irreversible. This reduces its usefulness as a realistic design goal for refrigeration systems. A more realistic approach to determine the optimum COP of a refrigeration system using a pure refrigerant is shown.

1.4.1 BACKGROUND

The design of vapor compression refrigeration cycle which attains the maximum possible coefficient of performance (COP) for specified heat exchanger sizes, capacitance rates, and external stream temperatures is of significant practical importance. The laws of thermodynamics and heat transfer mechanisms are considered to identify a realistic design goal for the COP of refrigeration cycles.

This COP differs from the Carnot COP, which is ordinarily used for the purpose as a design goal for actual cycles. Carnot introduced the concept of reversibility and the

principle that the thermal efficiency may be only expressed as a function of the heat source and heat sink. Nevertheless, the Carnot COP, which assumes a thermodynamical ideal cycle in which no irreversibilities exist and which yields the maximum COP, does not provide a realistic upper limit for design considerations because of various reasons.

The reversible heat transfer processes, assumed in the Carnot analyses, do not consider heat transfer mechanisms. Heat is added to the cycle in the evaporator by an external stream, which is cooled as it flows through the evaporator; heat is rejected from the cycle using an external stream, which is heated when it flows through the condenser. Heat transfer at a finite rate is necessarily an irreversible process and unavoidable in a refrigeration cycle. Further, heat exchangers represent a major size and cost constraint to refrigeration cycles, but the Carnot cycle can not provide any useful information on heat exchanger design.

The concept of constant temperature thermal reservoirs, as used in the Carnot cycle analyses, has no direct parallel in practice. In reality, refrigeration cycles receive and reject thermal energy from external streams. These streams, flowing at finite heat capacitance rates and with known inlet temperatures, do not represent an isothermal heat sink or heat source. This effect is not considered in the Carnot cycle analyses.

There is interest in non-azeotropic mixtures on refrigerants, for which the phase change in the evaporator and condenser does not occur at a constant temperature. Refrigerant mixtures offer the possibility of higher efficiencies and are possible substitutes for CFCs. A simple determination of the maximum COP for these fluids is desired and will be presented in the next chapter. This COP can not be calculated with a simple Carnot cycle analysis because of the varying temperature of the refrigerant during the phase changes and the heat exchanger limitations.

1.4.2 EXTERNAL BOUNDARY CONDITIONS

The performance of the ideal vapor compression cycle, with no internal irreversibilities is examined. The processes in the condenser and evaporator are assumed to be isobaric; the compression process in the compressor and turbine is assumed to be isentropic. The cycle is designed to provide a specified cooling load $\dot{Q}_L$ to an external stream with the heat capacity $\dot{C}_L$ entering the evaporator at the temperature $T_{L,in}$. Another stream with the heat capacity $\dot{C}_H$ rejects the heat and enters the condenser and at the temperature $T_{H,in}$. Figure 1.5 shows the cycle examined.

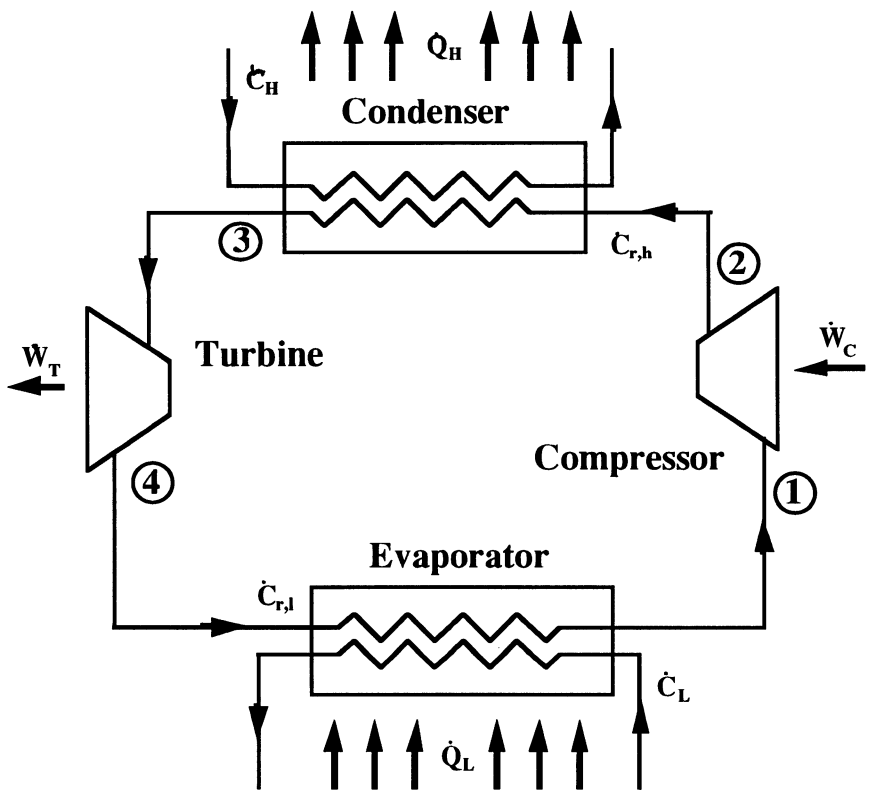

Figure 1.5 Refrigeration cycle with external streams

The evaluation of the heat transfer mechanism in the heat exchangers is based on the basic heat transfer relations [4,5]. All the components of the refrigeration cycle are modeled with the program Engineering Equation Solver (EES), [6] which is capable of solving large systems of algebraic equations and has built-in mathematical and thermophysical property functions.

1.4.3 IDENTIFICATION OF THE OPTIMUM REFRIGERATION CYCLE USING A PURE REFRIGERANT

The Carnot cycle is used as a starting point for the determination of a realistic upper bound on the COP

$$COP = \frac{\dot{Q}_L}{\dot{W}_C - \dot{W}_T} = \frac{T_l}{T_h - T_l} \tag{1.7}$$

where $\dot{Q}_L$ is the cooling load (or cooling capacity), $\dot{W}_C$ and $\dot{W}_T$ are the compressor and turbine power respectively. T_l is the temperature at which the heat is transferred from the refrigerated space through the low heat exchanger, the evaporator, to the cycle and T_h is temperature at which the heat is transferred from the cycle through the high heat exchanger, the condenser, to the heat sink. The Carnot COP is the maximum COP attainable for a refrigeration cycle with heat transfer at a constant temperature.

The determination of the Carnot COP is based only on the temperatures of the working fluid (refrigerant) in the cycle. It does not take into account the cooling load or any external conditions, like the external heat source (refrigerated space), external heat sink and the heat transfer mechanism from the cycle to the surrounding.

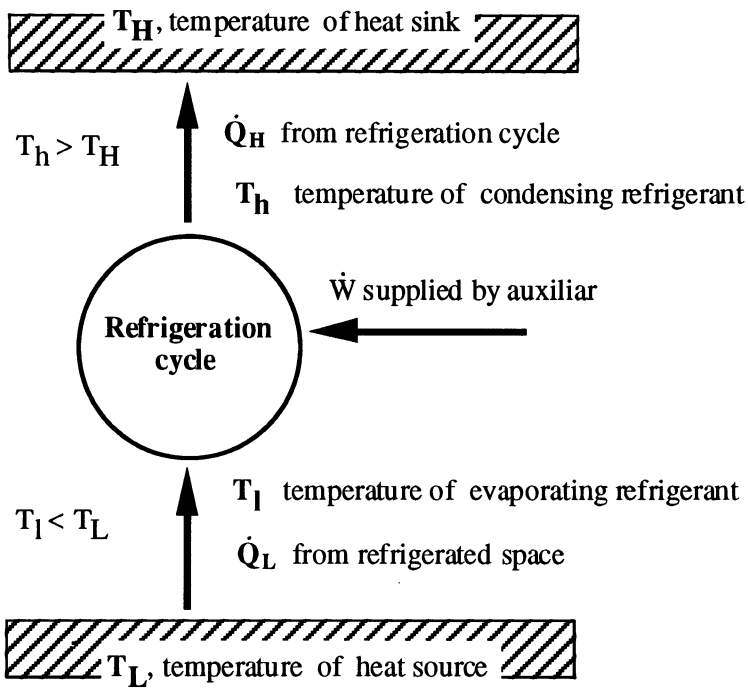

Figure 1.6 Schematic of a cooling engine

In addition, it does not consider the heat capacitance rates $\dot{C}_H$ and $\dot{C}_L$ of the heat transfer fluids in the condenser and evaporator, their overall heat transfer coefficients UA or the effectiveness ε_L and ε_H of the heat exchangers. Klein [7] found a more realistic expression for the Carnot COP in terms of the external conditions:

$$COP = \frac{T_{L,in} - \Delta T}{T_{H,in} - (T_{L,in} - \Delta T)} \tag{1.8}$$

where $T_{L,in}$ is the temperature at which the external fluid enters the low-temperature heat exchanger and $T_{H,in}$ is the temperature at which the external fluid enters the high-

temperature heat exchanger (Indices with capital letters refer to the external stream conditions and heat exchangers, whereas lower cases refer to the refrigerant.).
The remaining term ΔT, a temperature difference, is a measure for the performance of the cycle based on the above described external conditions and is defined as:

$$\Delta T = \dot{Q}_L \frac{\varepsilon_H \dot{C}_H + \varepsilon_L \dot{C}_L}{\varepsilon_H \dot{C}_H \varepsilon_{LI} \dot{C}_L} \tag{1.9}$$

The heat exchanger effectiveness, with one fluid undergoing isothermal heat transfer, is described by Kays and London [5] as

$$\varepsilon_L = 1 - \exp\left(-\frac{UA_L}{\dot{C}_L}\right) \tag{1.10}$$

$$\varepsilon_H = 1 - \exp\left(-\frac{UA_H}{\dot{C}_H}\right) \tag{1.11}$$

where UA_L and UA_H are the heat exchanger conductances for the low- and high-temperature heat exchanger respectively.
The COP defined in Equation (1.8) has its maximum for $\Delta T \rightarrow 0$. This limit is possible for a cooling capacity of $\dot{Q}_L = 0$, but it is of no practical interest, because it would result in a refrigeration cycle with zero cooling capacity. The heat capacitance rates have the largest influence on the ΔT. If both are increased to infinite values, heat transfer with the external streams becomes isothermal as assumed in the Carnot cycle analysis.

Figure 1.7 shows the two possibilities for the temperature distribution of the external streams for a coupling to a heat source and sink with infinite or finite heat capacitance rates.

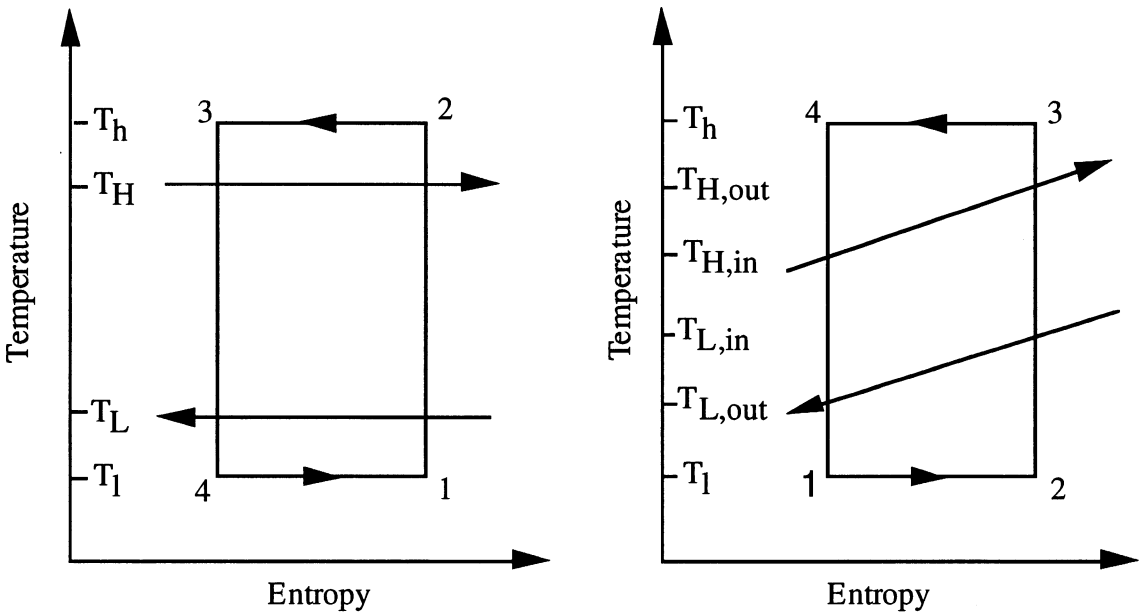

Figure 1.7 **Temperature vs. Entropy for a Carnot cycle coupled to a heat sink and heat source with infinite heat capacitance rates (left) or finite heat capacitance rate (right)**

In reality, the heat transfer to and from the external streams is not isothermal. Klein [7] shows that the optimum COP in that case is attained for equal products of the heat exchanger effectiveness and their heat capacitance rates

$$\varepsilon_H \dot{C}_H = \varepsilon_L \dot{C}_L \tag{1.12}$$

The temperature difference ΔT reduces then to

$$\Delta T = \frac{2\,\dot{Q}_L}{\varepsilon \dot{C}} \qquad \text{for } \varepsilon \dot{C} = \varepsilon_H \dot{C}_H = \varepsilon_L \dot{C}_L \tag{1.13}$$

For equal heat capacitance rates of the external streams $\dot{C}_H = \dot{C}_L$ becomes Equation (1.12) with Equations (1.9) and (1.10)

$$1 - \exp\left(-\frac{UA_L}{\dot{C}_L}\right) = 1 - \exp\left(-\frac{UA_H}{\dot{C}_H}\right) \tag{1.14}$$

This equation indicates, that the total heat exchanger conductance $UA_{total} = UA_L + UA_H$ should be split up equally $UA_L = UA_H$ for equal heat capacitance rates.

CHAPTER
TWO

IDENTIFICATION OF THE OPTIMUM REFRIGERATION CYCLE

In this chapter, the optimum refrigeration cycle is determined using a finite difference approach. The finite difference model is based on the Carnot cycle, but it considers the external boundary conditions e.g., the heat exchanger sizes, the inlet temperatures of the external stream at the heat exchangers and their heat capacitance rates. The model is able to predict the maximum obtainable COP. First design guidelines are established and the optimum refrigeration cycle shape is determined. The potential improvements of the COP in a refrigeration system using a NARM, compared to a pure refrigerant are shown.

2.1 DERIVATION OF A NUMERICAL SIMULATION MODEL

The Carnot cycle is used as starting point for the determination of a realistic upper limit on the COP. To simulate a non-isothermal phase, it is possible to break the one Carnot cycle into several smaller ones which together provide the same total cooling load. The shape of such a cycle is shown in Figure 2.1. The COP obtained with this finite difference model tends towards to the thermodynamical optimum COP (COP is maximum) as the number of segments is increased. The Carnot COP is the maximal thermodynamically possible COP and is simulated in each temperature range.

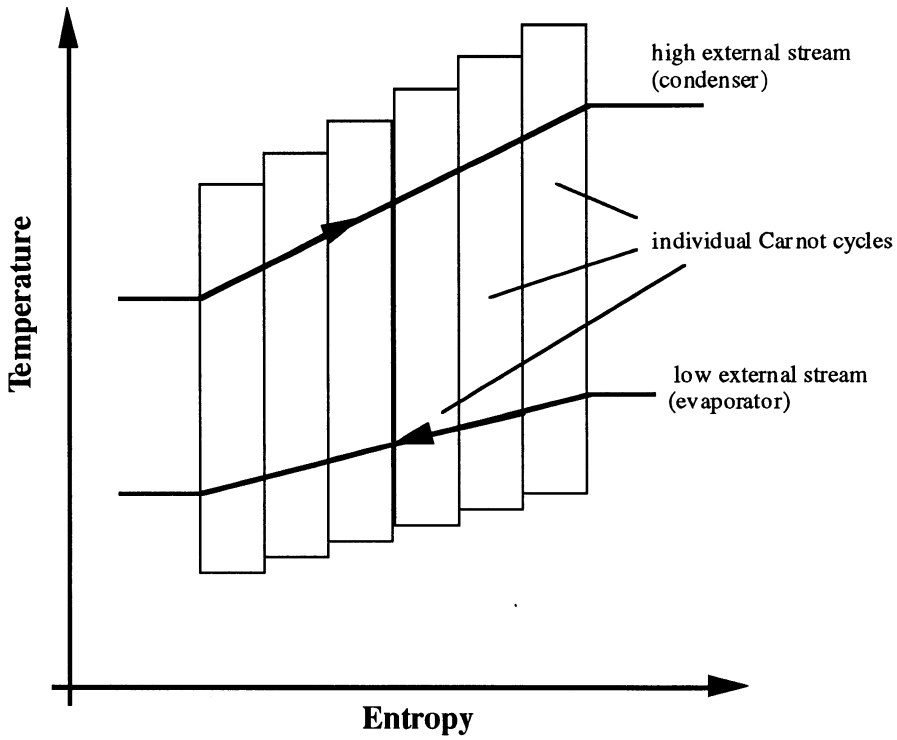

Figure 2.1 Refrigeration cycle broken into several individual Carnot cycles

The temperature of the refrigerant during the phase change processes in both heat exchangers of every single cycle remains constant, but it is different for each individual cycle. Hence, a discrete representation of a variable temperature distribution of the refrigerant throughout the phase changes is modeled. The temperature distribution of the external stream is necessarily changing along the heat exchangers and in general leads the trend of the refrigerant.

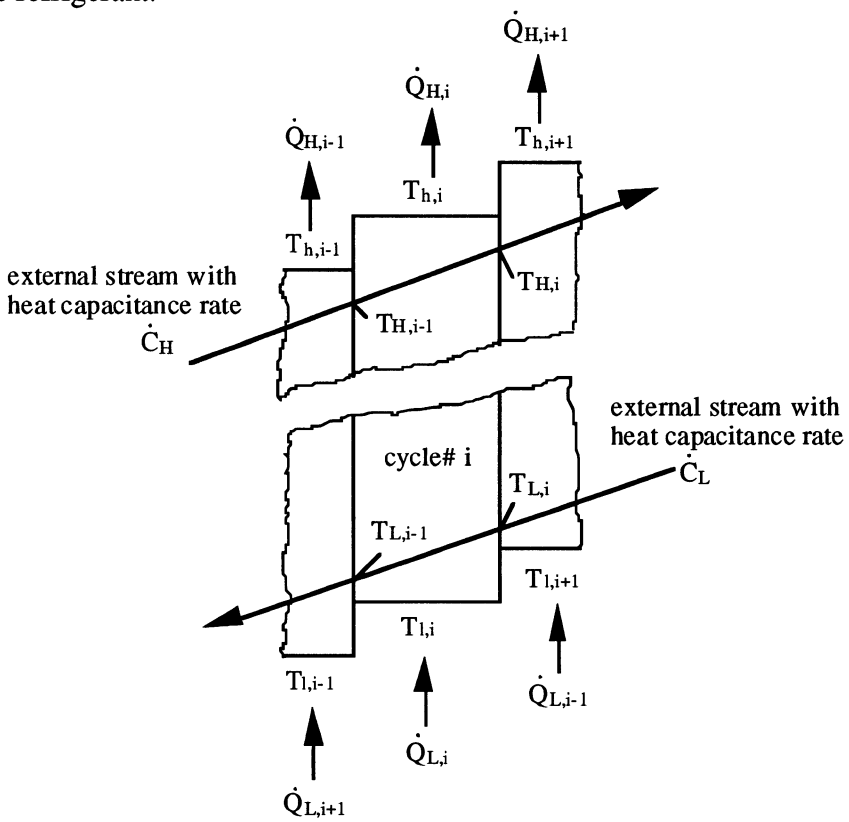

Figure 2.2 Individual Carnot cycle coupled to external streams

The first and second laws of thermodynamics for each reversible Carnot cycle may be expressed as

$$\dot{W}_i = \dot{Q}_{H,i} - \dot{Q}_{L,i} \tag{2.1}$$

and

$$\frac{\dot{Q}_{H,i}}{T_{h,i}} = \frac{\dot{Q}_{L,i}}{T_{l,i}} \tag{2.2}$$

$T_{h,i}$ is the temperature of the refrigerant in the high-temperature heat exchanger and $T_{l,i}$ is the temperature of the refrigerant in the low-temperature heat exchanger. The COP of this refrigeration cycle with n individual Carnot cycles is then obtained with

$$COP = \frac{\sum_{i=1}^{n} \dot{Q}_{L,i}}{\sum_{i=1}^{n} \dot{Q}_{H,i} - \sum_{i=1}^{n} \dot{Q}_{L,i}} = \frac{\sum_{i=1}^{n} \dot{Q}_{L,i}}{\sum_{i=1}^{n} \dot{W}_i} \tag{2.3}$$

where the heat rates and temperatures of all streams may vary for each individual cycle.

In order to determine the COP for this modified cycle, is it necessary to investigate each Carnot cycle. The examined system is shown in Figure 2.2. Energy balances and rate equations are to set up.

The energy balances for the external streams in the high and low-temperature heat exchanger respectively are

$$\dot{Q}_{H,i} = \dot{C}_{H,i} (T_{H,i} - T_{H,i-1}) \tag{2.4}$$

$$\dot{Q}_{L,i} = \dot{C}_{L,i} (T_{L,i} - T_{L,i-1}) \tag{2.5}$$

The rate equations between the refrigerant and the external streams in the high and low-temperature heat exchanger respectively become

$$\dot{Q}_{H,i} = \varepsilon_{H,i}\, \dot{C}_{H,i}\, (T_{H,i} - T_{H,i-1}) \tag{2.6}$$

$$\dot{Q}_{L,i} = \varepsilon_{L,i}\, \dot{C}_{L,i}\, (T_{L,i} - T_{l,i}) \tag{2.7}$$

where the heat exchanger's effectiveness are [5]

$$\varepsilon_L = 1 - \exp\left(-\frac{UA_{L,i}}{\dot{C}_{L,i}}\right) \tag{2.8}$$

$$\varepsilon_H = 1 - \exp\left(-\frac{UA_{H,i}}{\dot{C}_{H,i}}\right) \tag{2.9}$$

The heat capacitance rates of the external streams are assumed to be constant throughout the heat transfer process. This is a good assumption considering that fluids such as air or water will be used for these purpose and that the temperature change in each heat exchanger is usually relatively small.

The individual cooling load $\dot{Q}_{L,i}$ is specified for every single cycle. It is initially assumed, that the cooling load provided by each cycle is equal and that the sum of all individual cooling loads is equal to the total cooling load. The individual cooling load may be then expressed as:

$$\dot{Q}_{L,i} = \frac{\dot{Q}_L}{n} \tag{2.10}$$

In section 2.2.2 it is shown, that a significant increase of the COP does not occur if one tries to optimize the allocation of the heat transferred from the refrigerated space to the refrigerant and the heat exchanger conductance for every individual cycle.

Hence, the overall heat transfer coefficient area product of the heat exchangers is determined as

$$UA_i = \frac{UA}{n} \tag{2.11}$$

For the determination of the COP in terms of external conditions, it is necessary to specify the following boundary conditions: the heat capacitance rates of the external streams $\dot{C}_H$ and $\dot{C}_L$, the overall heat transfer coefficients area products of the high and low heat exchangers UA_H and UA_L, the desired total cooling load $\dot{Q}_L$ and the inlet temperatures $T_{H,in}$ and $T_{L,in}$ of the external fluids in both heat exchangers. With this information it is possible to calculate the COP with an arbitrary number of individual Carnot cycles.

2.2 RESULTS OBTAINED FROM THE FINITE DIFFERENCE MODEL

2.2.1 NECESSARY NUMBER OF INDIVIDUAL CARNOT CYCLES

The program FDM (Finite Difference Method, Appendix), written in EES is, is able to calculate the desired COP. All external parameters and the number of Carnot cycles may be varied. The COP_n, obtained for constant boundary conditions, is shown versus the number of individual Carnot cycles in sequence in Figure 2.3.

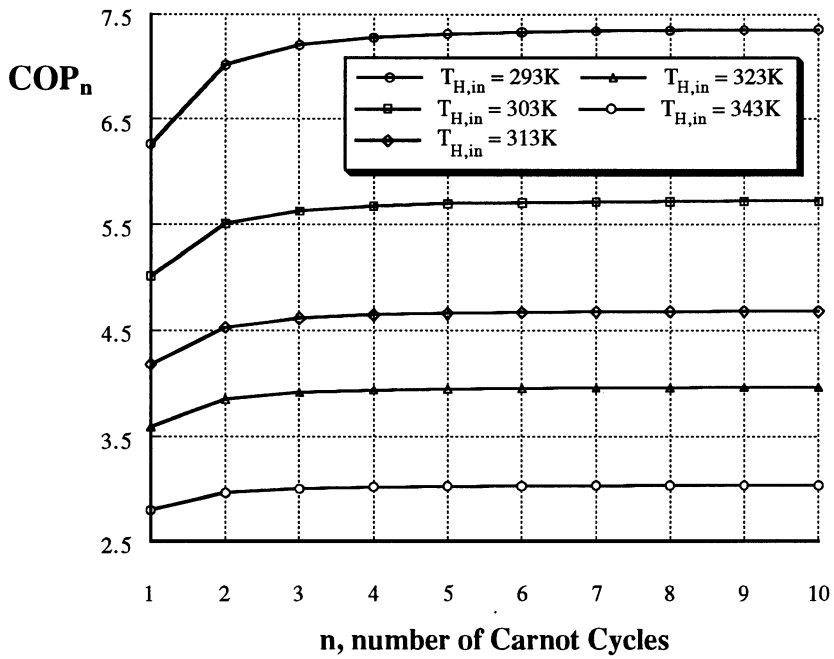

Figure 2.3 **COP_n vs. number of individual Carnot cycles for different high external stream inlet temperatures $T_{H,in}$ and low external stream inlet temperature of $T_{L,in}$ = 273 K, $UA_L = UA_H$ = 4 kW/K, $\dot{C}_L = \dot{C}_H = 1$ kW/K, $\dot{Q}_L = 10$ kW**

The inlet temperatures of the external fluid flowing into the high-temperature heat exchanger are varied for the different curves in the figure. It is first assumed that the heat capacitance rates ($\dot{C}$ = 1 kW/K) and heat exchanger conductances (UA = 4 kW/K) are the same in both heat exchangers.

The COP_n, determined with n individual Carnot cycles in sequence, increases in an asymptotic manner with increasing number of Carnot cycles, as shown in Figure 2.3, leveling off to a maximum which is independent of n .

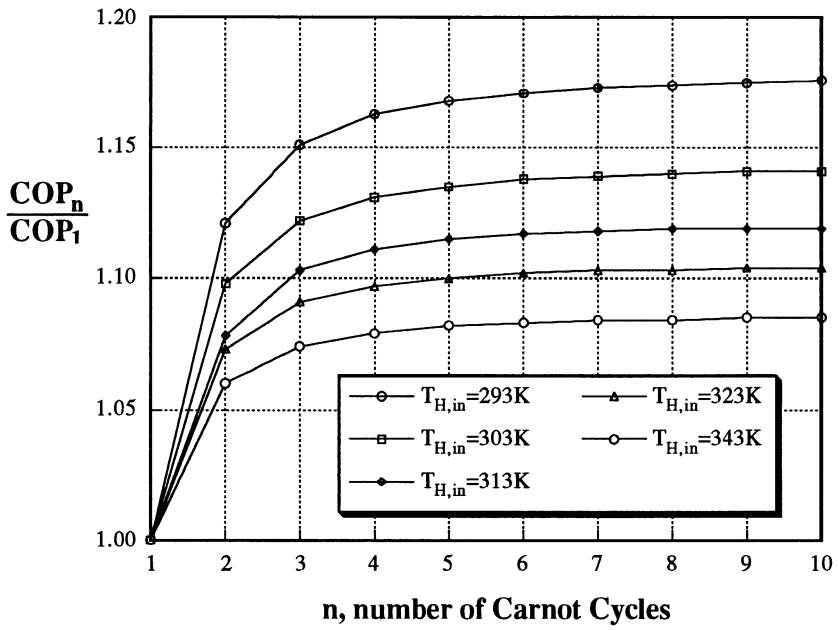

Figure 2.4 **COP_n/COP_1 vs. number of individual Carnot cycles for different high external stream inlet temperatures $T_{H,in}$ and low external stream inlet temperature of $T_{L,in}$ = 273 K, $UA_L = UA_H$ = 4 kW/K, $\dot{C}_L = \dot{C}_H = 1$ kW/K, $\dot{Q}_L = 10$ kW**

Figure 2.4 shows the potential COP improvement of COP_n/COP_1 versus the number of Carnot cycles in sequence. A COP_n/COP_1 of increase of more than 17% may be obtained. It depends on the operating conditions of the refrigeration cycle, a small $T_{H,in}$ leads to large potential performance increases. The lower the inlet temperature of $T_{H,in}$, the higher is the calculated COP, but also the higher the potential COP improvement of the COP.

The required number of Carnot cycles in sequence that will lead closely enough to the optimum COP of the refrigeration cycle is about 6 cycles. However, for all following simulations is the refrigeration cycle broken into 10 individual Carnot cycles.

2.2.2 INDIVIDUAL COOLING LOAD OF EACH CARNOT CYCLE

In order to derive this numerical model, the assumption of constant heat flow and equal heat exchanger conductances for every individual cycle was made. The effect of this assumption is shown in Figure 2.5. The individual cooling capacity and heat exchanger conductivity was optimized for each of the 8 individual Carnot cycles. The cycle is first broken into two sub-cycles in sequence. The COP of the total cycle is optimized with respect to the allocation of the cooling load and heat exchanger conductance on the two sub-cycles. Each sub-cycle is then broken into two other sub-cycles and the optimization is repeated for these cycles. At this state consists the refrigeration cycle of 4 individual sub-cycles. Every sub-cycle is broken into two further sub-cycles and the optimization procedure is repeated.

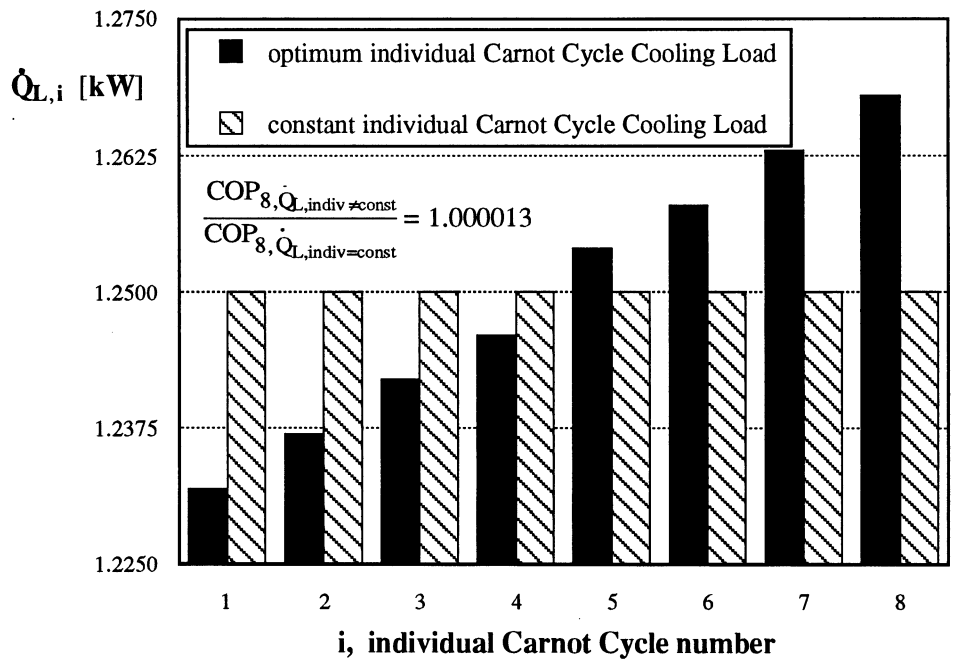

Figure 2.5 **Optimized individual cooling load $\dot{Q}_{L,i}$ of each individual Carnot cycle for $T_{L,in}$ = 273 K, $T_{H,in}$ = 313 K, UA_L = UA_H = 4 kW/K, $\dot{C}_L = \dot{C}_H$ = 1 kW/K, $\dot{Q}_L$ = 10 kW**

The optimized cooling load is for the Carnot cycles operating at relatively low temperatures smaller and at relative high operating temperatures larger than the equal average load. The optimized individual cooling load increases continuously throughout the heat exchanger, but the influence on the over all COP is negligible. The optimized heat exchanger conductances turn out to be nearly constant for all individual Carnot cycles. The potential improvement of the COP optimizing the allocation of the individual cooling loads $\dot{Q}_{L,i}$ to constant $\dot{Q}_{L,i}$ is less than 0.001%. The assumption of constant heat exchanger conductance and constant cooling load for every individual Carnot cycle is very good.

The optimum distribution of the heat exchanger conductances and heat capacitance rates in both heat exchangers is investigated next.

2.2.3 OPTIMIZED ALLOCATION OF THE HEAT EXCHANGER CONDUCTANCE

The influence of the distribution of the heat exchanger conductance UA_{total} with varying heat capacitance ratios $\dot{C}_H/\dot{C}_L$ of the external streams on the COP is shown in Figure 2.6. The inlet temperatures of the external fluids are fixed at $T_{L,in}$ = 273 K and $T_{H,in}$ = 313 K and the low heat capacitance is fixed at $\dot{C}_L$ = 1 kW/ K. The sum of the overall heat transfer coefficient area products UA_H and UA_L in the condenser and evaporator is held constant at UA_{total} = 1 kW/K. The allocation of the UA's is shifted between the two heat exchangers. Figure 2.6 indicates that the maximum COP is always obtained for $UA_L = UA_H$ (the deviation of UA_H to UA_H is less than 0.5 percent). The distribution of the COP is symmetrical about the even allocation line and exhibits a flat peak.

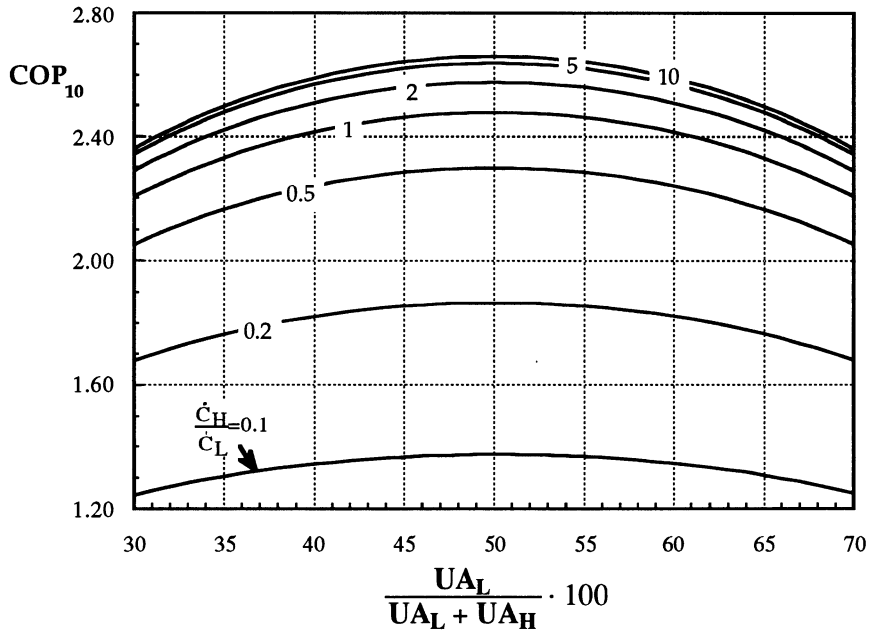

Figure 2.6 **COP_{10} vs. heat exchanger conductance UA fractions for different heat capacitance ratios with UA_{total} = 1 kW/K, $\dot{C}_L$ = 1 kW/K, $T_{L,in}$ = 273 K, $T_{H,in}$ = 313 K, $\dot{Q}_L$=10 kW**

A little deviation from the optimum allocation would still be very close to the maximum attainable COP. The heat capacitance rate in the evaporator $\dot{C}_L$ was fixed and the total heat capacitance rate $\dot{C}_{ext} = \dot{C}_H + \dot{C}_L$ changes for the different curves in Figure 2.6. The optimum allocation of the overall heat transfer coefficient is independent on the heat capacitance ratio $\dot{C}_H/\dot{C}_L$.

An increase of the high heat capacitance rate $\dot{C}_H$ strongly increases the COP for $\dot{C}_H < \dot{C}_L$. A further increase of the high heat capacitance rate for $\dot{C}_H > \dot{C}_L$ does not result in such a significant improvement of the COP. Hence there is a trade off, depending on the particular operating conditions, between the increase of $\dot{C}_H$ and the increase of the COP.

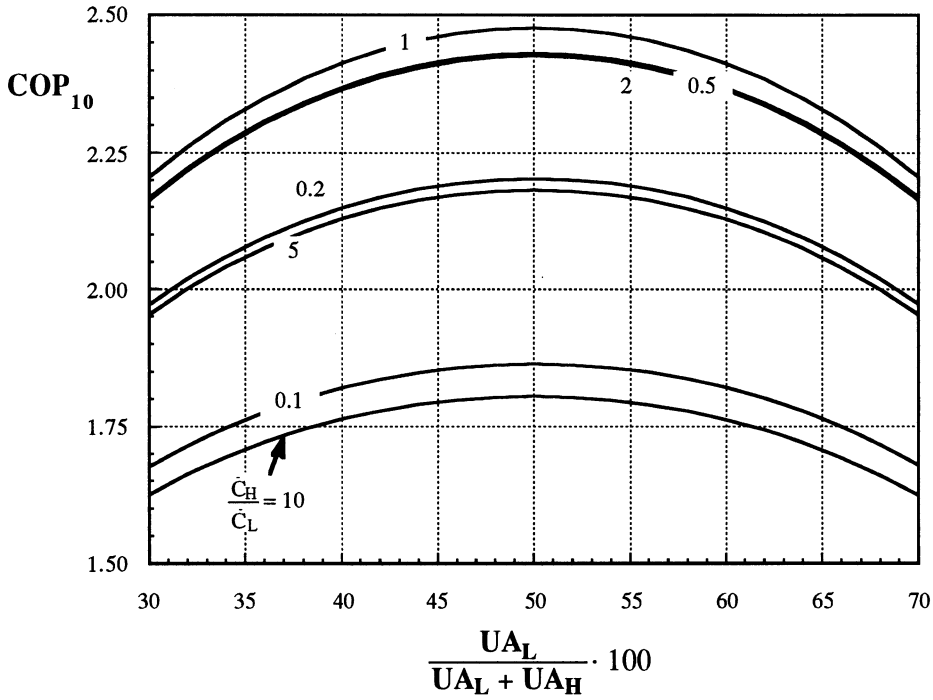

Figure 2.7 **COP_{10} vs. heat exchanger conductance UA fractions for different heat capacitance ratios with UA_{total} = 1 kW/K, $\dot{C}_{total}$ = 2 kW/K, $T_{L,in}$ = 273 K, $T_{H,in}$ = 313 K, $\dot{Q}_L$=10 kW**

The same boundary conditions as these applied in Figure 2.6 are used to create Figure 2.7, only this time the total heat capacitance rate and the total heat exchanger conductance are held constant. The total heat capacitance rate is fixed at $\dot{C}_{total}$ = 2 kW/K, so that the maximum curve in Figure 2.7 matches the curve of Figure 2.6 for equal heat capacitance rates. The maximum COP is obtained as before for equal heat exchanger conductances. In addition, it is best to allocate the total heat capacitance rate evenly on both external streams. The ratio of the two external heat capacitance rates is important, but in this analysis it does not matter which one of the heat capacitance rates larger.

2.2.4 OPTIMIZED ALLOCATION OF THE HEAT CAPACITANCE RATES

A result similar to that found in section 2.2.3 is obtained if the external heat capacitance rates in the evaporator and condenser are varied instead of the heat exchanger conductances. The same boundary conditions as these applied for Figure 2.7 are used to obtain the results shown in Figure 2.8. The only difference is the fixed total heat capacitance rate of $\dot{C}_{total}$ = 2 kW/K, which is now allocated between the two external streams and that the overall heat transfer coefficient area product ratio UA_H / UA_L is varied, where still UA_{total} = 1 kW/K. The different curves refer to different ratios of the heat exchanger conductances.

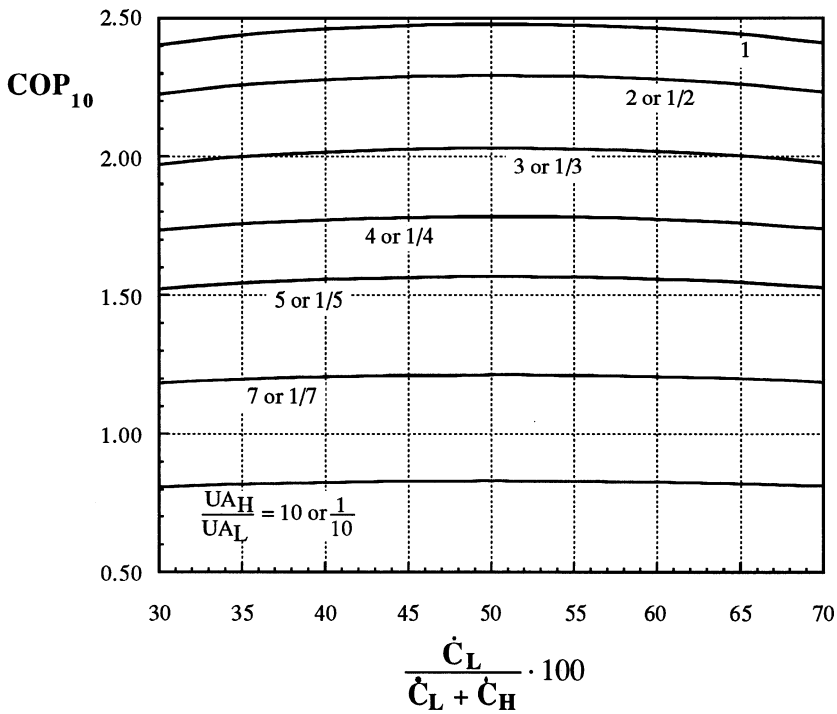

Figure 2.8 **COP_{10} vs. heat capacitance $\dot{C}$ fractions for different heat exchanger conductance ratios with UA_{total} = 1 kW/K, $\dot{C}_{total}$ = 2 kW/K, $T_{L,in}$ = 273 K, $T_{H,in}$ = 313 K, $\dot{Q}_L$=10 kW**

The optimum COP for the specified boundary conditions is, as expected, always obtained for equal heat capacitance rates $\dot{C}_H = \dot{C}_L$ and for equal heat exchanger conductances $UA_H = UA_L$. The peak again is flat and symmetrical to the even allocation line. A deviation of the optimum allocation is not severe for this special application. The calculated COP for constant UA_{total} is the same when UA_H / UA_L or UA_L / UA_H is used to calculate it. Hence, it would be possible to exchange the heat exchangers without changing the COP even if the heat exchanger sizes were different.

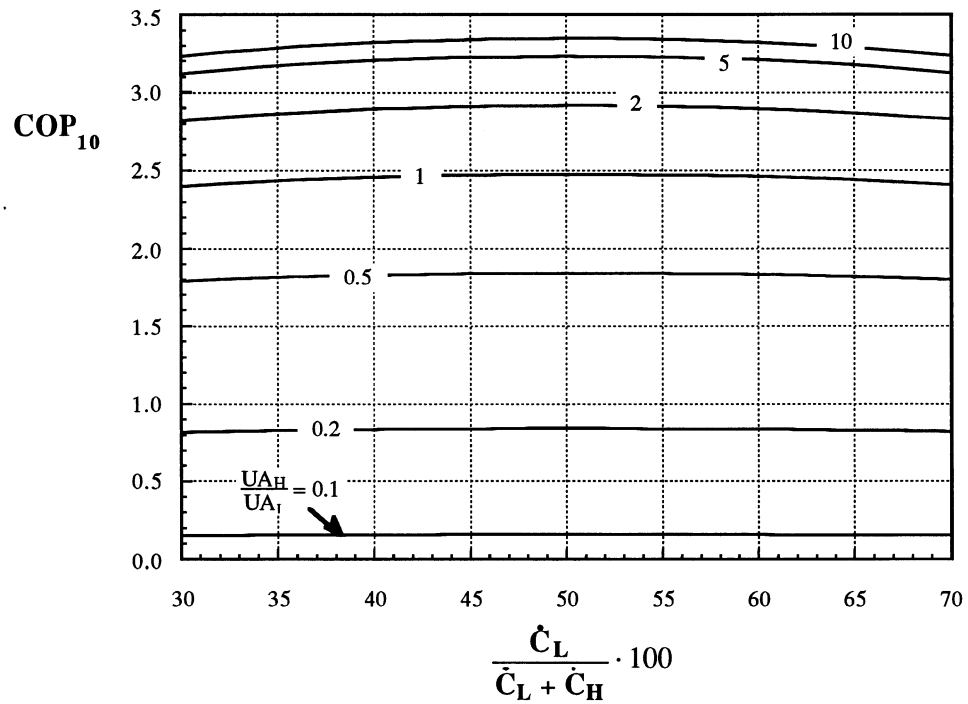

Figure 2.9 **COP_{10} vs. heat capacitance rate $\dot{C}$ fractions for different heat exchanger conductance ratios with UA_L = 0.5 kW/K, $\dot{C}_{total}$ = 2 kW/K, $T_{L,in}$ = 273 K, $T_{H,in}$ = 313 K, $\dot{Q}_L$ = 10 kW**

The total heat exchanger conductance is varied in Figure 2.9. An increase in the COP for larger ratios of UA_H/UA_L is obtained for constant UA_L. The total heat exchanger

conductance varies for the different curves and an increase of the COP for increasing ratios of UA_H/UA_L is obtained for constant UA_L.

Figure 2.10 shows results with the total heat exchanger conductance enlarged by the factor of 4. Larger values for the COP are obtained and the peak for the optimum COP sharpens with increasing UA_{total}. The larger UA_{total}, the more sensitive is the allocation of $\dot{C}_{total}$ on the two external streams.

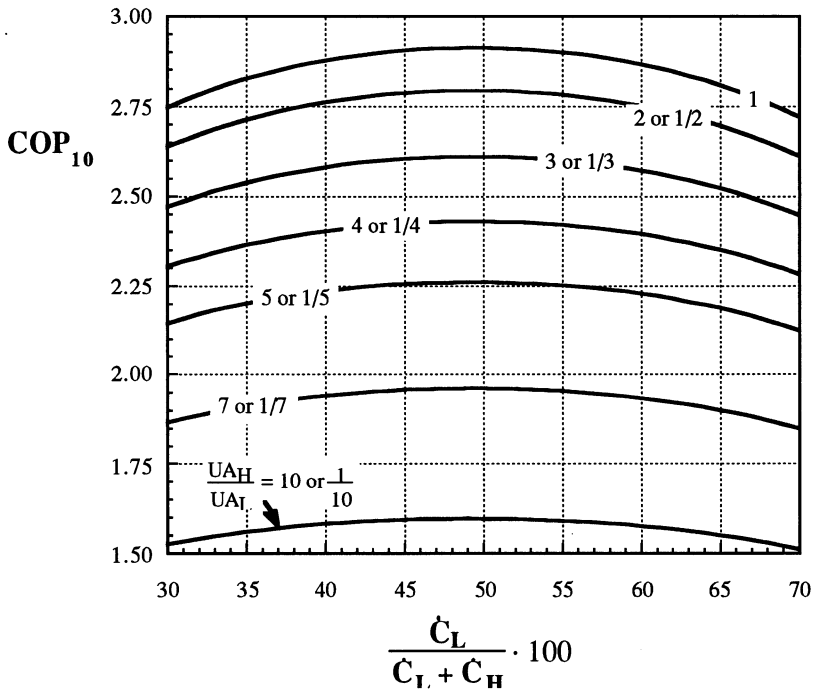

Figure 2.10 **COP_{10} vs. heat capacitance $\dot{C}$ fractions for different heat exchanger conductance ratios with UA_{total} = 2 kW/K, $\dot{C}_{total}$ = 2 kW/K, $T_{L,in}$ = 273 K, $T_{H,in}$ = 313 K, $\dot{Q}_L$=10 kW**

For Figure 2.11 is the total heat capacitance rate decreased by the factor of 4. The COP increases and again the peak for the optimum COP sharpens with decreasing $\dot{C}_{total}$. The smaller $\dot{C}_{total}$, the more sensitive is the allocation of $\dot{C}_{total}$ on the two external streams.

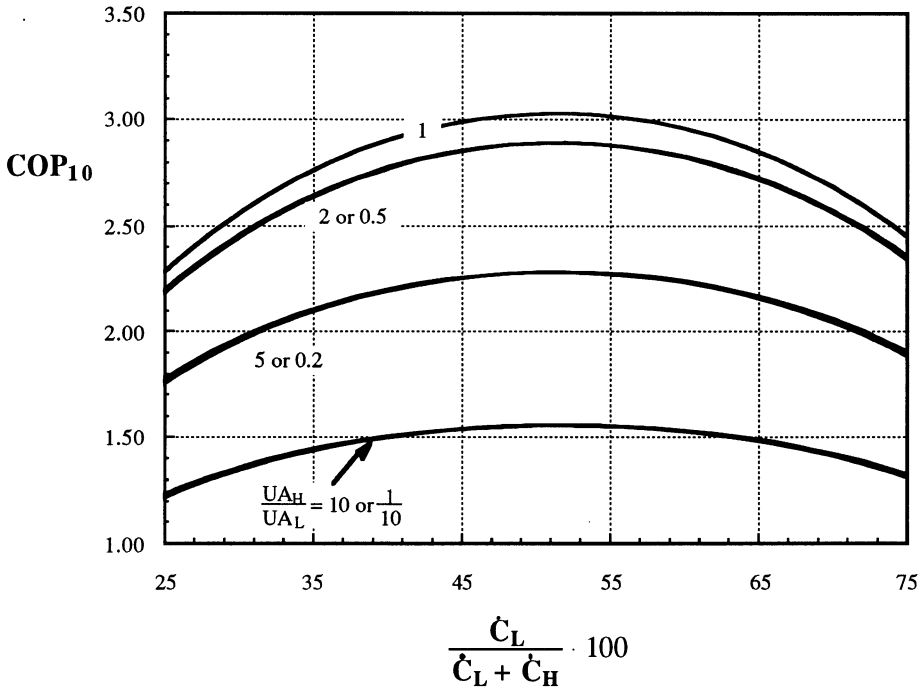

Figure 2.11 **COP_{10} vs. heat capacitance $\dot{C}$ fractions for different heat exchanger conductance ratios with UA_{total} = 2 kW/K, $\dot{C}_{total}$ = 0.5 kW/K, $T_{L,in}$ = 273 K, $T_{H,in}$ = 283 K, $\dot{Q}_L$=10 kW**

2.2.5 OPTIMUM REFRIGERATION CYCLE SHAPE

Figures 2.12, 2.13 and 2.14 show the shape of the optimum refrigeration cycle in a temperature-entropy transfer rate diagram for different heat capacitance ratios. The shape of the optimum refrigeration cycle as shown in Figure 2.12 assumes a constant total heat capacitance rate and total heat exchanger conductance which may be allocated between the two heat exchangers. The temperature difference between the heat transferring fluids in each heat exchanger is constant. For the cycle having the maximum COP, the heat exchange process between the refrigerant and the external stream occurs throughout the

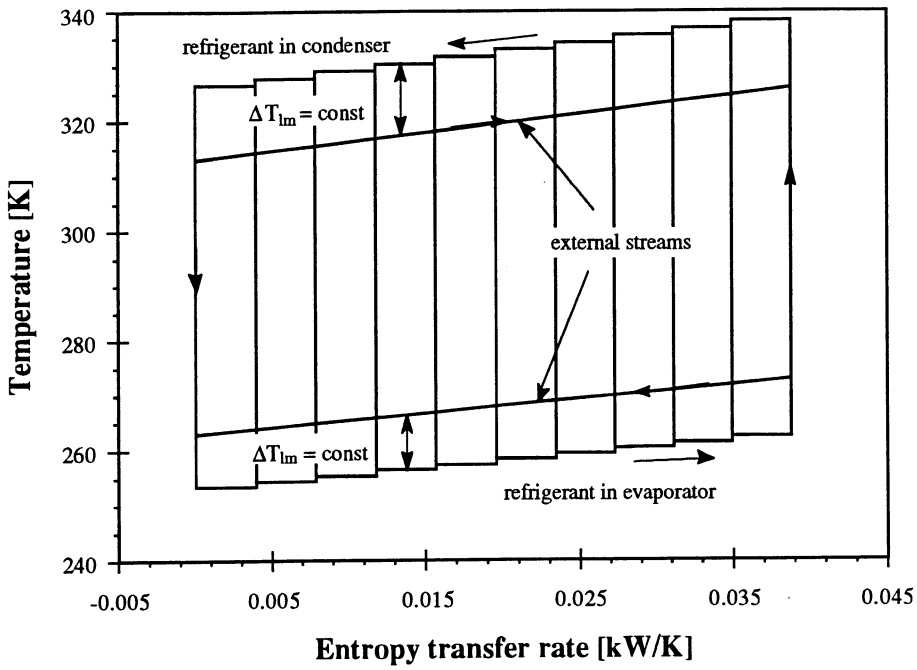

Figure 2.12 **Temperature vs. entropy transfer rate with low and high external stream inlet temperature of $T_{L,in} = 273$ K, $T_{H,in} = 313$ K respectively, $UA_L = UA_H = 1$ kW/K, $\dot{C}_L = \dot{C}_H = 1$ kW/K, $\dot{Q}_L$=10 kW**

whole heat transfer process at a constant temperature difference. Hence the temperature change of the external stream should match the temperature change of the refrigerant. The temperature profiles of the external stream and the refrigerant are parallel to each other in each heat exchanger as seen in Figure 2.12. It turned out that the COP_i for every individual cycle is constant and consequently equal to the total COP. A change of the heat capacitance rates to $\dot{C}_H << \dot{C}_L$ or $\dot{C}_H >> \dot{C}_L$ does not change this behavior significantly. The temperature difference in the evaporator remains constant, due to the equal heat rate in each single Carnot cycle in the evaporator. The temperature difference in the condenser is still fairly constant.

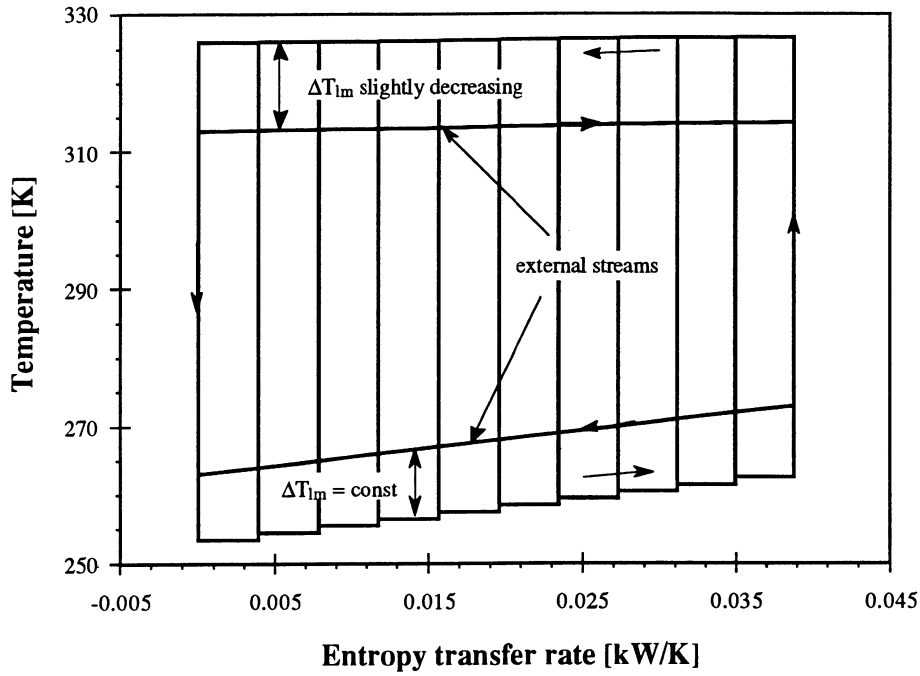

Figure 2.13 **Temperature vs. entropy transfer rate diagram with low and high external stream inlet temperature of $T_{L,in} = 273$ K, $T_{H,in} = 313$ K respectively, $UA_L = UA_H = 1$ kW/K, $\dot{C}_L = 1$ kW/K, $\dot{C}_H = 10$ kW/K, $\dot{Q}_L = 10$ kW**

Only for very small heat capacitance rates $\dot{C}_H$ ($\dot{C}_H << \dot{C}_L$) increases the temperature difference, between the external stream and refrigerant in the condenser. Nevertheless, the increase in the temperature difference is fairly small compared to the absolute increase of the fluid temperatures. The temperature change of the external stream should match the temperature change of the refrigerant also for refrigeration system with unequal heat capacitance rates of the external stream. The optimum refrigeration cycle shape will be investigated more thoroughly in the next chapter.

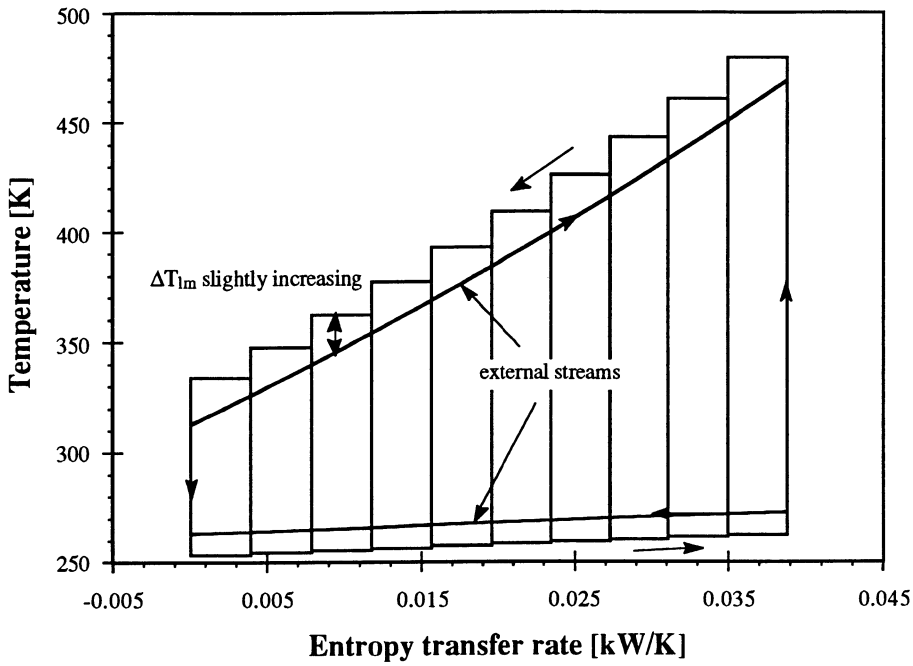

Figure 2.14 **Temperature vs. entropy transfer rate diagram with low and high external stream inlet temperature of $T_{L,in} = 273$ K, $T_{H,in} = 313$ K respectively, $UA_L = UA_H = 1$ kW/K, $\dot{C}_L = 1$ kW/K, $\dot{C}_H = 0.1$ kW/K, $\dot{Q}_L = 10$ kW**

2.3 CHAPTER SUMMARY

It was shown that a relatively small number of individual Carnot cycles is sufficient to obtain a COP very close to the maximum COP.

First design guidelines could be established:

For specified total heat exchanger conductance and specified total heat capacitance rates

- Equal allocation of the total heat exchanger conductance on the high- and low-temperature heat exchanger, independent on the heat capacitance ratio $\dot{C}_H/\dot{C}_L$ and the inlet temperatures of the external streams.
- Equal allocation of the total heat capacitance rates on the external streams, independent on the heat exchanger conductance ratio UA_H/UA_L and the inlet temperatures of the external streams.

For a varying total heat exchanger conductance and a varying total heat capacitance rates

- An increase of the total heat exchanger conductance increases the COP and increases the potential COP improvement.
- An increase of the total external heat capacitance rate increases the COP, but decreases the potential COP improvement.

For the temperature profiles of the external streams and the refrigerant

- The slope of the temperature change of the refrigerant in the heat exchanger should be parallel to that of the external stream flowing through that heat exchanger.

CHAPTER
THREE

ANALYTICAL SIMULATION MODEL

The calculation of the COP with the numerical model described in Chapter 2 leads to a large set of non-linear equations. The solution of the equations requires extensive calculations. So it is necessary to look for an analytic possibility to evaluate the optimum COP in terms of the external conditions.

In this chapter, another approach is presented for the determination of the optimum refrigeration cycle. This Analytical Simulation Model (AM, Appendix) does not provide information about the temperature distribution of the heat transferring fluids in the heat exchangers, but it is possible to specify internal heat capacitance rates of the refrigerant. A general and simple expression for the COP of an arbitrary system is found. The numerical and analytical model are then compared with each other.

3.1 DERIVATION OF AN ANALYTICAL MODEL

3.1.1 GENERAL EXPRESSION FOR THE COP

A refrigeration cycle broken into n individual Carnot cycles where $n \rightarrow \infty$ is assumed. Such a procedure leads to the optimum COP. The temperature of the external fluids and the refrigerant flowing through the heat exchangers change continuously. The general definition of the COP applied to this cycle is again

$$COP = \frac{\dot{Q}_L}{\dot{Q}_H - \dot{Q}_L} \tag{1.5}$$

In order to determine the COP, it is necessary to set up energy balances and rate equations for the high temperature heat exchanger (the condenser). The heat transfer does not occur isothermally for the refrigerant, as in each individual Carnot cycle, and the energy balance for the refrigerant in the condenser yields

$$\dot{Q}_H = \dot{C}_h (T_{h,in} - T_{h,out}) \tag{3.1}$$

where $\dot{C}_h$ is the heat capacitance rate of the refrigerant in the condenser and $T_{h,in}$ and $T_{h,out}$ are the temperatures of the refrigerant at the condenser inlet and outlet, respectively. An energy balance of the external stream yields

$$\dot{Q}_H = \dot{C}_H (T_{H,out} - T_{H,in}) \tag{3.2}$$

The energy balance for the refrigerant in the low temperature heat exchanger, the evaporator, is similar obtained as

$$\dot{Q}_L = \dot{C}_l (T_{l,out} - T_{l,in}) \tag{3.3}$$

where $\dot{C}_l$ is the heat capacitance rate of the refrigerant in the evaporator and $T_{l,out}$ and $T_{l,in}$ are the temperatures of the refrigerant at the condenser outlet and inlet, respectively. The energy balance for the external stream may be expressed as

$$\dot{Q}_L = \dot{C}_L (T_{L,in} - T_{L,out}) \tag{3.4}$$

The rate equations between the refrigerant and the external streams for the condenser are given as

$$\dot{Q}_H = \varepsilon_H \dot{C}_{H,min} (T_{h,in} - T_{H,in}) \tag{3.5}$$

and for the evaporator as

$$\dot{Q}_L = \varepsilon_L \dot{C}_{L,min} (T_{L,in} - T_{l,in}) \tag{3.6}$$

The heat exchanger effectiveness factor is defined as [5]

$$\varepsilon_H = \frac{1- \exp\left[-NTU_H\left(1 - \frac{\dot{C}_{H,min}}{\dot{C}_{H,max}}\right)\right]}{1 - \left(\frac{\dot{C}_{H,min}}{\dot{C}_{H,max}}\right)\exp\left[-NTU_H\left(1 - \frac{\dot{C}_{H,min}}{\dot{C}_{H,max}}\right)\right]} \tag{3.7}$$

for the high temperature heat exchanger and

$$\varepsilon_L = \frac{1- \exp\left[-NTU_L\left(1 - \frac{\dot{C}_{L,min}}{\dot{C}_{L,max}}\right)\right]}{1 - \left(\frac{\dot{C}_{L,min}}{\dot{C}_{L,max}}\right)\exp\left[-NTU_L\left(1 - \frac{\dot{C}_{L,min}}{\dot{C}_{L,max}}\right)\right]} \tag{3.8}$$

for the low temperature heat exchanger, where NTU_L and NTU_H are defined as

$$NTU_H = \frac{UA_H}{\dot{C}_{H,min}} \tag{3.9}$$

$$NTU_L = \frac{UA_L}{\dot{C}_{L,min}} \tag{3.10}$$

The heat capacitance rates appearing in Equations (3.5)-(3.10) are obtained with

$$\dot{C}_{H,max} = \max\left(\dot{C}_H, \dot{C}_h\right) \tag{3.11}$$

$$\dot{C}_{H,min} = \min\left(\dot{C}_H, \dot{C}_h\right) \tag{3.12}$$

$$\dot{C}_{L,max} = \max\left(\dot{C}_L, \dot{C}_l\right) \tag{3.13}$$

$$\dot{C}_{L,min} = \min\left(\dot{C}_L, \dot{C}_l\right) \tag{3.14}$$

If the heat capacitance rates ratio is $\dot{C}_{H,min}/\dot{C}_{H,max} = 1$, then the heat exchanger effectiveness for the condenser in Equation (3.7) reduces to [5]

$$\varepsilon_H = \frac{NTU_H}{NTU_H + 1} \qquad \text{for} \qquad \dot{C}_{H,min}/\dot{C}_{H,max} = 1 \tag{3.15}$$

The evaporator heat exchanger effectiveness in Equation (3.8) for $\dot{C}_{L,min}/\dot{C}_{L,max} = 1$ reduces to

$$\varepsilon_L = \frac{NTU_L}{NTU_L + 1} \qquad \text{for} \qquad \dot{C}_{L,min}/\dot{C}_{L,max} = 1 \tag{3.16}$$

The application of the second law of thermodynamics for this refrigeration cycle is more complex then for the Carnot cycle. The temperatures of the refrigerant in the low and high temperature heat exchanger are not constant. Suitable mean temperatures for non-isothermal heat transfer must be found so that the entropy balance for a reversible cycle becomes

$$\frac{\dot{Q}_L}{T_{l,mean}} = \frac{\dot{Q}_H}{T_{h,mean}} \tag{3.17}$$

The heat and entropy transfer must be examined carefully to determine these thermodynamic mean temperatures.

The entropy transfer rate due to the heat flow may be expressed as

$$\dot{S}_Q = \int_{T_1}^{T_2} \frac{d\dot{Q}}{T} = \frac{\dot{Q}}{T_m} \tag{3.18}$$

where the second equation defines the thermodynamic mean temperature for a non-isothermal heat transfer process.

$$T_m = \frac{\dot{Q}}{\int_{T_1}^{T_2} \frac{d\dot{Q}}{T}} = \frac{\dot{Q}}{\dot{S}} \tag{3.19}$$

In order to calculate the mean temperature Equation (3.19) is written as

$$T_m = \frac{\Delta \dot{Q}}{\Delta \dot{S}} = \frac{h_2 - h_1}{s_2 - s_1} \tag{3.20}$$

where 1 and 2 refer to inlet and outlet conditions respectively.

For a fluid with constant specific heat c_p, isobar enthalpy and entropy change and negligible kinetic and potential energy becomes the enthalpy

$$h_x = h_0 + c_p (T_x - T_0)) + v_0 (p_x - p_0) \tag{3.21}$$

and the entropy

$$s_x = s_0 + c_p \ln \frac{T_x}{T_0} - R \ln \frac{p_x}{p_0} \tag{3.22}$$

combining Equations (3.19) to (3.22) yields

$$T_m = \frac{(h_0 + c_p T_2) - (h_0 + c_p T_1)}{\left(s_0 + c_p \ln \frac{T_2}{T_0} \right) - \left(s_0 + c_p \ln \frac{T_1}{T_0} \right)} = \frac{T_2 - T_1}{\ln \frac{T_2}{T_1}} \tag{3.23}$$

where T_m is the thermodynamic mean temperature for non-isothermal heat transfer. The mean temperatures which are to be used in Equation (3.17) are

$$T_{h,mean} = \frac{T_{h,out} - T_{h,in}}{\ln\left(\frac{T_{h,out}}{T_{h,in}}\right)} \tag{3.24}$$

$$T_{l,mean} = \frac{T_{l,out} - T_{l,in}}{\ln\left(\frac{T_{l,out}}{T_{l,in}}\right)} \tag{3.25}$$

It is now possible to evaluate the coefficient of performance only in terms of external conditions. Solving the Equations (1.5), (3.1) to (3.17), (3.24) and (3.25) for the COP leads to the following general expression.

$$COP = \frac{\dot{Q}_L\left[1 + \beta\left(\varepsilon_H \frac{\dot{C}_{H,min}}{\dot{C}_h} - 1\right)\right]}{T_{H,in}\varepsilon_H\dot{C}_{H,min}(\beta - 1) - \dot{Q}_L\left[1 + \beta\left(\varepsilon_H \frac{\dot{C}_{H,min}}{\dot{C}_h} - 1\right)\right]} \tag{3.26}$$

where β is defined by

$$\beta = \left[\frac{\dot{C}_{L,min}}{\dot{C}_l} \cdot \frac{\dot{Q}_L\,\varepsilon_L}{(T_{L,in}\,\varepsilon_L\,\dot{C}_{L,min} - \dot{Q}_L)} + 1\right]\left(\frac{\dot{C}_l}{\dot{C}_h}\right) \tag{3.27}$$

3.1.2 PARTIALLY OPTIMIZED COP

The optimum refrigeration cycle shape was shown in a temperature-entropy transfer rate diagram in Figure 2.12. Parallel temperature curves of the fluids in each heat exchanger have been obtained for that cycle. That indicates, that the heat capacitance rates of the refrigerant and the external fluid flowing through the same heat exchangers ($\dot{C}_{L,ext} = \dot{C}_{l,ext}$ & $\dot{C}_{H,ext} = \dot{C}_{h,refr}$) should be equal in order to obtain an optimized COP. Equation (3.26) reduces then to

$$COP = \dot{Q}_L \frac{\left[1 + \lambda\,(\varepsilon_H - 1)\right]}{T_{H,in}\,\varepsilon_H\,\dot{C}_H(\lambda - 1) - \dot{Q}_L\left[1 + \lambda\,(\varepsilon_H - 1)\right]} \tag{3.28}$$

where λ is defined by

$$\lambda = \left[\frac{\dot{Q}_L\,\varepsilon_L}{(T_{L,in}\,\varepsilon_L\,\dot{C}_L - \dot{Q}_L)} + 1\right] \tag{3.29}$$

Equations (3.28) and (3.29) do not require equal heat capacitance rates of the external streams flowing through the different heat exchangers ($\dot{C}_{L,ext} \neq \dot{C}_{H,ext}$). The COP in Equation (3.28) is only optimized with respect to the ratio of external to refrigerant heat capacitance rate ($\dot{C}_{L,ext}/\dot{C}_{l,refr}$ & $\dot{C}_{H,ext}/\dot{C}_{h,refr}$), hence it is called a partially optimized COP. A verification of that result is fairly simple. COP's obtained with the expression in Equation (3.28) must be equal or slightly larger then the COP calculated with the Finite Difference Method for 10 cycle. The two models are compared in section 3.3.

3.2 RESULTS FROM THE ANALYTICAL MODEL

3.2.1 VARIATION OF THE EXTERNAL INLET TEMPERATURES $T_{L,in}$ AND $T_{H,in}$

The influence of different external inlet temperatures $T_{H,in}$ and $T_{L,in}$ will be investigated along with different temperature drops $T_{L,in}$ - $T_{L,out}$ of the external stream in the low-temperature heat exchanger.

The same boundary conditions applied as these for the numerical investigation in the previous chapter with the additional assumption of equal heat exchanger conductances, $UA_H = UA_L$ and equal heat capacitance rate in each heat exchanger, $\dot{C}_H = \dot{C}_h$ & $\dot{C}_L = \dot{C}_l$. A new parameter, the potential improvement of the COP named Ω, is defined as

$$\Omega = \frac{COP_\infty}{COP_1} \tag{3.30}$$

COP_∞ represents the COP obtained from the Analytical Simulation Model and COP_1 is the COP obtained from the Numerical Simulation Model with n=1 (one Carnot cycle).

Figure 3.1 shows a schematic temperature - entropy diagram. The external inlet temperatures and a temperature difference, the gliding temperature difference GTD are labeled in the figure. The GTD refers to the total temperature change which a fluid acquires during the heat transfer process. These and other parameters will be investigated. Ω decreases as the difference between $T_{H,in}$ and $T_{L,in}$ increases. Figure 3.2.a indicates also, that Ω increases with increasing heat exchanger conductance. This behavior is especially significant for small temperature differences and becomes less important for higher incoming temperatures $T_{H,in}$ ($T_{L,in}$ is fixed at $T_{L,in}$ = 273 K).

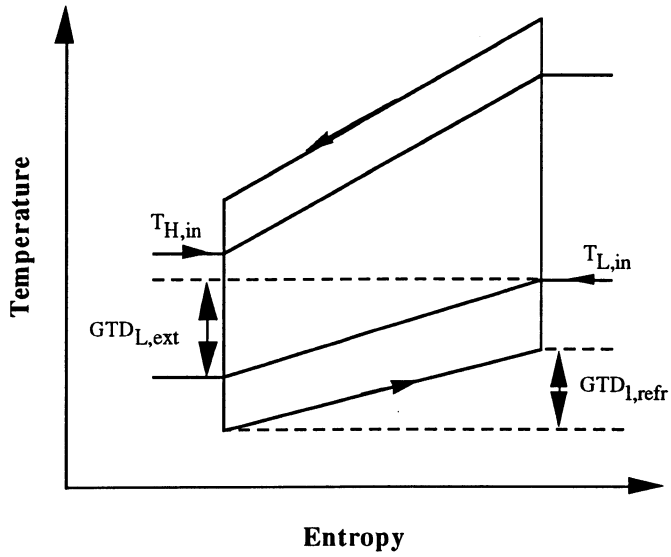

Figure 3.1 Schematic Temperature - Entropy diagram

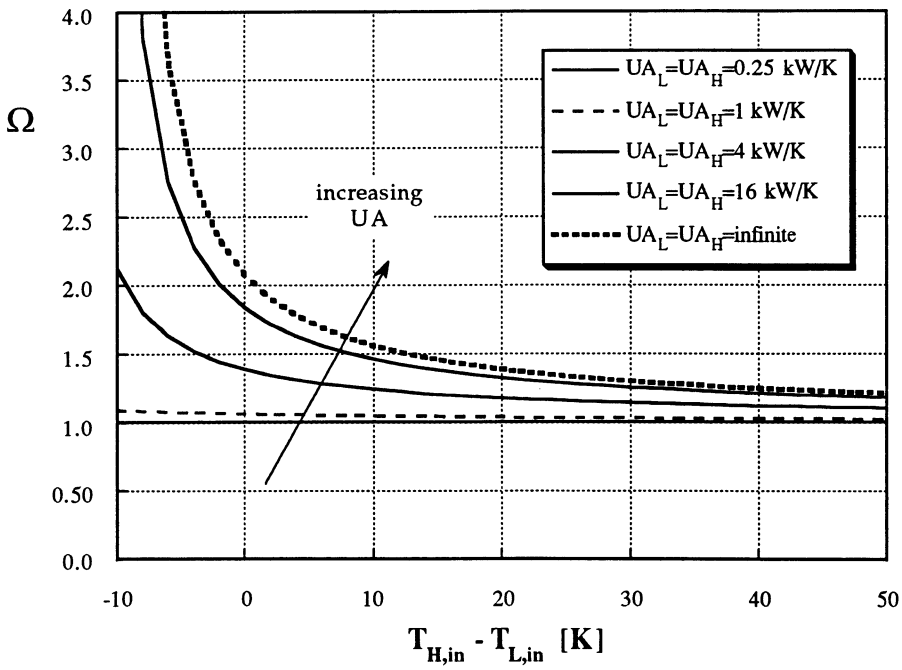

Figure 3.2.a Potential COP improvement Ω vs. temperature difference $T_{H,in} - T_{L,in}$ for different heat exchanger conductances, low external stream inlet temperature of $T_{L,in} = 273$ K, $\dot{C}_L = \dot{C}_H = 1$ kW/K, $\dot{Q}_L$=10 kW

The range of larger temperature differences represents the realistic operating conditions of a refrigeration system. $T_{H,in}$ will ordinarily be well above $T_{L,in}$. It is unlikely that the fluid which has to be cooled enters the low-temperature heat exchanger at the same or little higher temperature than the temperature of the high external stream, which enters the high-temperature heat exchanger usually at ambient temperature $T_{H,in}$. The section of interest is enlarged and shown in Figure 3.2.b. The potential improvement Ω can be as high as 50 % for infinite heat exchanger size.

The smaller the inlet temperature difference of the external streams $T_{H,in}$ - $T_{L,in}$, the larger the potential COP improvement Ω. The larger the total heat exchanger conductance UA_{total}, the larger the potential COP improvement Ω.

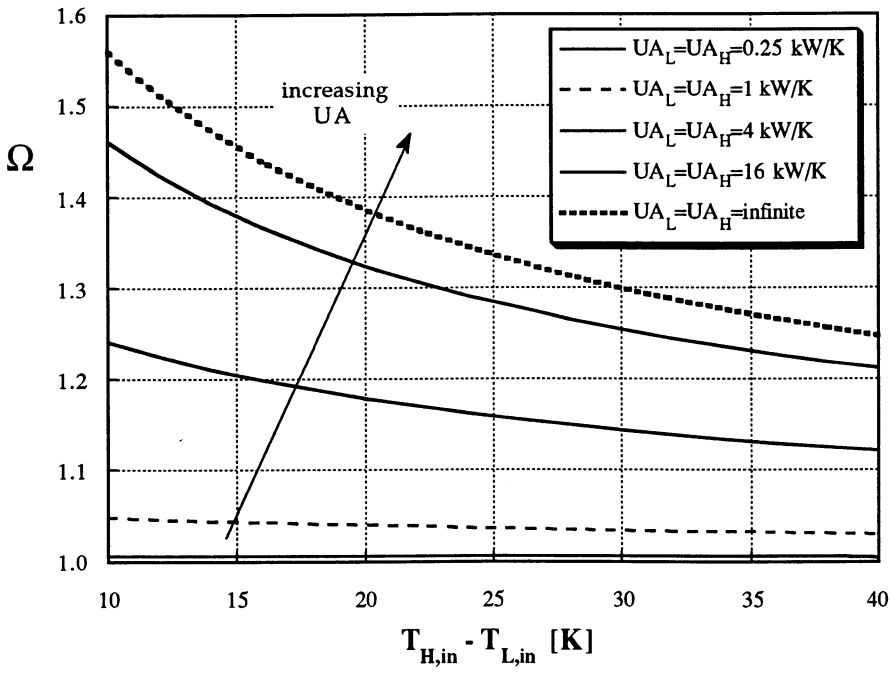

Figure 3.2.b Potential COP improvement Ω vs. temperature difference $T_{H,in}$ - $T_{L,in}$ for different heat exchanger conductances, low external stream inlet temperature of $T_{L,in} = 273$ K, $\dot{C}_L = \dot{C}_H = 1$ kW/K, $\dot{Q}_L$=10 kW

3.2.2 VARIATION OF THE GLIDING TEMPERATURE DIFFERENCES $GTD_{l,refr}$ AND THE COOLING LOAD $\dot{Q}_L$

3.2.2.1 Gliding Temperature Difference $GTD_{l,refr}$ at constant Heat Capacitance Rates

The temperature drop of the low external stream represents the ability of the refrigeration system to cool down a fluid to a certain temperature. The temperature drop of the system investigated in chapter 3.2.1 was fixed at $T_{L,in} - T_{L,out} = 10$ K. What is the influence of other temperature differences?

The temperature difference of the low external stream is now called external gliding temperatures difference $GTD_{L,ext}$ and defined as

$$GTD_{L,ext} = T_{L,in} - T_{L,out} \tag{3.29}$$

The heat capacitance rates of the streams in each heat exchanger are assumed equal and consequently the temperature drop of the external stream is equal to the temperature drop of the refrigerant.

$$GTD_{l,ext} = T_{l,out} - T_{l,in} = GTD_{L,ext} \tag{3.30}$$

A variation of the $GTD_{l,ext}$ is attained by varying the cooling capacity $\dot{Q}_L$ or by varying the heat capacitance rates. An increase of $GTD_{l,ext}$ increases the potential improvement Ω. It is possible to double the COP for very large gliding temperatures $GTD_{l,ext}$ in the low-temperature heat exchanger, but the refrigeration system at this operating conditions would operate at a very low COP. The COP and the potential improvement are strongly dependent on the operating conditions. In Figure 3.3 for example is a $COP_\infty = 3$ and a

$\Omega = 1.10$ (10%) obtained for a system at $GTD_{l,refr} = 20$ K. The external high inlet temperature is $T_{H,in} = 313$ K = 40 °C.

The COP of the system decreases with increasing $GTD_{l,refr}$. This behavior is non-intuitive and the reader might ask why it is useful to apply a refrigerant mixture when the COP decreases. Actually the cooling capacity is increased in order to vary the $GTD_{l,refr}$. The refrigeration system itself is not changed and the same system has to cope with a higher cooling load which explains the reduced COP. Nevertheless it is seen, that a system operating at large GTD and using a suitable refrigerant mixture would perform better than a pure refrigerant.

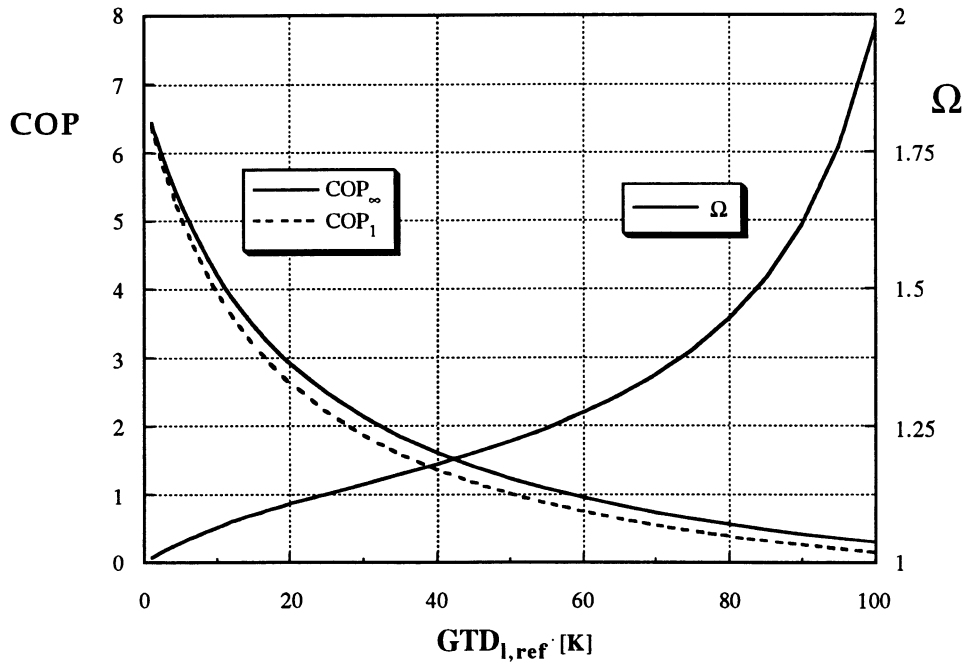

Figure 3.3 **COP_∞, COP_1 and potential COP improvement Ω vs. temperature difference $T_{l,in} - T_{l,out}$ with external stream inlet temperature of $T_{L,in} = 273$ K, $T_{H,in} = 313$ K and $UA_L = UA_H = 2$ kW/K, $\dot{C}_L = \dot{C}_H = 1$ kW/K**

$T_{H,in}$ in Figure 3.3 is fairly high for ambient heat rejection. If the temperature $T_{H,in}$ is decreased from $T_{H,in}$ = 313 K to $T_{H,in}$ = 293 K = 20 °C, which is more realistic, then the COP increases to $COP_\infty = 4$, and Ω increases even to $\Omega = 1.13$ (13%), as shown in Figure 3.4. Consequently there is a trade off between the attainable COP, the potential improvement Ω, and the operating conditions.

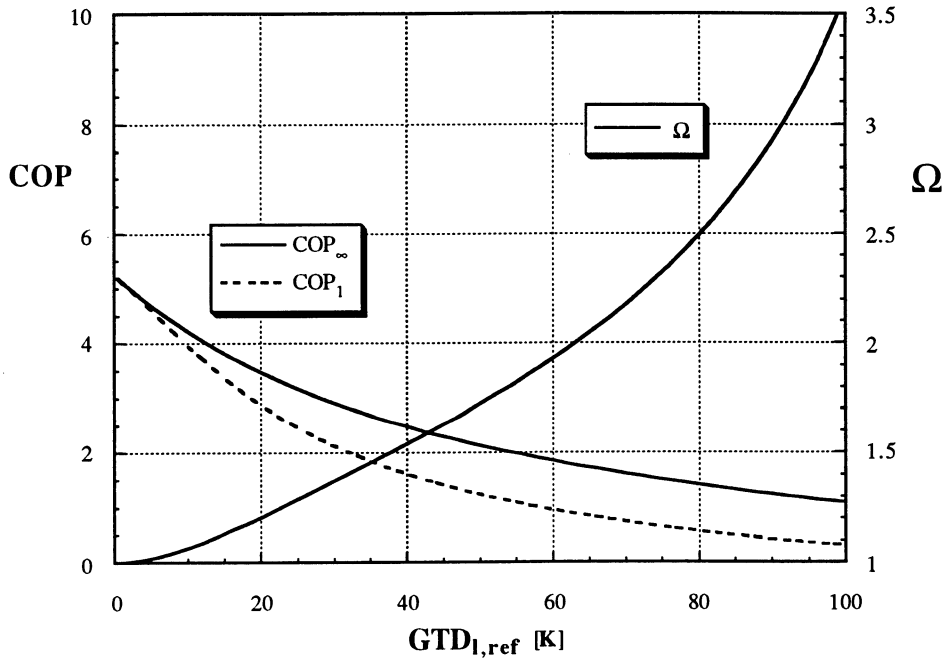

Figure 3.4 **COP_∞, COP_1 and potential COP improvement Ω vs. temperature difference $T_{l,in} - T_{l,out}$ with external stream inlet temperature of $T_{L,in} = 273$ K, $T_{H,in} = 293$ K and $UA_L = UA_H = 2$ kW/K, $\dot{C}_L = \dot{C}_H = 1$ kW/K**

3.2.2.2 Influence of Cooling Load

The variation of $GTD_{l,refr}$ at constant heat capacitance rates causes also a variation of the cooling load, $GTD_{l,refr} \sim \dot{Q}_L$. Hence refrigeration systems of very different sizes have been compared in section 3.2.2.1. The cooling capacity changed from

$\dot{Q}_L > 0$ to $\dot{Q}_L = 100$ kW. In Figure 3.5 is the influence of $\dot{Q}_L$ on the COP for a refrigeration cycle operating at different external high heat capacitance rates $\dot{C}_H$ shown. The COP decreases very quickly with an increasing cooling load. An increase of $\dot{C}_H$ at constant $\dot{C}_L$ certainly helps the system, but does not change the tendency.

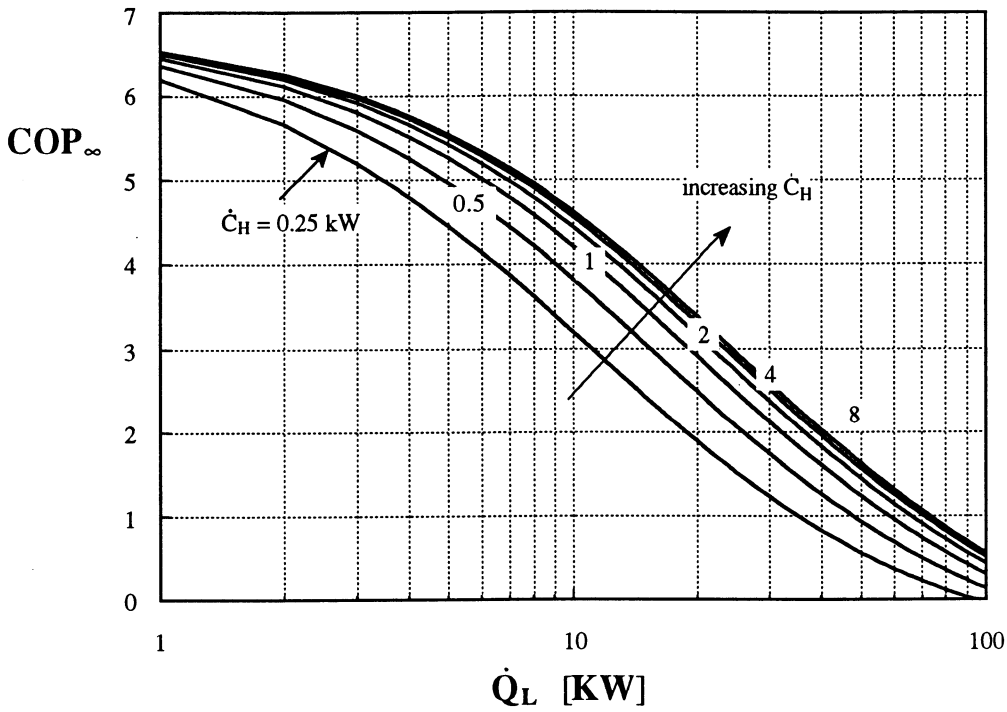

Figure 3.5 COP_∞ vs. cooling capacity $\dot{Q}_L$ with external stream inlet temperatures of $T_{L,in} = 273$ K, $T_{H,in} = 313$ K and $UA_L = UA_H = 2$ kW/K, $\dot{C}_L = 1$ kW/K

An accompanying plot for the potential performance increase Ω is given in Figure 3.6. It indicates that Ω increases very rapidly for large cooling loads $\dot{Q}_L$. On the one hand, large Ω may be obtained for large $\dot{Q}_L$, but on the other hand would such a refrigeration system run at a low COP.

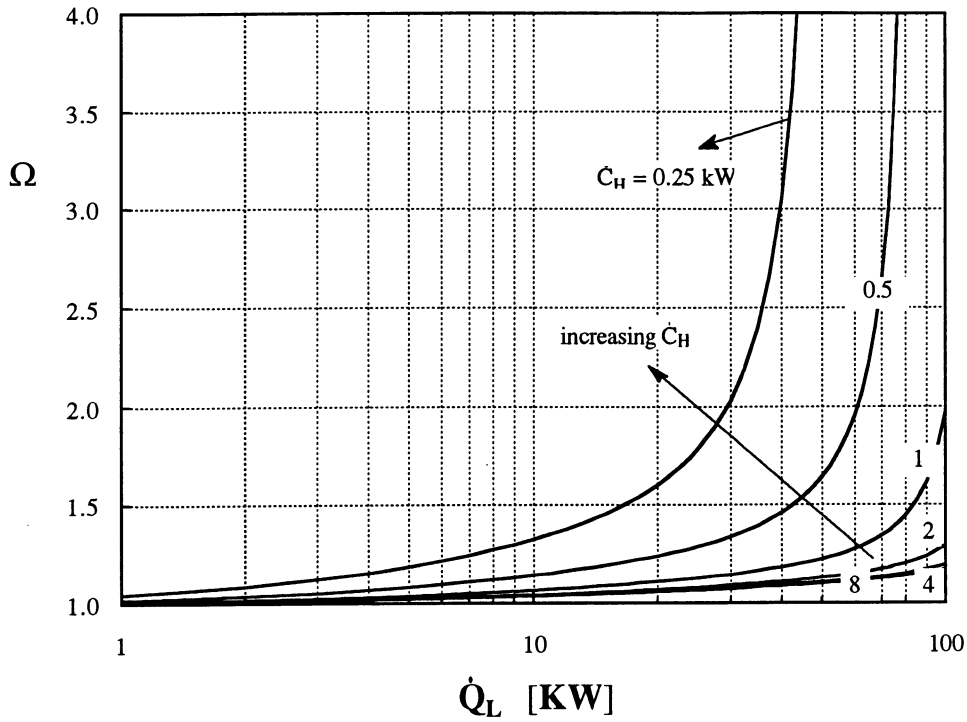

Figure 3.6 **Ω vs. cooling capacity $\dot{Q}_L$ with external stream inlet temperatures of $T_{L,in} = 273$ K, $T_{H,in} = 313$ K , $UA_L = UA_H = 2$ kW/K, $\dot{C}_L = 1$ kW/K**

3.2.2.3 Gliding Temperature Difference $GTD_{l,refr}$ at constant Cooling Load

The $GTD_{l,refr}$ can be varied at a constant $\dot{Q}_L$ by a variation of the heat capacitance rate $\dot{C}_L$. Figure 3.7 shows the same tendency as these indicated by Figure 3.3, but the potential improvement Ω and the COP_∞ are larger. For a gliding temperature difference of $GTD_{l,refr} = 20$ K is a COP of $COP_\infty = 3.7$ and a Ω of $\Omega = 1.18$ (18%) obtained. Ω increases more rapidly and the COP levels off slower than in the case of non-constant cooling capacity.

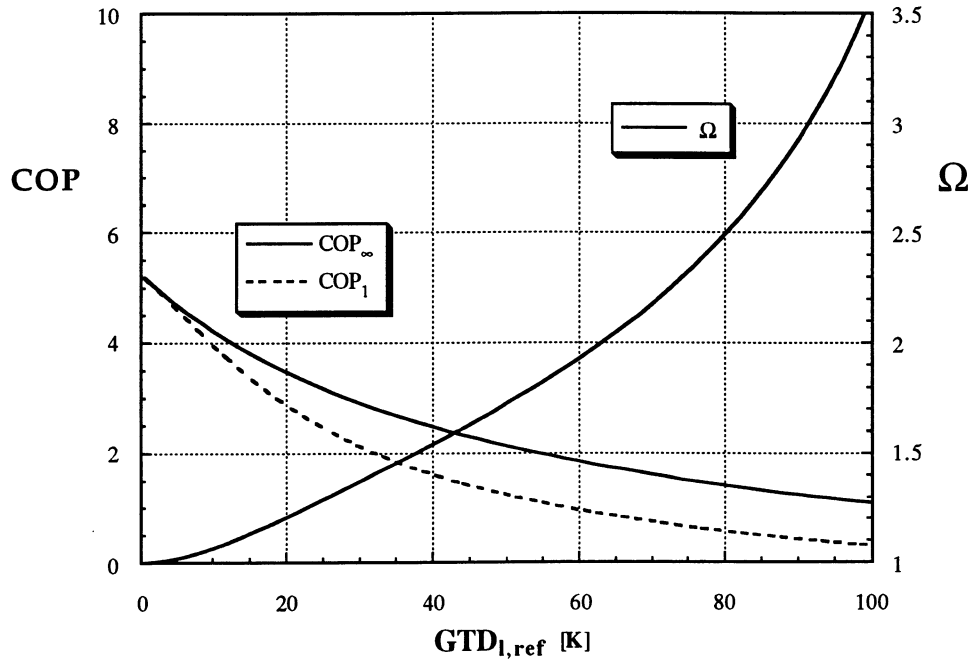

Figure 3.7 **COP_∞, COP_l and potential COP improvement Ω vs. temperature difference $T_{l,in} - T_{l,out}$ with external stream inlet temperature of $T_{L,in} = 273$ K, $T_{H,in} = 313$ K and $UA_L = UA_H = 2$ kW/K, $\dot{Q}_L = 10$ kW, $\dot{C}_L = 1$ kW/K**

A decrease of $T_{H,in}$ from $T_{H,in} = 313$ K to $T_{H,in} = 293$ K yields to the same tendency as before. The COP and Ω increases become even more significant as seen in Figure 3.8. At a $GTD_{l,refr}$ of $GTD_{l,refr} = 20$ K is now a COP of $COP_\infty = 4.9$ and an Ω of $\Omega = 1.28$ (28%) obtained.

The potential performance improvement Ω becomes more significant with increasing gliding temperature differences $GTD_{l,refr}$, but the COP itself decreases. Ω alone does not provide sufficient information about the performance of the system.

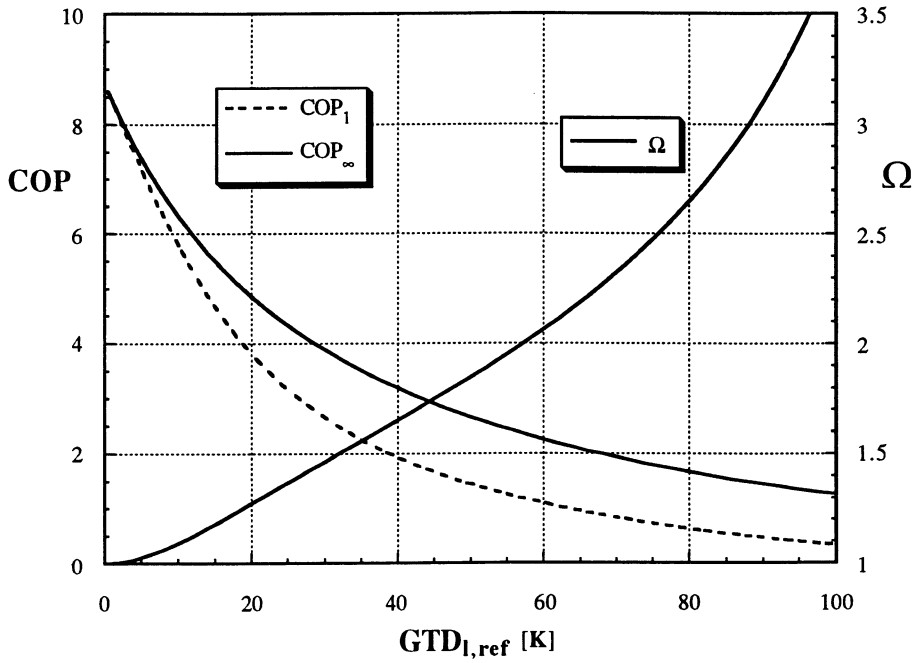

Figure 3.8 **COP_∞, COP_l and potential COP improvement Ω vs. temperature difference $T_{l,in} - T_{l,out}$ with external stream inlet temperature of $T_{L,in} = 273$ K, $T_{H,in} = 293$ K and $UA_L = UA_H = 2$ kW/K, $\dot{Q}_L = 10$ kW, $\dot{C}_L = 1$ kW/K**

3.2.3 INFLUENCE OF TOTAL HEAT EXCHANGER CONDUCTANCES

The next investigation is devoted to the question how significant the potential performance increase Ω is for different total heat exchanger conductances. The performance of a refrigeration system which has to meet two different loads, $\dot{Q}_L = 10$ kW and $\dot{Q}_L = 50$ kW is shown in Figure 3.9. The COP increases with increasing UA_{total} and also does the potential performance improvement Ω. The refrigeration system which has to meet the smaller cooling load $\dot{Q}_L$ achieves the larger COP and also the smaller Ω. The larger the cooling load $\dot{Q}_L$ and the larger the total heat exchanger size UA_{total}, the larger the potential performance improvement Ω.

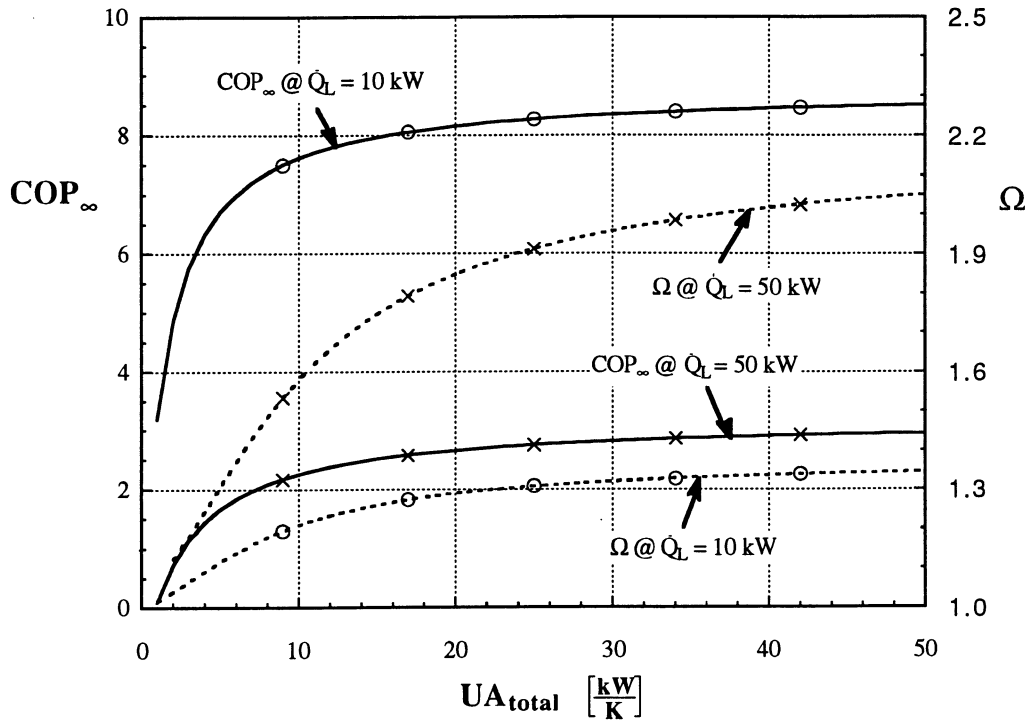

Figure 3.9 **COP_∞ and potential COP improvement Ω vs. UA_{total} with external stream inlet temperature of $T_{L,in} = 273$ K, $T_{H,in} = 293$ K and $UA_L = UA_H$, $\dot{C}_L = \dot{C}_H = 1$ kW/K, $\dot{Q}_L$ =10 kW and $\dot{Q}_L$ =50 kW**

3.2.4 INFLUENCE OF TOTAL HEAT CAPACITANCE RATES

It is interesting to consider the influence of the total external heat capacitance rate $\dot{C}_{ext,total} = \dot{C}_{L,ext} + \dot{C}_{H,ext}$ on the COP and Ω. An increase of $\dot{C}_{ext,total}$ results in a smaller $GTD_{l,refr}$, which reduces the potential COP improvement but increases the COP. The heat transfer approaches an isothermal process for $\dot{C}_{ext,total} \rightarrow \infty$ and hence there are no further improvements possible in operating the cycle with a working fluid which undergoes non-isothermal heat transfer (COP_∞) instead of a working fluid undergoing isothermal heat transfer.

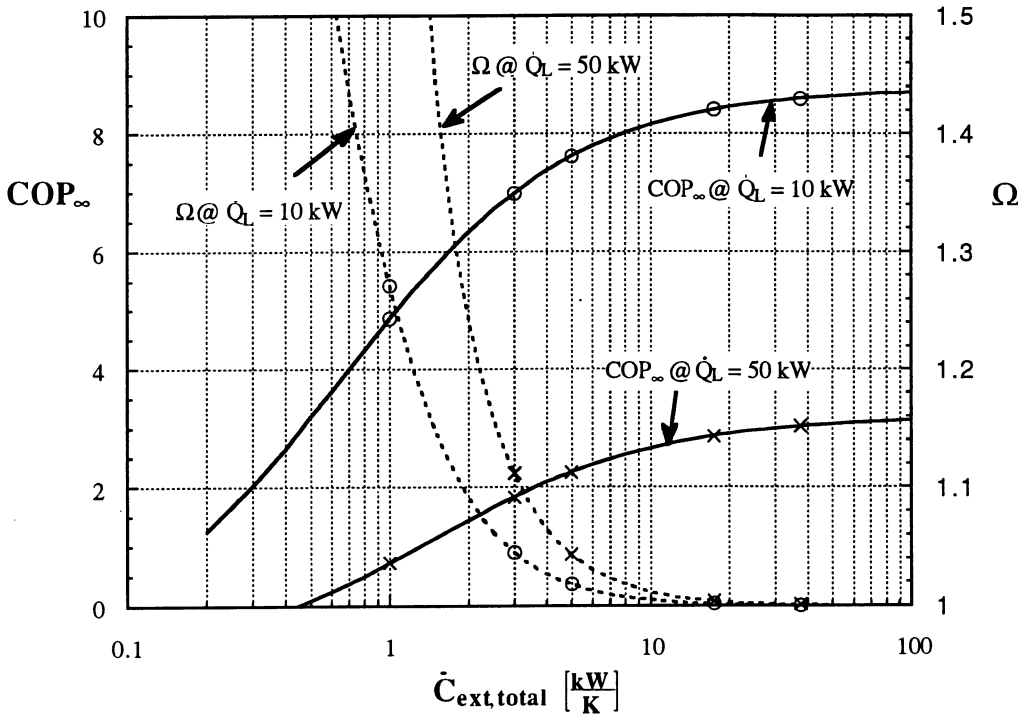

Figure 3.10 **COP_∞, and potential COP improvement Ω vs. $\dot{C}_{ext,total}$ with external stream inlet temperature of $T_{L,in} = 273$ K, $T_{H,in} = 293$ K and $UA_L = UA_H = 2$ kW/K, $\dot{C}_L = \dot{C}_H$, $\dot{Q}_L$ =10 kW or $\dot{Q}_L$ =50 kW**

3.2.5 OPTIMUM REFRIGERANT HEAT CAPACITANCE RATE

Up to now is it assumed in this chapter that the heat capacitance rates of the streams in each heat exchanger ($\dot{C}_{L,ext} = \dot{C}_{l,refr}$ and $\dot{C}_{H,ext} = \dot{C}_{h,refr}$) are equal, whereas the heat capacitance rates of the external streams in the different heat exchangers have not been necessarily the same ($\dot{C}_L \neq \dot{C}_H$). Consequently as a result of this assumption are the refrigerant heat capacitance rates in the different heat exchangers different. It is surely not easy to find a fluid with these required properties. It is now time to look at a refrigerant

with constant heat capacitance rate $\dot{C}_{refr}$ in order to find the corresponding optimum heat capacitance rate of the refrigerant for arbitrary given external heat capacitance rates. The optimum heat capacitance rate of the refrigerant $\dot{C}_{refr,opt}$ is shown in Figure 3.11 and plotted versus the external heat capacitance ratios $\dot{C}_H/\dot{C}_L$.

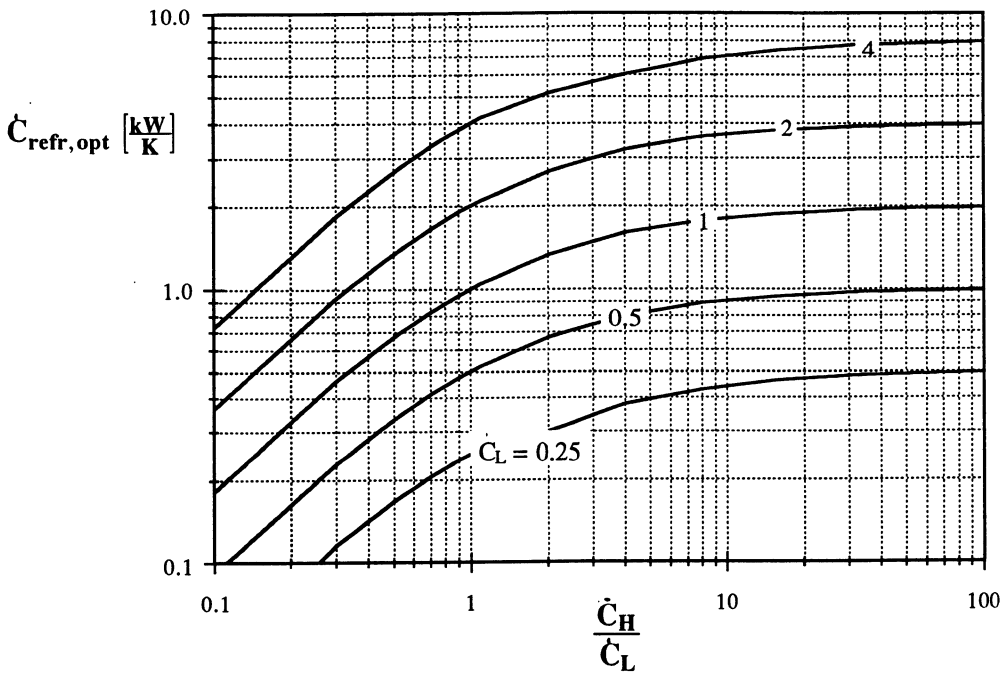

Figure 3.11 Optimum refrigerant heat capacitance rate $\dot{C}_{refr,opt}$ vs. external heat capacitance rate ratio $\dot{C}_H/\dot{C}_L$ for different fixed $\dot{C}_L$ and $\dot{U}A_L = \dot{U}A_H$

The low heat capacitance rate $\dot{C}_L$ is fixed at different values for each curve in Figure 3.11. The heat exchanger conductance of the low- and high-temperature heat exchanger are equal, $UA_L = UA_H$. All curves level off to a constant $\dot{C}_{refr,opt}$, which is always twice as much as the constant $\dot{C}_L$. These values represent the optimum $\dot{C}_{refr}$ for an refrigeration cycle with isothermal heat rejection.

The optimum $\dot{C}_{refr,opt}$ does not change for different inlet temperatures of the external stream, different total heat exchanger conductances or different cooling loads. The optimum heat capacitance rate of the refrigerant $\dot{C}_{refr,opt}$ is solely dependent on the two heat capacitance rates of the external streams. The $\dot{C}_{refr,opt}$ for the optimum heat exchanger conductance allocation $UA_L = UA_H$ may be expressed as

$$\frac{1}{\dot{C}_{refr,opt}} = \frac{1}{2}\left(\frac{1}{\dot{C}_L} + \frac{1}{\dot{C}_H}\right) \tag{3.31.a}$$

$$\dot{C}_{refr,opt} = 2\left(\frac{\dot{C}_L \dot{C}_H}{\dot{C}_L + \dot{C}_H}\right) \tag{3.31.b}$$

3.3 COMPARISON OF THE NUMERICAL AND ANALYTICAL MODEL

3.3.1 COP OF THE DIFFERENT MODELS

The coefficients of performances calculated with the different models are compared. The four most interesting COP's are:

- The COP_1 calculated from the numerical model with one single Carnot Cycle
- The COP_{10} calculated from the numerical model with 10 Carnot cycle in sequence
- The COP_∞ calculated from the analytical model with fluids of the same heat capacitance rates in each heat exchanger ($\dot{C}_{L,ext} = \dot{C}_{l,refr}$ & $\dot{C}_{H,ext} = \dot{C}_{h,refr}$)
- The COP^*_∞ calculated from the analytical model with a constant heat capacitance rate $\dot{C}_{refr}$ of the refrigerant

In Figures 3.12 to 3.15, plots of COP^*_∞ vs. a constant heat capacitance rate of the refrigerant $\dot{C}_{refr}$ are shown. The heat capacitance rates of the external streams are varied for the different figures; all other boundary conditions are constant. In order to note the similarities and the differences, the corresponding COP_1 , COP_{10} and COP_∞ are plotted as horizontal lines. The value of the optimized $\dot{C}_{refr}$ is indicated in each figure. This value is calculated with the optimization process in EES and gives the same result as Equation (3.31.a).

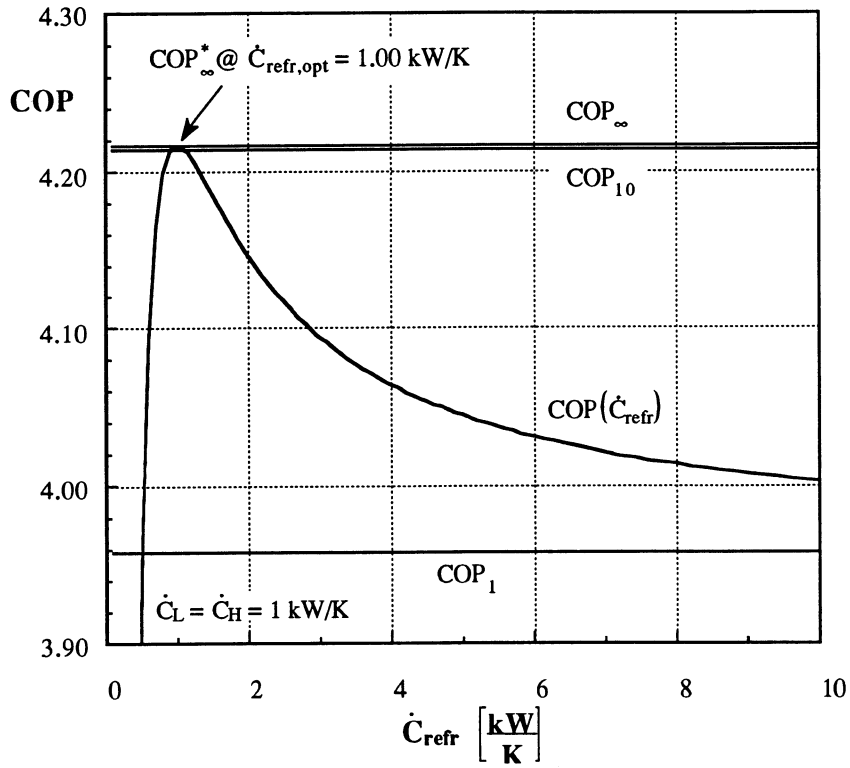

Figure 3.12 COP vs. heat constant capacitance rate of the refrigerant $\dot{C}_{refr}$ for $T_{L,in} = 273$ K, $T_{H,in} = 313$ K, $UA_L = UA_H = 2$ kW/K, $\dot{C}_L = \dot{C}_H = 1$ kW/K

COP^*_∞ levels off to the COP_1 for increasing heat capacitance rate $\dot{C}_{refr}$. The heat transfer is isothermal for $\dot{C}_{refr} \rightarrow \infty$ and is identical to a Carnot cycle process. The heat

capacitance rate $\dot{C}_{refr}$ should be at least $\dot{C}_{refr} \geq \dot{C}_L$. Otherwise the COP^*_∞ may drop rapidly.

An increase of the high external heat capacitance to $\dot{C}_H = 4$ kW/K results in a higher COP, but COP^*_∞ can not be higher than the value of the COP_∞. The optimum COP would be obtained for $\dot{C}_H = \dot{C}_{h,refr} = 4$ kW/K and $\dot{C}_L = \dot{C}_{l,refr} = 1$ kW/K$_L$ which would lead to the optimum temperature matching where the gliding temperature differences are equal, $GTD_{ext} = GTD_{refr}$. It is not possible to meet both conditions for a refrigerant with a constant heat capacitance rate throughout the whole refrigeration process.

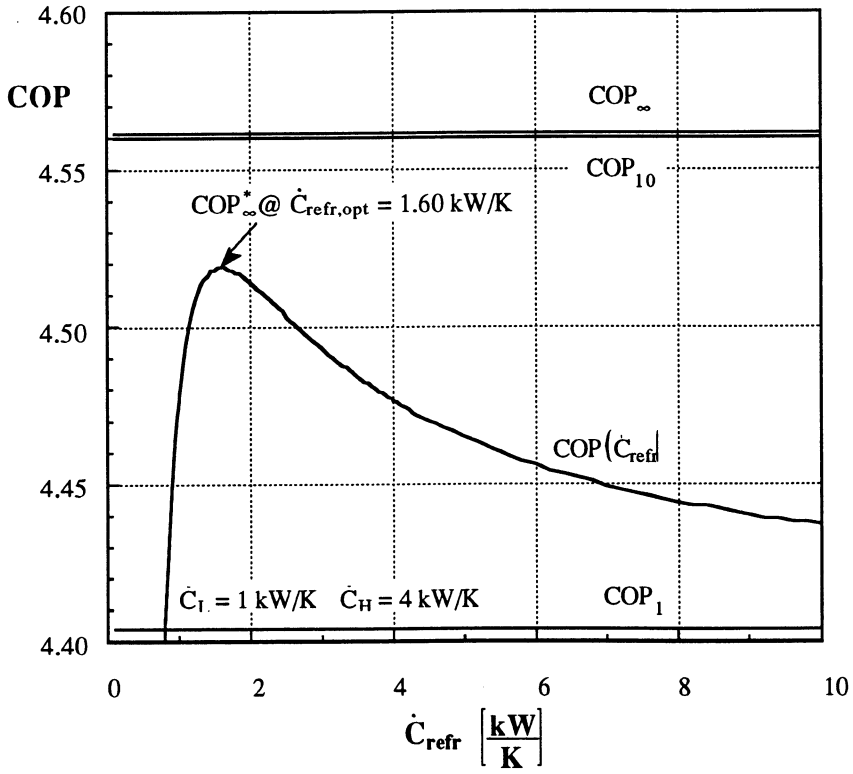

Figure 3.13 **COP vs. heat constant capacitance rate of the refrigerant $\dot{C}_{refr}$ for $T_{L,in} = 273$ K, $T_{H,in} = 313$ K, $UA_L = UA_H = 2$ kW/K $\dot{C}_L = 1$ kW/K and $\dot{C}_H = 4$ kW/K**

The corresponding $\dot{C}_{refr,opt}$ is somewhat between the external heat capacitance rates $\dot{C}_L$ and $\dot{C}_H$ and indicated in Figure 3.13. The value is obtained by optimizing the COP with respect to $\dot{C}_{refr}$. This number is identical to the $\dot{C}_{refr,opt}$ obtained with Equation (3.31.a).

The difference between the COP_∞ and COP_∞^* becomes even larger for a further increase of the heat capacitance rate to $\dot{C}_H = 20$ kW/K , as Figure 3.14 shows. The heat rejection becomes virtually isothermal and the optimum $\dot{C}_{refr,opt}$ approaches the number of $\dot{C}_{refr} \rightarrow 2\ \dot{C}_L = 2$ kW/K.

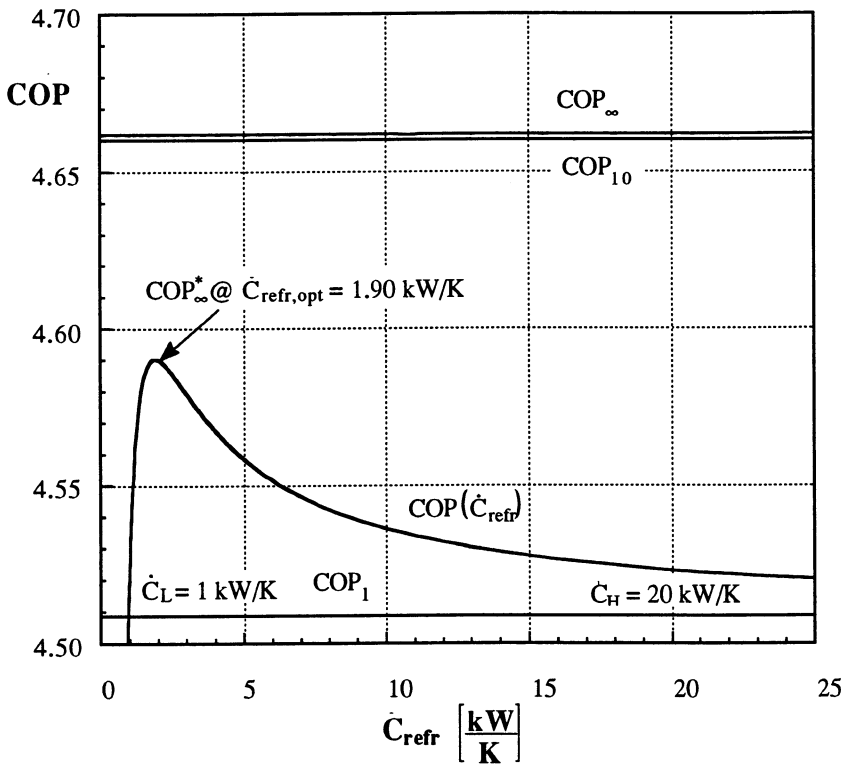

Figure 3.14 COP vs. heat constant capacitance rate of the refrigerant $\dot{C}_{refr}$ for $T_{L,in} = 273$ K, $T_{H,in} = 313$ K, $UA_L = UA_H = 2$ kW/K $\dot{C}_L = 1$ kW/K and $\dot{C}_H = 20$ kW/K

The same behavior is obtained for a very small heat capacitance rate of $\dot{C}_H = 0.25$ kW/K. The optimized $\dot{C}_{refr,opt}$ is again somewhat between the external heat capacitance rates $\dot{C}_L$ and $\dot{C}_H$ as indicated in Figure 3.15. A deviation of the $\dot{C}_{refr}$ from the $\dot{C}_{refr,opt}$ results in a significant decrease. The heat capacitance rate of the refrigerant should be at least $\dot{C}_{refr} \geq \min(\dot{C}_L, \dot{C}_H)$.

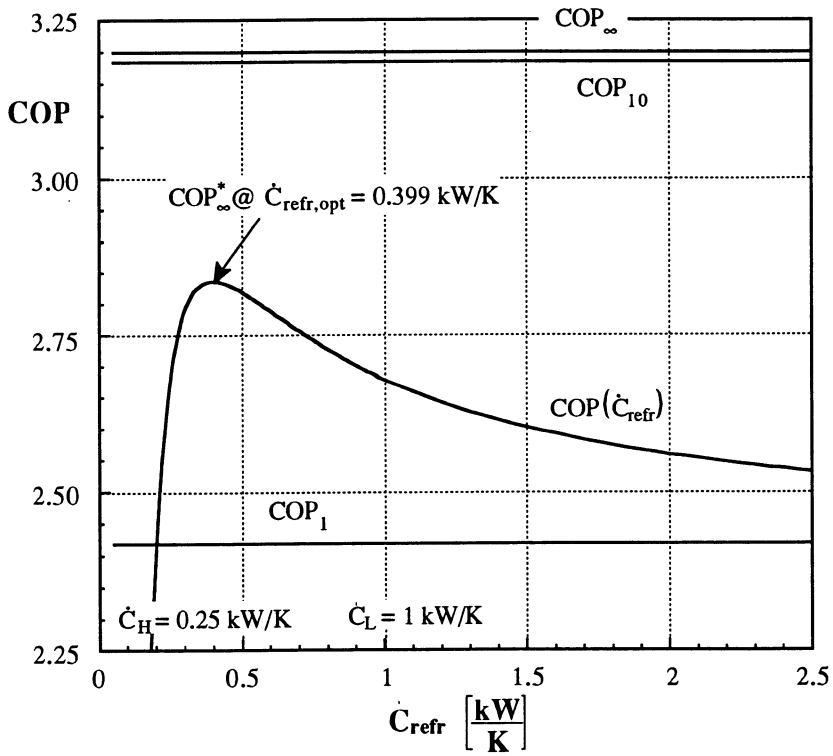

Figure 3.15 **COP vs. heat constant capacitance rate of the refrigerant $\dot{C}_{refr}$ for $T_{L,in} = 273$ K, $T_{H,in} = 313$ K, $UA_L = UA_H = 2$ kW/K $\dot{C}_L = 1$ kW/K and $\dot{C}_H = 0.25$ kW/K**

3.3.2 ACCURACY OF THE NUMERICAL MODEL

In this section is first shown, that the solutions of the numerical and analytical model are nearly identical. Then is the distribution of the total heat exchanger conductance UA_{total} on the two heat exchangers presented.

Some arbitrary conditions have been picked to compare the models in Figure 3.16. The cooling load $\dot{Q}_L$ is changed for the different curves in the Figure and the ratio of COP_n/COP_∞ vs. the incoming external temperature $T_{L,in}$ is shown.

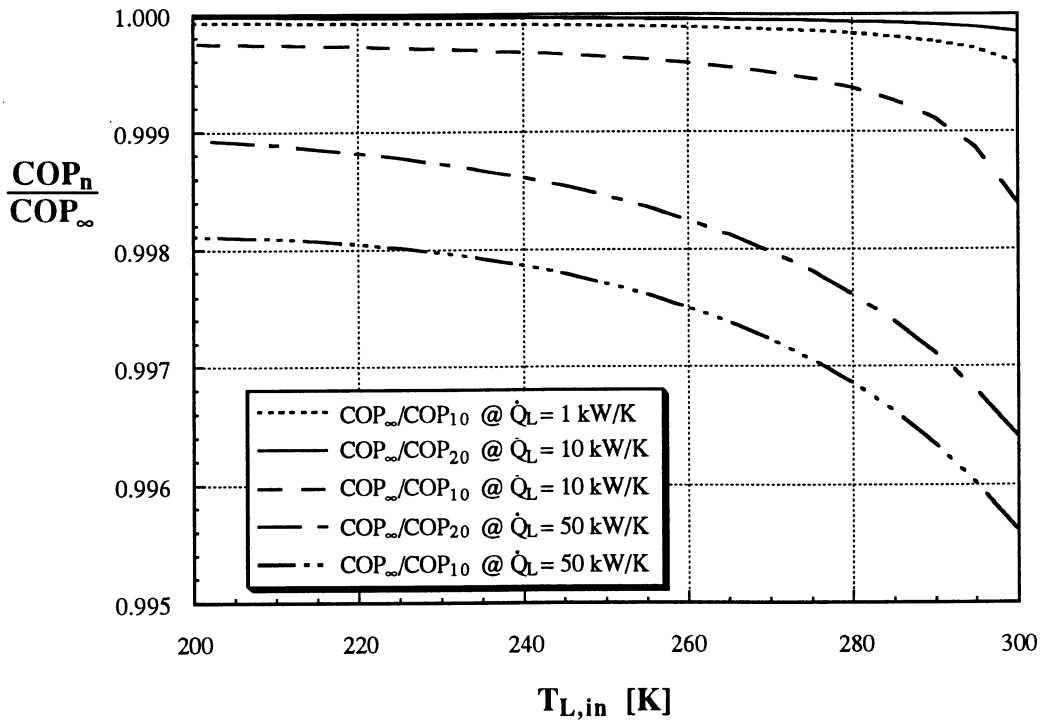

Figure 3.16 **COP_∞/COP_n vs. different low external inlet temperatures $T_{L,in}$ for different cooling loads $\dot{Q}_L$ for $T_{H,in} = 313$ K, $UA_L = 2$ kW/K, $UA_H = 4$ kW/K, $\dot{C}_L = 1$ kW/K and $\dot{C}_H = 5$ kW/K**

The COP's are always nearly identical. A model of 10 Carnot cycles in sequence calculates the COP accurately. The error is less than 0.5% for the system with a cooling

load of $\dot{Q}_L$ = 50 kW/K. For large $\dot{Q}_L$ is the agreement less than for smaller ones. Large $\dot{Q}_L$ leads to a stronger temperature change of the fluids, so that the alignment of several Carnot cycles in sequence to the continuous temperature change of the external stream becomes more difficult. The deviation is still less than 0.5 % for relatively large $\dot{Q}_L$.

The numerical model has the advantage of being able to solve for the temperature distribution of the fluids throughout the heat exchangers and it represents close enough the maximum possible COP. On the other side, it is not possible to specify the heat capacitance rates of the refrigerant. This is the great benefit of the analytical model. Furthermore it offers a single algebraic equation only in terms of external boundary conditions for the determination of the COP.

3.3.3 ALLOCATION OF HEAT EXCHANGER CONDUCTANCE AND HEAT CAPACITANCE RATE FOR AN ISOTHERMAL PROCESS

3.3.3.1 Heat Exchanger Conductance

It is known from previous investigations with the numerical model that the total heat exchanger conductance UA_{total} and total heat capacitance rate should be allocated equally for constant $\dot{C}_{ext,total}$ and UA_{total}. The analytical model leads to the same result as Figure 3.17 indicates. The corresponding COP_1 for an isothermal heat transfer process is also presented. The optimum allocation of the UA_{total} is not equal for the different simulations. As expected, the analytical simulation shows an even allocation of the total heat exchanger conductances, whereas this is not true for the simulation with one Carnot cycle. For this system, an even allocation is only recommended for equal heat capacitance rates of the external stream. Otherwise it is useful to reallocate the UA for a given UA_{total} between the heat exchangers.

As shown in Figure 3.18, the optimum allocation of the UA_{total} depends on the heat capacitance ratio $\dot{C}_H/\dot{C}_L$. For ratios of $\dot{C}_H/\dot{C}_L < 1$ is the optimum allocation shifted to larger UA_L, whereas it is shifted to larger UA_H for $\dot{C}_H/\dot{C}_L > 1$.

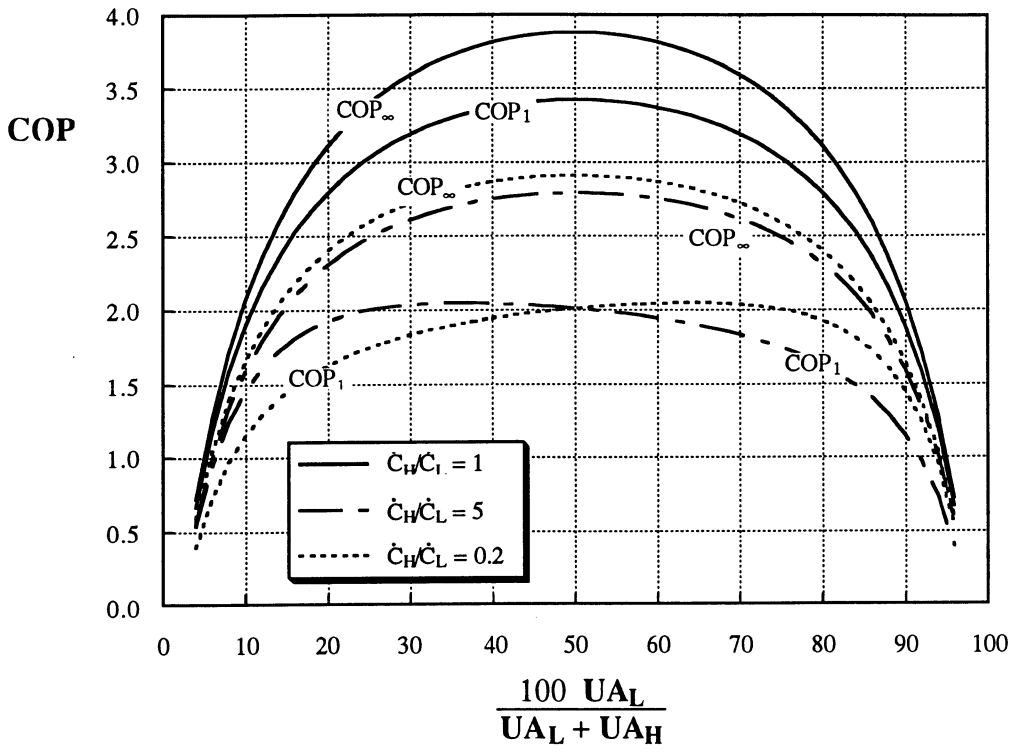

Figure 3.17 **COP_∞ and COP_1 vs. heat exchanger conductances fractions UA_L for different external heat capacitance rates ratios with $\dot{C}_{ext,\,total} = 2$ kW/K, $UA_{total} = 4$ kW/K, $T_{H,in} = 293$ K, $T_{L,in} = 273$ K and $\dot{Q}_L = 20$ kW**

The different curves in the figure refer to different total heat exchanger conductances and it is seen that the larger the total heat exchanger conductance is, the more sensitive is the allocation of the UA_{total}. Nevertheless the optimum COP_1 is always obtained at the same operating point, which are equal heat exchanger conductance and heat capacitance rates.

Hence Figure 3.18 is a little misleading for heat capacitance rates $\dot{C}_H/\dot{C}_L$ far off unity, because such a system would probably not be designed.

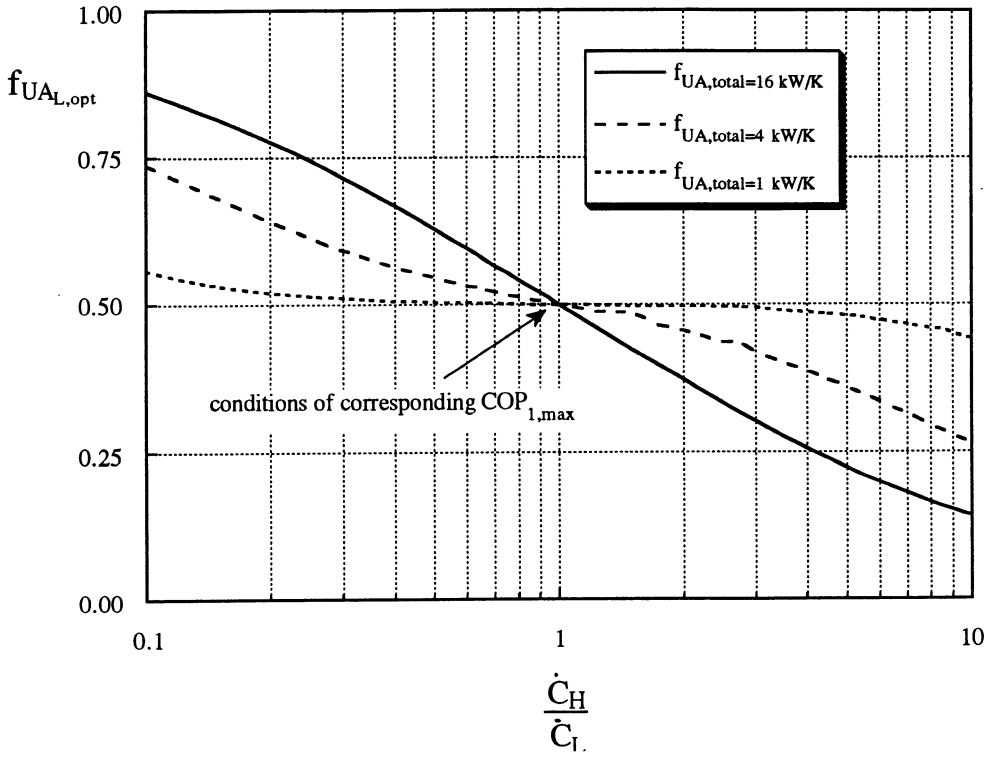

Figure 3.18 Optimum allocation of the total heat exchanger conductance UA_{total} for a single Carnot cycle system vs. external heat capacitance rates ratios $\dot{C}_H/\dot{C}_L$ with $\dot{C}_{ext,\,total} = 2$ kW/K, $T_{H,in} = 293$ K, $T_{L,in} = 273$ K, $\dot{Q}_L = 20$ kW and varying UA_{total}

3.3.3.2 Heat Capacitance Rates

An investigation of the allocation of the total heat capacitance rate $\dot{C}_{ext,total}$ on the two, external streams leads to very similar results to these of section 3.3.3.1. The analytical

simulation results in a even distribution of $\dot{C}_{ext,total}$ on the external streams, whereas this is not always the case for the refrigeration cycle applying a pure refrigerant.

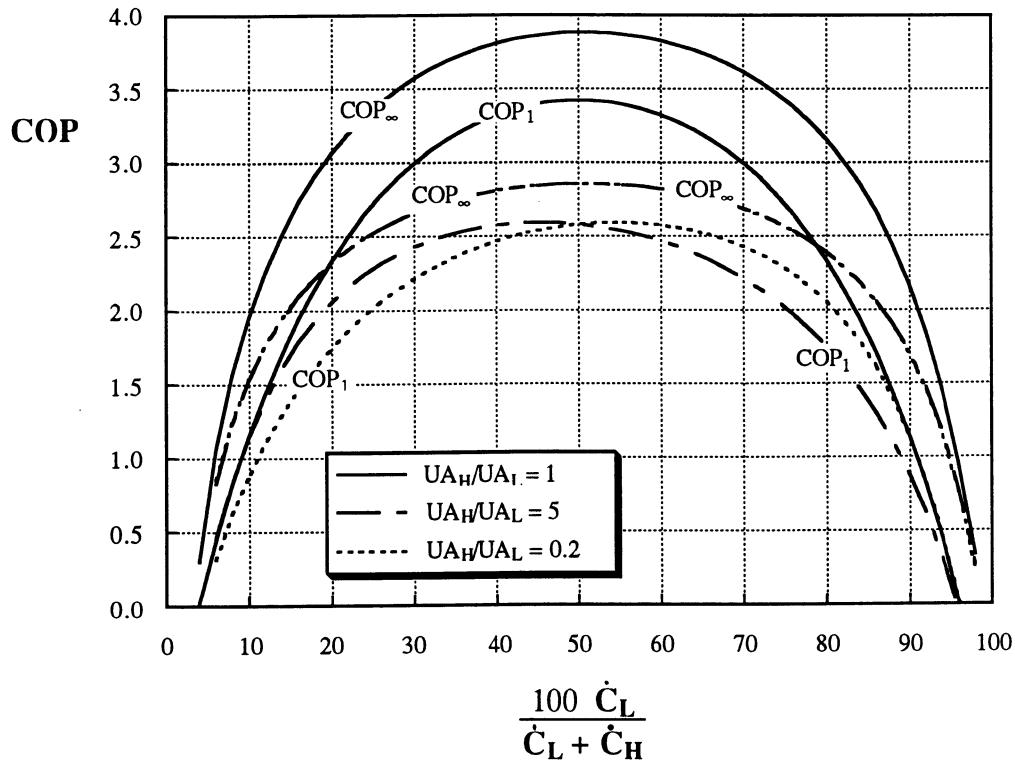

Figure 3.19 **COP_∞ and COP_1 vs. heat capacitance rates fractions $\dot{C}_L$ for different heat exchanger conductance ratios UA_H/UA_L with $\dot{C}_{ext,\,total} = 2$ kW/K, $UA_{total} = 4$ kW/K, $T_{H,in} = 293$ K, $T_{L,in} = 273$ K and $\dot{Q}_L = 20$ kW**

An even allocation of heat capacitance rates is optimum only if the UA_{total} is distributed equal, but the cycle achieves the maximum COP_1 under these operating conditions. For ratios of $UA_H/UA_L < 1$ is the optimum allocation shifted to larger $\dot{C}_L$, whereas it is shifted to larger $\dot{C}_H$ for $UA_H/UA_L > 1$. The allocation of the $\dot{C}_{ext,total}$ for the chosen operating conditions was most sensitive for a total external heat capacitance rate of $\dot{C}_{ext,total}$ = 2.7 kW/K. Nearly 60 % of the total heat capacitance rate should have been

passed through the low temperature heat exchanger at a ratio of $UA_H/UA_L = 0.1$ kW/K. It is less sensitive for other ratios.

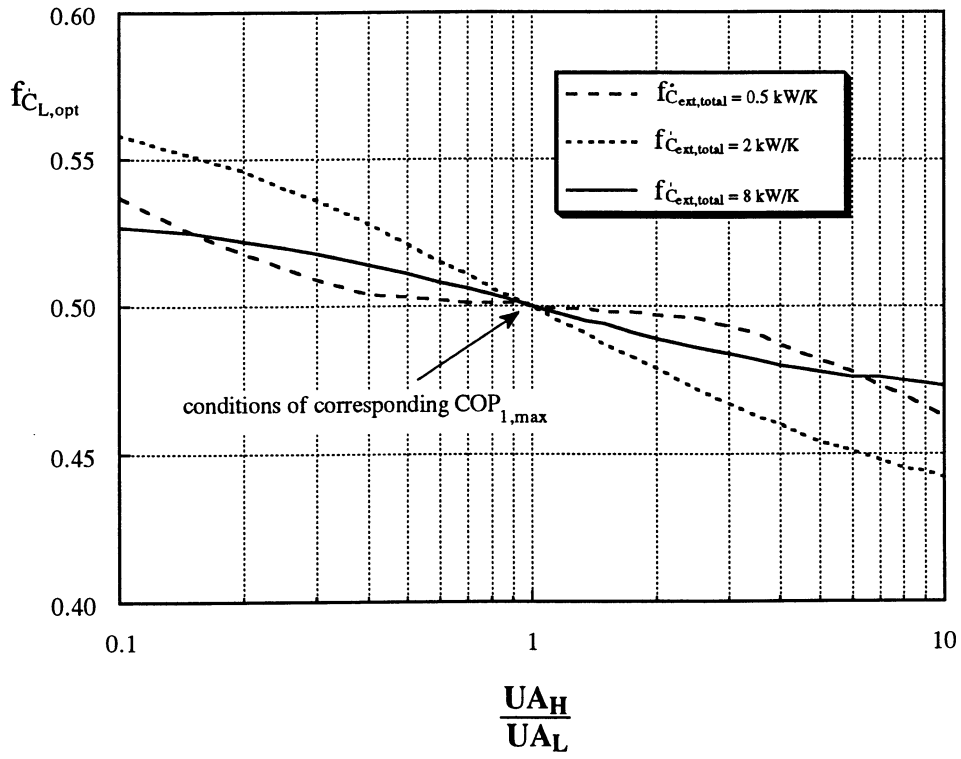

Figure 3.20 Optimum allocation of the total heat capacitance rates $\dot{C}_{ext,total}$ for a single Carnot cycle system vs. external heat exchanger conductance ratios UA_H/UA_L with $UA_{total} = 4$ kW/K, $T_{H,in} = 293$ K, $T_{L,in} = 273$ K, $\dot{Q}_L = 20$ kW and varying $\dot{C}_{ext,total}$

It has been demonstrated, that the optimum allocation of $\dot{C}_{ext,total}$ and UA_{total} for a refrigeration system applying a pure refrigerant should be both equal in order to obtain the optimum COP_1. If one of these parameters is not allocated evenly, then the remaining parameter is also not equally allocated for the corresponding optimum COP_1.

3.4 COMPARISON OF DIFFERENT REFRIGERATION CYCLES

The COP for an arbitrary system in terms of external boundary conditions was developed in chapter 3.1. First are the general Equations (3.28) and (3.29) recalled.

$$COP = \frac{\dot{Q}_L\left[1 + \beta\left(\varepsilon_H \frac{\dot{C}_{H,min}}{\dot{C}_h} - 1\right)\right]}{T_{H,in}\varepsilon_H\dot{C}_{H,min}(\beta - 1) - \dot{Q}_L\left[1 + \beta\left(\varepsilon_H \frac{\dot{C}_{H,min}}{\dot{C}_h} - 1\right)\right]} \tag{3.26}$$

with

$$\beta = \left[\frac{\dot{C}_{L,min}}{\dot{C}_l} \cdot \frac{\dot{Q}_L\,\varepsilon_L}{(T_{L,in}\,\varepsilon_L\,\dot{C}_{L,min} - \dot{Q}_L)} + 1\right]^{\left(\frac{\dot{C}_l}{\dot{C}_h}\right)} \tag{3.27}$$

3.4.1 CARNOT REFRIGERATION CYCLE

The Carnot refrigeration cycle assumes a isothermal heat transfer in the evaporator and condenser. Consequently the heat capacitance rates of the refrigerant are infinite, it is $\dot{C}_L \to \infty$ and $\dot{C}_h \to \infty$. Klein [7] shows that

$$COP = \frac{T_{L,in} - \Delta T}{T_{H,in} - (T_{L,in} - \Delta T)} \tag{1.7}$$

where

$$\Delta T = \dot{Q}_L \frac{\varepsilon_H\dot{C}_H + \varepsilon_L\dot{C}_L}{\varepsilon_H\dot{C}_H\,\varepsilon_{LI}\dot{C}_L} \tag{1.8}$$

3.4.3 BRAYTON REFRIGERATION CYCLE

A constant heat capacitance rate $\dot{C}_{refr} = \dot{C}_h = \dot{C}_l$ for the refrigerant is assumed. The Equations (3.28) and (3.29) reduce then to

$$COP = \frac{T_{L,in} - \Delta T'}{T_{H,in} - (T_{L,in} - \Delta T')} \tag{3.32}$$

where

$$\Delta T' = \dot{Q}_L \frac{\varepsilon_H \dot{C}_{H,min}\, \dot{C}_{refr} + \varepsilon_L \dot{C}_{L,min}\, \dot{C}_{refr} - \varepsilon_L \dot{C}_{L,min}\, \varepsilon_H \dot{C}_{H,min}}{\varepsilon_H \dot{C}_{H,min}\, \varepsilon_L \dot{C}_{L,min}\, \dot{C}_{refr}} \tag{3.33}$$

This equation holds for the ideal Brayton refrigeration cycle. The heat exchanger effectiveness factors are defined by the Equations (3.15) and (3.16). The temperature difference $\Delta T'$ is a measurement of the performance of the system. The smaller $\Delta T'$, the larger the COP.

3.4.4 OPTIMUM CYCLE

A expression for a partially optimized COP with equal heat capacitance rates in each heat exchanger was given in the Equations (4.30) and (4.31).

It was shown, that the optimum cycle is obtained for equal allocation of the total heat exchanger conductance, equal allocation of the external heat capacitance rates, and equal heat capacitance rate of the refrigerant and external stream in each heat exchanger. The COP for this cycle may be expressed as

$$COP = \dot{Q}_L \frac{\left[1 + \lambda'(\varepsilon\text{-}1)\right]}{T_{H,in}\,\varepsilon\,\dot{C}\left(\lambda' - 1\right) - \dot{Q}_L\left[1 + \lambda'(\varepsilon\text{-}1)\right]} \tag{3.34}$$

where λ' is defined as

$$\lambda' = \left[\frac{\dot{Q}_L\,\varepsilon}{\left(T_{L,in}\,\varepsilon\,\dot{C} - \dot{Q}_L\right)} + 1\right] \tag{3.35}$$

The heat exchanger effectiveness and heat capacitance rates in the Equations (3.34) and (3.35) are $\varepsilon = \varepsilon_L = \varepsilon_H$ (defined by Equation (3.15)) and $\dot{C} = \dot{C}_L = \dot{C}_H$, respectively.

3.5 CHAPTER SUMMARY

A analytical simulation model was developed in this chapter. It is possible to specify different heat capacitance rates of the refrigerant in the low and high-temperature heat exchanger. However, the analytical model does not provide the temperature profile of the refrigerant, as for the numerical model.

Important aspects and design guidelines for the optimum cycle are:

- It was shown, that very high Ω may be obtained, but the corresponding COP was always very small for unreasonable high Ω.
- The potential improvement of the performance Ω increases significantly with increasing gliding temperature differences GTD_{refr}.
- The Ω increases with increasing total heat exchanger conductance UA_{total}.
- The Ω decreases with increasing total heat capacitance rates $\dot{C}_{ext,total}$.

- The UA_{total} should be allocated evenly on the two heat exchangers, independent on $\dot{C}_H$, $\dot{C}_L$, $T_{H,in}$, $T_{L,in}$, $\dot{Q}_L$
- The $\dot{C}_{ext,total}$ should be allocated evenly on the two external heat capacitance rates independent on UA_H, UA_L, $T_{H,in}$, $T_{L,in}$, $\dot{Q}_L$.
- The COP does not vary significantly for moderate deviations of the optimum distribution of UA_{total} and $\dot{C}_{ext,total}$.
- The heat capacitance rate of a refrigerant with constant heat capacitance rate $\dot{C}_{refr} = \dot{C}_h = \dot{C}_l$ should be at least $\dot{C}_{refr} > \min(\dot{C}_L, \dot{C}_H)$.

Design guideline for a refrigeration system undergoing iso-thermal heat transfer.

- The UA_{total} and $\dot{C}_{ext,total}$ should be also for this system allocated evenly for the two heat exchangers.
- The total heat exchanger conductance should not be allocated evenly if $\frac{UA_H}{UA_L} \neq 1$ for $\dot{C}_H \neq \dot{C}_L$
- The total heat capacitance rate should not be allocated evenly if $\frac{\dot{C}_H}{\dot{C}_L} \neq 1$ for $UA_H \neq UA_L$

CHAPTER
FOUR

NARMs IN A STANDARD VAPOR COMPRESSION CYCLE

In this chapter, a realistic simulation of a standard vapor compression cycle is reported. A simulation program, Cycle11 [14,16,17,18] is used to investigate the performance of a specified refrigeration system. The use of a non-azeotropic mixture (NARM), as an option to improve the performance of the system is investigated and compared to a pure refrigerant. The optimum possible COP_∞ for this system is determined with the Analytical Model from Chapter 3 and compared to the COP obtained with the simulation from Cycle11.

4.1 DESCRIPTION OF NARM

4.1.1. PHASE CHANGE PROCESS OF A NARM

A non-azeotropic refrigerant mixture (NARM) behaves differently from a pure refrigerant or an azeotropic mixture. It may be described most easily as a fluid which changes its composition in the liquid and vapor phases during boiling or condensation.

NARMs have different vapor and liquid lines as shown in Figure 4.1. This results in a different composition of the refrigerant in the boiling or condensing liquid phase and the corresponding vapor phase. For example, a binary NARM with a mole fraction of f_{A0} and a temperature of T_1 is heated isobarically to the liquid line. The refrigerant with the lower boiling point will preferentially evaporate first at the temperature T_2.

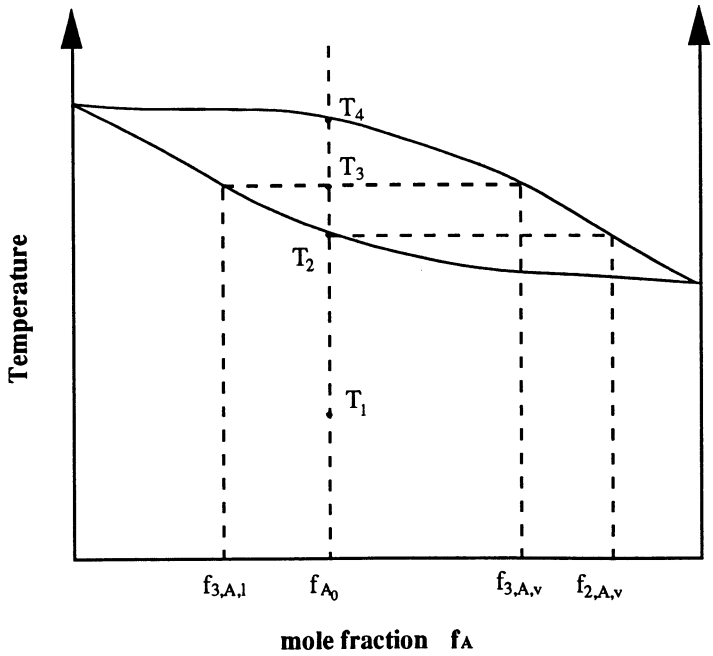

Figure 4.1 Evaporation process of a binary NARM in a Temperature-Concentration diagram

The composition of the vapor phase in equilibrium with the liquid is $f_{2,A,v}$ and the composition of the remaining liquid is f_A. The mole fraction f_A of the less volatile component A is larger than the initial mole fraction f_{AO}. Consequently the boiling temperature of the remaining liquid shifts to the component with the higher boiling temperature for instance to the temperature T_3. The composition of the liquid and vapor phase at that state is $f_{3,A,l}$ and $f_{3,A,v}$, respectively. At the temperature T_4 the NARM consists only of saturated vapor with the same composition f_{A0} as at the temperature T_1.

Hence, the isobaric evaporation and condensation occur over a temperature range. This temperature range is strongly dependent on the mixture components and the composition. The choice of the mixture composition offers an additional degree of freedom which may be used as a design parameter. For instance, a NARM consisting of two components of very different boiling temperature and with a suitable initial composition will result in a mixture with a large temperature range.

4.1.2 COMPONENTS FOR A NARM

The use of any fully halogenated CFCs is to avoided. Refrigerants like R11, R12, R113, R114 and R115 are in the Montreal Protocol [23] classified as group 1 chemicals, which have to be replaced. Other aspects like low toxicity, non-flammability, chemical and thermal stability, non-aggressive behavior towards design materials and commercial availability should also be taken into account.

4.2 DESCRIPTION OF THE SIMULATION MODEL CYCLE11

The CYCLE11 model was developed by Domanski and McLinden [14,16,17,18] at the National Institute of Standards and Technology. It is able to evaluate the performance of a theoretical standard vapor compression refrigeration cycle. The investigated refrigeration cycle works like the cycle described in section 1.3.1, but with an polytropic compressor efficiency η smaller than unity and it accounts for pressure drops in the condenser and evaporator.

4.2.1 HEAT EXCHANGER MODEL

Counterflow heat exchangers are assumed in the evaporator and condenser. The performance of the heat exchangers is specified in terms of an average effective temperature difference ΔT_{hx} between the refrigerant and the external streams and pressure drops in the condenser and evaporator.

Domanski [14] assumes for his model the same overall heat transfer coefficients, U = const, of the heat exchanger and a linear pressure drop Δp in the heat exchangers with respect to the length L, dp/dL = constant. The heat exchanger average temperature difference is defined as

$$\Delta T_{hx} = \frac{\dot{Q}_{hx}}{UA_{hx}} \tag{4.1}$$

Individual temperature differences are considered in different sections of the heat exchangers. The two phase region in the condenser is broken into several individual

sections, because the temperature profile of the refrigerant may be non-linear. Cycle11 splits the two-phase portion of the heat exchangers into a number of sub-sections, computes the log mean temperature of each of them and then evaluates the heat exchanger average effective temperature difference consistently with Equation (4.4). The individual rate equation between the refrigerant and the external stream is

$$\dot{Q}_i = UA_i \Delta T_i \tag{4.2}$$

where A_i and ΔT_i are the individual heat transfer area and temperature difference in each section. The total heat transferred in the heat exchanger is

$$\dot{Q}_{hx} = \sum \dot{Q}_i \tag{4.3}$$

Domanski expressed the average effective temperature difference as a mean weighted with the fraction of heat transferred in the individual sections of the heat exchanger.

$$\frac{1}{T_{hx}} = \frac{1}{\dot{Q}_{hx}} \sum \frac{\dot{Q}_i}{\Delta T_i} \tag{4.4}$$

4.2.2 REFRIGERANT PROPERTIES

Morrison and McLinden [16] developed a routine for the calculation of the refrigerant properties. In that are the refrigerant thermodynamic properties represented by the Carnahan-Starling-DeSantis (CSD) equation of state [17].

$$\frac{pV}{RT} = \frac{1 + y + y^2 - y^3}{(1 - y)^3} - \frac{a}{RT(V + b)} \tag{4.5}$$

where R is the universal gas constant, T is the fluid temperature, V is the molar volume of the mixture and p is the pressure. The values of the parameter a and b are strong functions of the mixture composition and the temperature. The parameter y is defined by

$$y = \frac{b}{4V} \tag{4.6}$$

McLinden [15, 24] showed that the CSD equation of state accurately represents the vapor and liquid phase for CFC refrigerants and their mixtures. This routine was built in Cycle11 by Domanski.

4.3 SIMULATIONS WITH CYCLE11

A vapor compression cycle is considered with the following simplifications. No pressure losses occur in the evaporator and condenser and no heat and pressure losses occur in the manifold. The electric efficiency of the compressor is assumed to be unity.

The performance of the system is investigated following this procedure:

1. Specify the initial operating conditions, assuming arbitrary heat exchanger conductance UA allocation on the condenser and evaporator
2. Optimize the COP with respect to the mole fraction f_{R22}

3. Match the gliding temperature differences GTD_{evap} to $GTD_{L,ext}$ and GTD_{cond} to $GTD_{H,ext}$ in the evaporator and condenser, respectively
4. Optimize the COP with respect to the UA allocation

4.3.1 BASE CASE SYSTEM

The initial operating conditions are given in table 4.1. The chosen numbers are similar to a small refrigeration application like a household refrigerator.

Electric motor efficiency	1
Polytropic efficiency	0.5/ 0.7/ 1.0
Compressor swept volume [m^3]	0.170
Compressor RPM	1800
External fluid entering condenser [K]	293.1
External fluid exiting condenser [K]	323.1
GTD of the external stream in the condenser [K]	30
UA for condenser [kW/K]	0.35
External fluid entering evaporator [K]	283.1
External fluid exiting evaporator [K[	268.1
GTD of the external stream in the evaporator [K]	15
UA for evaporator [kW/K]	0.25

Table 4.1 Operating conditions for the standard vapor compression cycle

Irreversibilities such as pressure drops in the heat exchangers are not taken into account, because, by far, the largest irreversibilities, besides these generated by the heat transfer, occur in the compressor. The potential improvement of the COP increases with larger GTD_{ext} if the GTD_{refr} of the refrigerant mixture matches the temperature change of the

external streams. The gliding temperature differences of the incoming and outgoing external streams in the heat exchangers $GTD_{L,ext}$ and $GTD_{H,ext}$ are 15 and 30 K, respectively. These GTD's will be varied in section 4.3.5.

A refrigerant mixture of R22/R141b is used to investigate this cycle. The components R22 and R141b are possible replacements for the CFCs.

4.3.2 OPTIMUM COMPOSITION OF THE NARM

Figure 4.3 shows the COP vs. the mole fraction f_{R22} for a refrigeration system operating at the conditions specified in Table 4.1. The different curves refer to different polytropic compressor efficiencies, $\eta = 1.0$, $\eta = 0.7$ and $\eta = 0.5$. The maximum COP is always obtained at a mole fractions of about $f_{R22} \approx 0.1$. All three curves demonstrate the same behavior. The COP obtained for a system employing the pure refrigerant R141b is in every case about twice as high as the COP obtained when pure R22 is employed.

The COP of the NARM might be considered in a first approach as a weighted average of the COPs of the pure components. A composition with a large mole fraction f_{R22}, the refrigerant which leads to a low COP, does not show any improvement of the mixture COP relative to the COP of pure R141b. Otherwise is for a mixture with a small mole fraction f_{R22} a significant improvement of the COP obtained. The COP obtained with such a mixture would always out performance the COP obtained with pure R141b. The increase of the COP is about 16% for the isentropic compressor and about 13% for the systems with the lower polytropic compressor efficiencies.

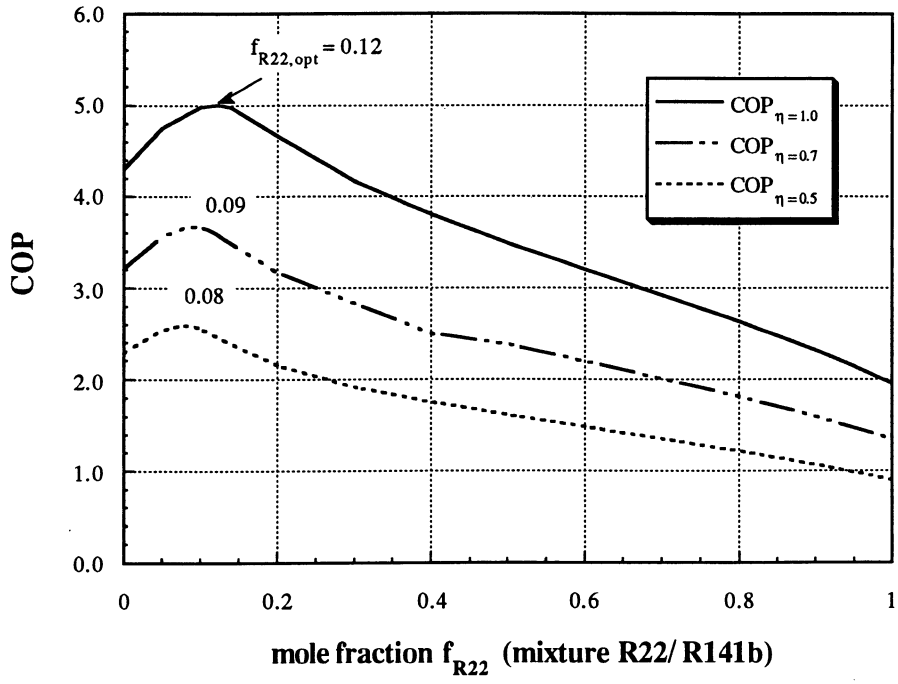

Figure 4.2 COP vs. mole fraction f_{R22} for a refrigerant mixture of R22/R141b and different polytropic compressor efficiencies

It is of interest to know how large the heat transferred in the superheated region in the condenser $\dot{Q}_{sh}$ is and how well the GTD_{refr} of the refrigerant matches the GTD_{ext} of the external streams for different mole fractions.

4.3.3 ACCOMPANYING SUPERHEAT

In Figure 4.4 is the mole fraction f_{R22} vs. the fraction of heat transferred in the condenser in the superheated region f_{sh} shown. The parameter f_{sh} is defined as

$$f_{sh} = \frac{\dot{Q}_{cond} - \dot{Q}_{main}}{\dot{Q}_{cond}} = \frac{\dot{Q}_{sh}}{\dot{Q}_{cond}} \tag{4.1}$$

where $\dot{Q}_{cond}$ is the total heat transferred in the condenser, $\dot{Q}_{main}$ is the heat transferred in the two phase vapor liquid region in the condenser and $\dot{Q}_{sh}$ is the heat transferred in the superheated region in the condenser.

The f_{sh} is small for NARMs at lower mole fractions f_{R22}. The minimum occurs about $f_{sh} = 0.3$. Only about 5% or less of the heat is transferred in the superheated region. Whereas the superheat is large at higher mole fractions f_{R22}. A system using pure R22 as the refrigerant instead of a mixture would run with a f_{sh} of 20% or more.

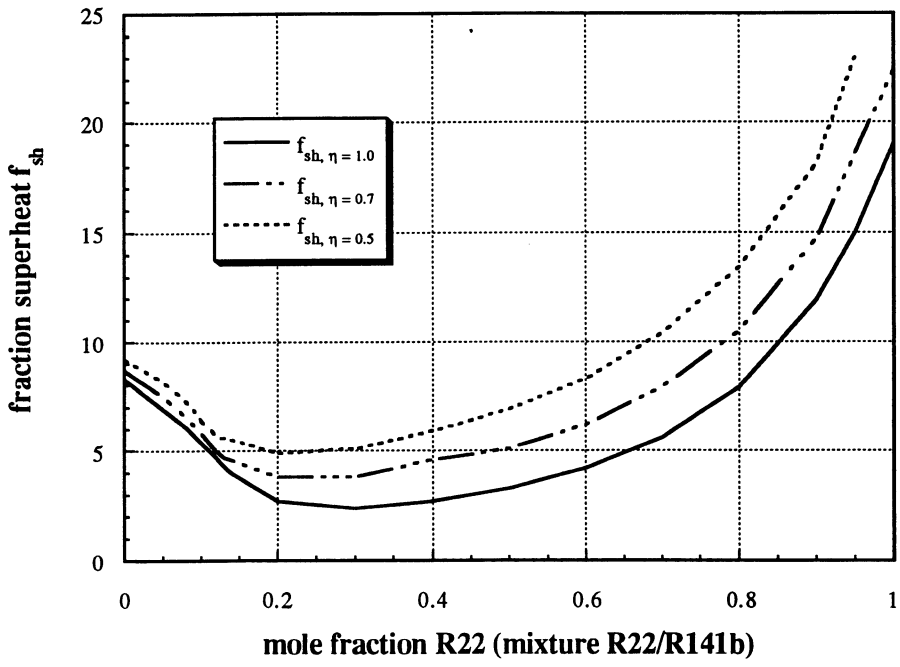

Figure 4.3 **Fraction superheat f_{sh} vs. mole fraction f_{R22} for a refrigerant mixture of R22/ R141b and different polytropic compressor efficiencies**

At these operating conditions is it due to the large superheat not possible that the temperatures of the two streams in the condenser are well matched. A larger condenser superheat is corresponding to a worse temperature matching and should be avoided.

4.3.4 DEVIATION OF THE OPTIMUM TEMPERATURE MATCHING

As described in Chapter 2, the optimum temperature matching is obtained for equal GTDs in the evaporator ($GTD_{L,ext} = GTD_{evap}$) and for equal GTDs in the condenser ($GTD_{H,ext} = GTD_{cond}$).

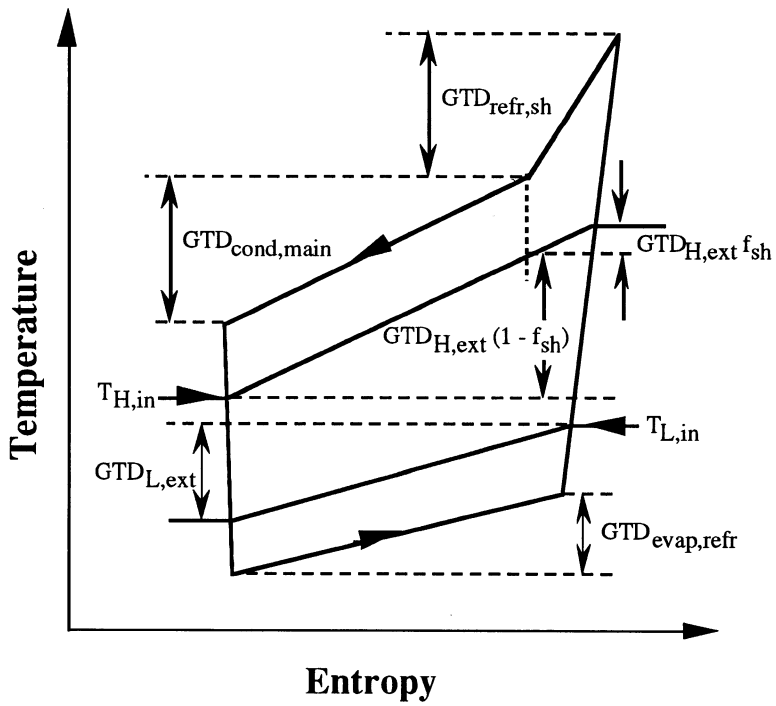

Figure 4.4 Location of gliding temperature differences

A measurement for the deviation of the optimum temperature matching is introduced as ψ:

$$\psi = \Delta GTD_{evap} + \Delta GTD_{cond} \tag{4.7}$$

where the ΔGTD_{evap} is the absolute difference of the GTDs of the refrigerant $GTD_{evap,refr}$ and the external stream $GTD_{L,ext}$ in the evaporator.

$$\Delta GTD_{evap} = || GTD_{evap,refr} | - | GTD_{L,ext} || \tag{4.8}$$

The absolute difference of the GTDs from the refrigerant and the external stream in the condenser ΔGTD_{cond} is broken into two regions. These regions, the liquid vapor phase and superheated region, are weighted by the fraction of heat transferred in each region.

$$\Delta GTD_{cond} = \Delta GTD_{cond,main} (1- f_{sh}) + \Delta GTD_{sh} f_{sh} \tag{4.9}$$

where $\Delta GTD_{cond,main}$ is the difference of the GTD of the refrigerant and the external stream in the two phase region in the condenser and ΔGTD_{sh} is the difference of the GTD in the superheated region respectively. The $\Delta GTD_{cond,main}$ is defined as

$$\Delta GTD_{cond,main} = || GTD_{H,ext} (1-f_{sh}) | - | GTD_{cond,refr,main} || \tag{4.10}$$

where $GTD_{cond,refr,main}$ is the GTD of the refrigerant in the two phase region and $GTD_{H,ext}(1-f_{sh})$ is the GTD of the external stream in the two phase region.

The deviation of the GTDs in the superheated region is determined by

$$\Delta\ GTD_{sh} = || GTD_{refr,sh} | - | GTD_{H,ext}\ f_{sh} || \qquad (4.11)$$

where $GTD_{refr,sh}$ is the GTD of the refrigerant in the superheated region and $GTD_{H,ext}\ f_{sh}$ is the GTD of the external stream in the superheated region.

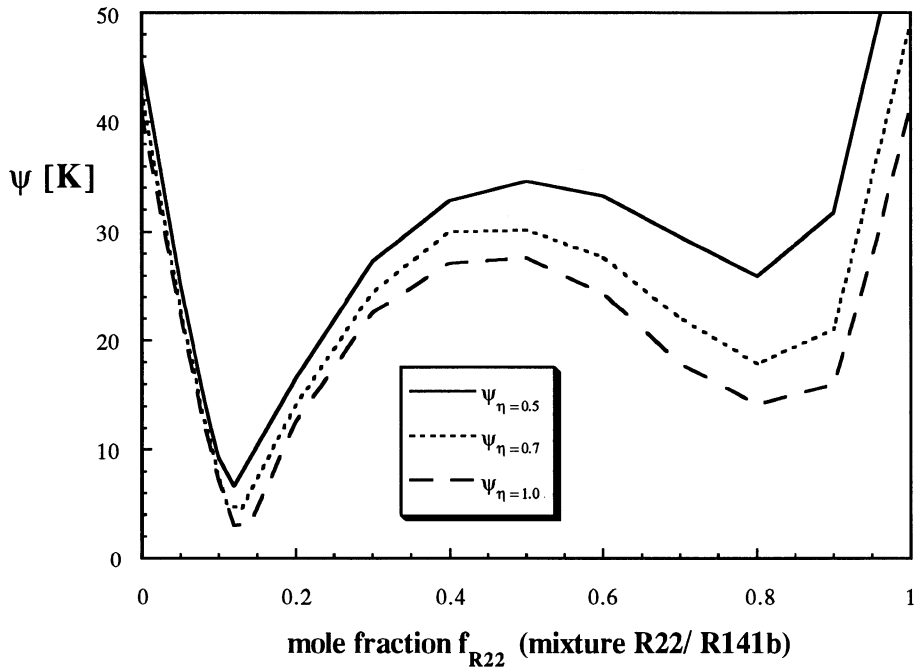

Figure 4.5 Deviation of optimum temperature matching ψ vs. mole fraction f_{R22} for a refrigerant mixture of R22/R141b and different polytropic compressor efficiencies

In Figure 4.5, the deviation of the optimum temperature matching ψ, is plotted as a function of the mole fraction f_{R22} shown. The curves are very similar to each other and two minima at the same mole fractions of about $f_{R22} = 0.12$ and $f_{R22} = 0.8$ are obtained

for each of the systems with the different polytropic compressor efficiencies η. ψ increases with decreasing η, due to the larger superheat occurring in the condenser. The smaller minimum of ψ is obtained for mixtures at a mole fractions of about $f_{R22} = 0.12$. This mole fraction corresponds to the mole fraction which leads to the maximum COP, as indicated in Figure 4.3.

It could be expected that another peak for the COP in Figure 4.3 occurs at a mole fraction of about $f_{R22} = 0.8$. At this conditions is ψ also relatively small and the temperature matching of such a mixtures is relative good. The problem is, that the COP of the pure refrigerant R22 is compared to the R141b very small so that the benefit of the relative well matched GTDs is not sufficient to cause an increase of the COP at that large mole fraction f_{R22}.

An accompanying scaled temperature-entropy diagram of the system at minimum ψ of $\psi = 7$ K is shown in Figure 4.6 for a polytropic compressor efficiency of $\eta = 0.5$. The in- and outlet temperatures of all fluids in the heat exchangers, the saturated vapor temperature of the refrigerant in the condenser and the corresponding entropies are used to present the diagram. The Cycle11 program does not provide information concerning the temperature profiles of the fluids in the heat exchangers so the temperature profile is approximated as straight lines.

The temperature matching of the fluids in each temperature heat exchanger at this operating condition (Table 4.1, $f_{R22} = 0.12$) indicates nearly parallel temperature profiles in the evaporator and in the condenser. The temperature profiles of the streams are nearly ideal matched, except in the superheated region. The amount of heat transferred in the

superheated region is less than 5% of the total energy and the mismatch of the GTDs in that region is negligible.

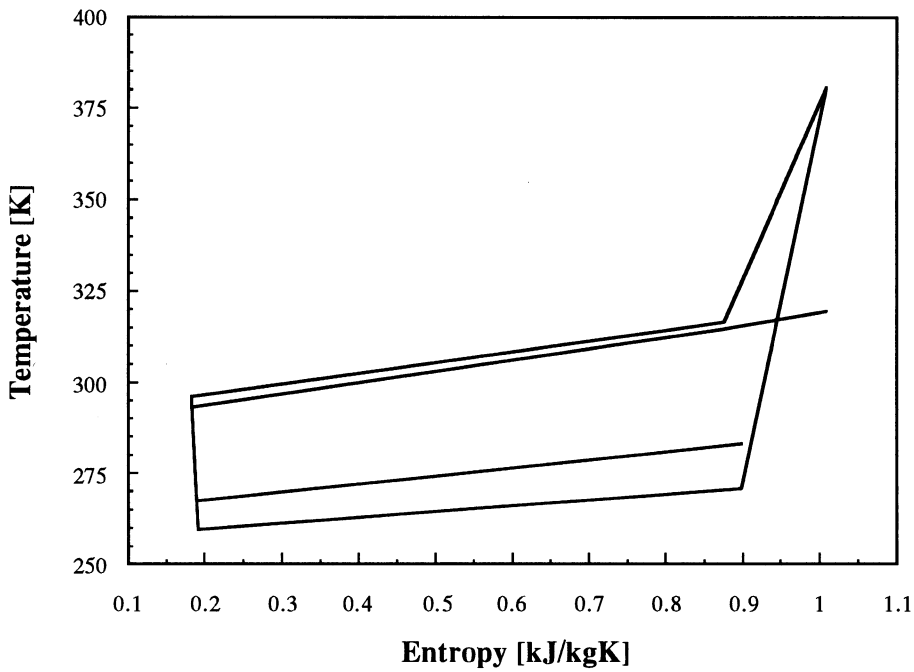

Figure 4.6 Temperature-Entropy diagram for the system with a polytropic compressor efficiency of $\eta = 0.5$

4.3.5 HEAT EXCHANGER CONDUCTANCE ALLOCATION

The GTD of the external streams may be altered until $\psi \rightarrow$ min. Such a system transfers the heat in the evaporator and condenser at the best possible temperature matching. The outlet temperatures of the external streams are changed until ψ reaches a minimum. The change of the GTD causes a change of the heat capacitance rates of the external streams, because $\dot{C}_{ext} = \dot{Q}/\text{GTD}$ and $\dot{Q}$ remains nearly constant. The refrigeration systems differ

now not only in different compressor polytropic efficiencies η, but also in different external heat capacitance rates (Table 4.2). The GTDs of both external streams were reduced, which results in larger heat capacitance rates of the external streams and hence in a higher COP. This alteration increased the COP compared to the COP obtained with the optimum mole fraction (section 4.2.2). The improvement is for $\eta = 0.5$, $\eta = 0.7$ and $\eta = 1.0$ in average about 9%, 2.5% and 5%, respectively.

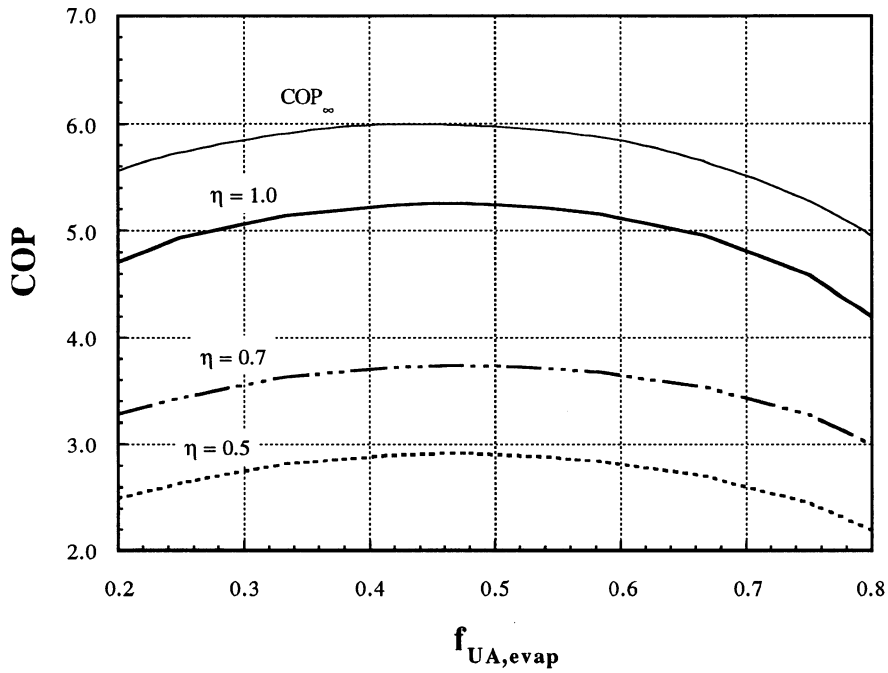

Figure 4.7 **COP vs. heat exchanger conductance fraction $f_{UA,evap}$ for a refrigerant mixture of R22/ R141b and different polytropic compressor efficiencies**

The distribution of the total heat exchanger conductances on the evaporator and condenser is now optimized. The heat exchanger conductance of the evaporator and condenser have been initially fixed at $UA_{evap} = 0.25$ kW/K and $UA_{cond} = 0.35$ kW/K. The total heat

exchanger conductance $UA_{total} = 0.60$ kW/K remains constant, but the allocation is varied. Figure 4.7 indicates, that the total heat exchanger size should be allocated nearly evenly for the two heat exchangers, independent on the compressor polytropic efficiency η. The optimum distribution for the three different systems occurs if 48% of the total heat exchanger conductance UA_{total} are allocated to the evaporator. The optimum distribution is always about $UA_{cond} = 0.315$ kW/K and $UA_{evap} = 0.285$ kW/K. A moderate deviation of the optimum distribution does not decrease the COP significantly. This indicates, that the UA_{total} should be allocated even for that system.

4.3.6 COMPARISON OF ANALYTICAL MODEL AND RESULTS FROM CYCLE11

The COP_∞ for the system with $\eta = 1.0$ obtained with the analytical ideal model from Chapter 3 is also shown in Figure 4.7. In the plot the upper line represents the upper limit of the COP. This COP is determined with considerations of heat transfer mechanism. The COP of the refrigeration system with the isentropic compressor is very close to that limit and reaches nearly the optimum COP_∞. The difference between the COPs of the systems with the non-isentropic compressor and the optimum COP_∞ is of course larger.

The external heat capacitance rates have been changed to obtain the best temperature matching (section 4.3.5). For this reason, the optimum COP_∞ for the systems with the different polytropic compressor efficiency η varies. Table 4.2 shows the different operating conditions and the corresponding COPs.

polytropic compressor efficiency η	low ext.heat capacit. rate $\dot{C}_{L,ext}\left[\frac{kW}{K}\right]$	high ext. heat capacit. rate $\dot{C}_{H,ext}\left[\frac{kW}{K}\right]$	COP (Cycle11)	COP_∞ (AM)	$\frac{COP}{COP_\infty}$
1.0	$123.8\ 10^{-3}$	$87.6\ 10^{-3}$	5.25	6.00	0.88
0.7	$135.9\ 10^{-3}$	$94.6\ 10^{-3}$	3.73	7.02	0.53
0.5	$161.4\ 10^{-3}$	$125.3\ 10^{-3}$	2.91	7.76	0.38

Table 4.2 COPs calculated from Cycle11 and AM

The external heat capacitance rates are calculated as the heat transferred in each heat exchanger over the corresponding gliding temperature difference.

$$\dot{C}_{L,ext} = \frac{\dot{Q}_{evap}}{GTD_{L,ext}} \tag{4.12}$$

$$\dot{C}_{H,ext} = \frac{\dot{Q}_{cond}}{GTD_{H,ext}} \tag{4.13}$$

The COP of the cycle with $\eta = 1.0$ falls only 12% short of the optimum $COP_\infty = 6.0$ determined from the analytical model. Vapor-slip and reduced heat transfer coefficients in the heat exchanger leads to smaller COPs than predicted. For the system with lower polytropic compressor efficencies is the difference to the optimum COP larger. A parallel temperature profile as obtained for $\psi \rightarrow 0$ corresponds to identical heat capacitance rates of the external stream and the refrigerarant. An energy balance for the refrigerant in the condenser leads to

$$\dot{Q}_{cond,refr} = \dot{C}_{cond,refr}\ GTD_{cond,refr} \tag{4.14}$$

and for the external stream flowing through the condenser

$$\dot{Q}_{H,ext} = \dot{C}_{H,ext}\, GTD_{ext} \tag{4.15}$$

The heat exchanger as a closed system yields $\dot{Q}_{cond,refr} = \dot{Q}_{H,ext}$ and for equal GTDs ($GTD_{H,ext} = GTD_{cond,refr}$) must be $\dot{C}_{H,ext} = \dot{C}_{cond,refr}$.

The same result is for the evaporator attained, so that the heat capacitance rates of the external stream and the refrigerant are also equal, $\dot{C}_{L,ext} = \dot{C}_{evap,refr}$.

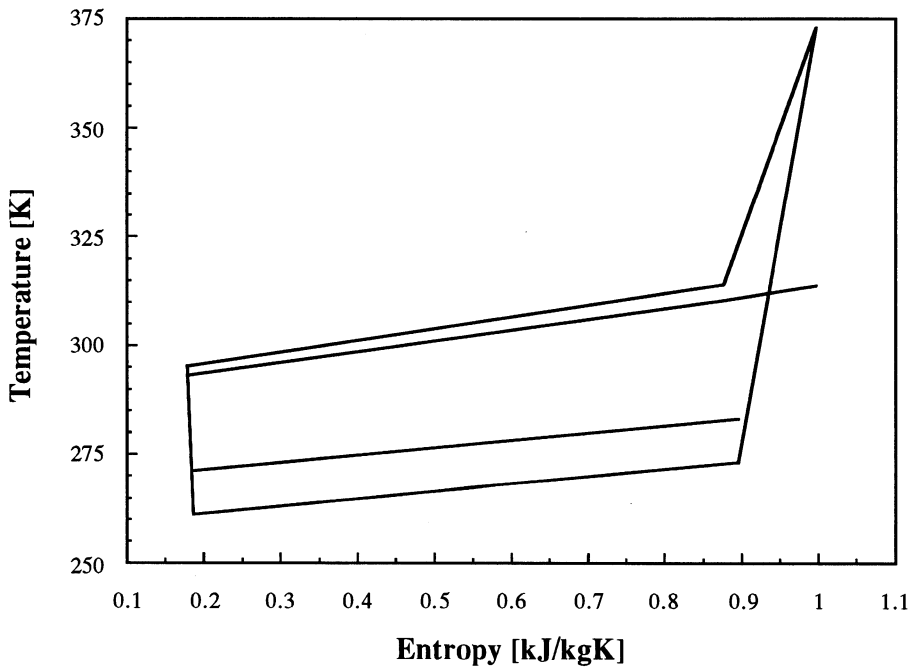

Figure 4.8 Temperature-Entropy diagram for the system with a polytropic compressor efficiency of $\eta = 0.5$ and optimized UA allocation

A accompanying T-S diagram for optimized $f_{R22} = 0.08$, $f_{UA_{evap}} = 0.48$ and $\eta = 0.5$ is presented in Figure 4.8. The change of the initial UA allocation (for which the GTDs

have been matched) to the optimum UA allocation alters the temperature profile a little. Nevertheless are the temperature profiles nearly parallel lines.

4.3 CHAPTER SUMMARY

In this chapter was a binary NARM in a standard vapor compression refrigeration cycle investigated and compared to the COP_∞ determined from the Analytical Model developed in Chapter 3.

- The COP reaches a maximum for a refrigerant compositions which lead to the smallest deviation of parallel temperature profiles of the external stream and the refrigerant in each heat exchanger.

  $$COP \rightarrow COP_{max} \quad \text{for } \psi \rightarrow 0$$

- A parallel temperature profile corresponds to identical heat capacitance rates of the external stream and the refrigerant. The heat capacitance rate of the external stream should match the heat capacitance in the heat exchanger.

  $$\dot{C}_{ext} = \dot{C}_{hx,refr}$$

- Matching the gliding temperature difference in the evaporator and condenser to the corresponding gliding temperature difference of the external stream is not sufficient to obtain an increase of the COP.

- The COPs obtained with a refrigeration system employing the pure refrigerants of the mixture should be reasonable large, otherwise the benefit of the temperature matching is undermined by the low COP of one of the components.

- The mixture should consist of a less and a more volatile component, depending on the desired gliding temperature difference.

- The COP experiences an optimum for equal allocation of the total heat exchanger conductance if the gliding temperature differences are matched to each other.

- The analytical COP defined by Equation (3.26) represents an upper limit for the Carnot COP considering heat transfer mechanism and may be used as a design goal.

CHAPTER
FIVE

CONCLUSIONS AND RECOMMENDATIONS

5.1 CONCLUSIONS

The Carnot cycle places an upper limit on the COP of a refrigeration cycle. This Carnot COP assumes a thermodynamic cycle with no internal irreversibilities. It does not consider heat transfer mechanism, which are necessarily a irreversible process. The Carnot COP may only be obtained for a refrigeration cycle with zero cooling capacity. Furthermore the Carnot analysis assumes that the heat transfer from and to the cycle occurs at a constant temperature. All this reduces its usefulness as a realistic design goal for a refrigeration system.

The maximum possible COP for a standard vapor compression cycle, which takes specified external boundary conditions into account and does not require an isothermal heat transfer for the refrigerant and the heat transferring external fluid, is given by Equations (3.28) and (3.29). The COP is determined by the cooling load, the heat

exchanger conductances of the low- and high temperature heat exchangers, the inlet temperatures of the external heat transferring fluids in each heat exchanger and their heat capacitance rates. A numerical and an analytical simulation model for the refrigeration cycle has been developed. The investigation of the cycle leads to several design guidelines for the cycle obtaining the maximum COP. The most important are:

- The slope of the temperature change (or gliding temperature difference (GTD)) of the refrigerant in the heat exchangers should be parallel to that of the external stream flowing through that heat exchanger. This result corresponds to equal heat capacitance rates of the refrigerant and the external stream flowing through the heat exchanger.
- The total heat exchanger conductance should be evenly allocated between the two heat exchangers independent on the cooling load, the inlet temperatures and heat capacitance rates of the external streams.
- The total external heat capacitance rate should be evenly allocated between the two external heat capacitance rates independent on the inlet temperature of the external stream, the cooling load and the heat exchanger conductances.

The potential performance improvement of the COP, Ω, is defined as the COP of a system employing a refrigerant undergoing non-isothermal heat transfer to a system employing a refrigerant undergoing isothermal heat transfer. Ω is strongly dependent on the gliding temperature difference GTD (temperature difference between the in- and outlet temperature of the refrigerant or external stream in the heat exchanger) of the refrigerant and the external streams. Assuming, that the GTD of the refrigerant matches the GTD of the external system:

- The larger the GTD of the refrigerant, the larger the potential COP improvements of the refrigeration system.
- A change of the refrigerant GTD as the GTD of the external streams remains constant results in a smaller COP.

A simulation of a standard vapor compression cycle with internal irreversibilities and real non-azeotropic refrigerant mixtures (NARMs) developed by Domanski showed that the COP of a specified system experiences a maximum for the best possible GTD matching (GTD of the refrigerant in the heat exchanger nearly identical to the GTD of the external stream flowing through that heat exchanger). In addition it was found, that the total heat exchanger conductance for the two heat exchanger should be evenly allocated, as shown for the ideal model.

The COP determined by Equation (3.26) and (3.27) offers a realistic upper limit of the COP of a vapor compression refrigeration cycle employing a NARM. Contrary to Equations (3.28) and (3.29) is it possible to specify the heat capacitance rates of the refrigerant. This becomes important for refrigeration systems where the GTDs of the refrigerant and external stream in each heat exchanger are not matched and Equations (3.28) and (3.29) do not apply.

NARMs offer the potential for significant improvements of the COP in refrigeration systems. These potential gains are strongly dependent on the fluid properties. A mixing of two refrigerants often yields lower COPs than the COPs which would be obtained if the pure refrigerants were used in the same system. The choice of the components is difficult because several properties like ozone depletion potential, toxicity and commercial

availability exclude many refrigerants. The refrigerant mixture should consist out of refrigerants with different boiling point temperatures depending on the desired gliding temperature difference of the refrigerant.

5.1 RECOMMENDATIONS FOR FUTURE WORK

In this work simulation models are used to investigate the performance of a refrigeration cycle and to establish design guidelines. A verification of the design guidelines using measurements of a real refrigeration cycle employing NARMs should be performed. Data for the temperature profile of all fluids in the heat exchangers, the corresponding heat capacitance rates, cooling load and COP are most important. The potential performance improvements are significant, but experimental results have shown, that they might be quite smaller than expected.

A refrigeration system using dedicated mechanical subcooling is of interest. In such a refrigeration system, a second smaller vapor compression is applied, which task it is to subcool the refrigerant flowing out of the main cycle's condenser. Studies have shown [22], that large energy savings are possible for systems employing pure refrigerants. A investigation with a NARM instead of a pure refrigerant might lead to even larger energy savings. Potential performance improvements should be evaluated and design guidelines should be established.

APPENDIX

{**********

Matthias Rauck November 1992

Calculation for the Coefficient of Performance (COP) for an ideal Refrigeration cycle

Modeled with :

I) single Carnot cycle

II) Numerical Solution Model - Finite Difference Method (FDM) with n Carnot Cycle

III) Analytical Solution Model (AM)

****

****

INPUT DATA:

****

Specification of the operating conditions of the refrigeration cycle:

**********}

{Number of individual Carnot Cycles in sequence, use replace command to change n change 10{n} to #{n} }

n=10{n}

{cooling load QL_total}

QL_total=10 {kW}

{Low and high temperature heat exchanger conductance}

UAL=5 {kW/K}

UAH=5

{Low and high external heat capacitance rates}

CextL=2 {kW/K}

CextH=3

```
{Inlet temperature low (cold) external fluid in low temperature heat exchanger}
DUPLICATE a=n,n
TLext[10{n}]=273      {K}
END

{inlet tenperature high (warm) external stream in high temperature heat exchanger}
THext[0]=313  {K}
```

{ I & III) Refrigeration cycle modeled with one and n Carnot Cycle

```
**********************************************************************
NOTE:  Infinite heat capacitance rates of the working fluid for Carnot analysis}

{Define low and high inlet temperatures for single Carnot cycle}
DUPLICATE a=n,n
TLextin=TLext[10{n}]
END
THextin=THext[0]
```

{III) Analytical Solution Model (AM)

```
**********************************************************************
NOTE:  Specify heat capacitance rates of the refrigerant and external stream}


{Define low and high inlet temperatures of the external stream for AM}
THextanalyin=THext[0]
TLextanalyin=TLext[10{n}]


{NOTE: Put non corresponding paragraph in brackets (A or B), depending on
which definition of the heat capacitance rates is required
{

A) for optimum cycle (COP @ maximum): equal heat capacitance rates of
                    external stream and refrigerant (wf, working fluid)}
CwfL=CextL
CwfH=CextH

{corresponding heat exchanger effectiveness factors for the
low and high temperature heat exchangers @ CwfL=CextL & CwfH=CextH !!}
  EpsanalyH=NTUanalyH/(NTUanalyH+1)
  EpsanalyL=NTUanalyL/(NTUanalyL+1)
}
```

{**B**) for arbitrary cycle (COP not @ maximum): unequal heat capacitance rates of external stream and refrigerant (wf, working fluid)}

{specify heat capacitance rates of the refrigerant}
CwfL=1.5 {kW/K}
CwfH=2.5

{corresponding heat exchanger effectiveness factors for the low and high temperature heat exchangers @ CwfL unequal CextL & CwfH unequal CextH !!}

EpsanalyH=(1-exp(-NTUanalyH*(1-A)))/(1-A*exp(-NTUanalyH*(1-A)))
A=min(CextH/CwfH, CwfH/CextH)
EpsanalyL=(1-exp(-NTUanalyL*(1-B)))/(1-B*exp(-NTUanalyL*(1-B)))
B=min(CextL/CwfL, CwfL/CextL)

{**********
CALCULATIONS:
****

Refrigeration cycle modeled with one Carnot Cycle as reference:
**********}

{Determination of Number of Transfer Units NTU for the low and high hx}
NTUCa1H=UAH/CextH
NTUCa1L=UAL/CextL

{heat exchanger effectiveness factors for the low and high temperature hx}
EpsCa1H=1-exp(-NTUCa1H)
EpsCa1L=1-exp(-NTUCa1L)

{Energy balances and rate equations: (wf=refrigerant (working_fluid)=Carnot cycle)}
QHCa1=CextH*(THextout-THextin)
QL_total=CextL*(TLextin-TLextout)
QHCa1=EpsCa1H*CextH*(TwfHCa1-THextin)
QL_total=EpsCa1L*CextL*(TLextin-TwfLCa1)

{Entropy transfer rate balance}
QL_total/TwfLCa1=QHCa1/TwfHCa1

{compressor work}
WorkCa1=QHCa1-QL_total

{COP definition: (reversibel) }
COPCa1=QL_total/WorkCa1

{Refrigeration cycle modeled with 10{n} Carnot Cycle:
**********}
{Creating the required equation set for n=10{n} Carnot cycles:}

DUPLICATE i=1,10{n}

{single cooling load per cycle:}
QL[i]=QL_total/10{n}

{heat exchanger effectiveness factors for the low and high temperature hx
for each individual Carnot cycle}
EpsCanH[i]=1-exp(-NTUCa1H/10{n})
EpsCanL[i]=1-exp(-NTUCa1L/10{n})

{Energy balances and rate equations: wf=refrigerant (working_fluid)=Carnot cycle)}
QH[i]=CextH*(THext[i]-THext[i-1])
QL[i]=CextL*(TLext[i]-TLext[i-1])
QH[i]=EpsCanH[i]*CextH*(Tcon[i]-THext[i-1])
QL[i]=EpsCanL[i]*CextL*(TLext[i]-Tevap[i])

{Entropy transfer rate balance}
QL[i]/Tevap[i]=QH[i]/Tcon[i]

{Entropy transferred with heat transfer in high hx}
{ a) for refrigerant}
Scon[i]=QH[i]/Tcon[i]

{ b) for high external stream}
SH[i]=QH[i]/((THext[i-1]-THext[i])/(ln(THext[i-1]/THext[i])))

{Entropy transferred with heat transfer in low hx}
{ a) for refrigerant}
Sevap[i]=QL[i]/Tevap[i]

{ b) for low external stream}
SL[i]=QL[i]/((TLext[i-1]-TLext[i])/(ln(TLext[i-1]/TLext[i])))

{Determination of the logarithm mean temperature differences:}
{logarithm mean temperature difference in low hx}
dtL[i]=((TLext[i-1]-Tevap[i])-(TLext[i]-Tevap[i]))/look1[i]
  look1[i]=ln((TLext[i-1]-Tevap[i])/(TLext[i]-Tevap[i]))

{temperature difference between external streams}
dtext_fl[i]=THext[i]-TLext[i]

```
{logarithm mean temperature difference in high hx}
dtH[i]=-((THext[i-1]-Tcon[i])-(THext[i]-Tcon[i]))/look2[i]
   look2[i]=ln((THext[i-1]-Tcon[i])/(THext[i]-Tcon[i]))

END

{compressor work}
W=sum(QH[i],i=1,10{n})-QL_total


{total rejected heat}
QHCan=sum(QH[i],i=1,10{n})

{total entropy generated by heat transfer}
{in high temperature hx}
EntropyH=sum(SH[i]-Scon[i],i=1,10{n})

{in low temperature hx}
EntropyL=sum(Sevap[i]-SL[i],i=1,10{n})

{COP for n Carnot cycles}
COPCan=QL_total/(W)

{potential COP improvement}
COPimprCanvsCa1=COPCan/COPCa1    {performance increase vs one cycle}

{Average temperature differences for one complete circulation (n cycles)
between the refigerant and external stream in the each hx}
dtevap_Lext_av=sum(dtL[i],i=1,10{n})/10{n}
dtHext_con_av=sum(dtH[i],i=1,10{n})/10{n}
dtHext_Lext=sum(dtext_fl[i],i=1,10{n})/10{n}

{Standard deviation for the temperature difference between
the external stream and working fluid}
stdv_evap_Lext=(sum((dtevap_Lext_av)^2,i=1,10{n}))^0.5/(10{n}-1)
stdv_Hext_con=(sum((dtHext_con_av)^2,i=1,10{n}))^0.5/(10{n}-1)
```

{Analytical Model (AM):
**********}

{NOTE: We have different heat exchanger effectiveness factors depending on the
ratio of the heat capacitance rates of the external fluid and refrigerant.

Possible: a) CwfH=CwfL and CextL=CextH than Eps=NTU/(1+NTU)

b) CwfH=CextH=CwfL=CextL than Eps=NTU/(1+NTU)

c) CwfH=CwfL unequal to CextL=CextH than Eps=Epsanaly (earlier defined}

{Determination of Number of Transfer Units NTU for the low and high hx}
NTUanalyH=UAH/CminH
CminH=min(CextH, CwfH)
NTUanalyL=UAL/CminL
CminL=min(CextL, CwfL)

{Energy balances and rate equations:}
QHanaly=CextH*(THextanalyout-THextanalyin)
QHanaly=CwfH*(Twf_analyH_in-Twf_analyH_out)
QHanaly=EpsanalyH*CminH*(Twf_analyH_in-THextanalyin)
QL_total=CextL*(TLextanalyin-TLextanalyout)
QL_total=CwfL*(Twf_analyL_out-Twf_analyL_in)
QL_total=EpsanalyL*CminL*(TLextanalyin-Twf_analyL_in)

{Entropy transfer rate balance}
QHanaly/TmeanwfH=QL_total/TmeanwfL
TmeanwfH=(Twf_analyH_in-Twf_analyH_out)/ln(Twf_analyH_in/Twf_analyH_out)
TmeanwfL=(Twf_analyL_out-Twf_analyL_in)/ln(Twf_analyL_out/Twf_analyL_in)

{COP definition:}
COPanaly=QL_total/(QHanaly-QL_total)

{potential COP improvement}
COP_impr_analy_vs_Can=COPanaly/COPCan

{Additional}

{equations (3.26) and (3.27)
{Unequal heat capacitance rates of external stream and refrigerant}
Cop_general=QL_total*alpha/(THextanalyin*(betha-1)*gamma-QL_total*alpha)

{where}
alpha=CwfH+betha*(EpsanalyH*CminH-CwfH)
betha=((QL_total*EpsanalyL*CminL)/(CwfL*(TLextanalyin*EpsanalyL*CminL-QL_total))+1)^delta
gamma=EpsanalyH*CminH*CwfH
delta=CwfL/CwfH

```
{equations (3.28) and (3.29)}
{{Equal heat apacitance rates of external stream and refrigerant}
{CwfH=CwfL; Cwfl=cwf}
COPpart_op_=(TLextanalyin-omega)/(THextanalyin-(TLextanalyin-omega))
  omega=QL_total*(1/(EpsanalyH*CminH)+1/(EpsanalyL*CminL)-1/(Cwfpart_op_))
Cwfpart_op_=CwfH}

{Deviation of Numerical and Analytical Model}
Accuracy=COPCan/COPanaly
}
```

REFERENCES

1. Holusha, J., *The Refrigerator of the Future, for Better and Worse* , New York Times, August 30, 1992

2. Moran, M. and Shapiro, H. N., *Fundamentals of Engineering Thermodynamics*, John Wiley & Sons, New York (1988)

3. Baehr, H. D., *Thermodynamik*, 7th Edn., Springer-Verlag Berlin/ Heidelberg (1989)

4. Incropera, F. P. and DeWitt D. P., *Fundamentals of Heat and Mass Transfer,* 3rd Edn., John Wiley & Sons, New York (1990)

5. Kays, W. M. and London, A. L., *Compact Heat Exchanger*, 2nd Edn, McGraw-Hill, New York (1964)

6. Klein, S.A. and Alvardo, F.L., *EES: Engineering Equation Solver F-Chart Software*, 4406 Fox Bluff Road Middleton, WI 53562 (1990)

7. Klein, S. A., *Design Considerations for Refrigeration Cycles,* accepted for the publication in the International Journal of Refrigeration, (November 1991)

8. Atwood, T., *NARBs (Non-azeotropic Refrigerant Blends) The Promise and the Problems,* ASHRAE Paper No. 86-WA/HT-61, presented at the 1986 Winter Annual Meeting, Dec 7-12, 1986

9. Vineyard, E.A., Sand, J.R. ,Statt, T.G., *Selection of Ozone-Safe, Nonazeotropic Refrigerant Mixtures for Capacity Modulation in Residential Heat Pumps,* ASHRAE Transactions 1989, Vol. 95, Pt. 1, No. 3199

10. Spauschus, H.A., *Refrigerant mixtures challenges and opportunities*, ASHRAE Journal, pp. 28-41, November 1989

11. Atwood, T., *(The ABCs of NARBs (Nonazeotropic Refrigerant Blends)*, ASHRAE Transactions, Vol. 91, Pt. 2, Paper HI-85-18 No. 1, 1985

12. Kruse, H., Hesse, U., *Possible substitutes for fully halogenated chlorofluorcarbons using fluids already marketed*, International Journal of Refrigeration, Vol. 11, pp. 276-283, July 1988

13. Kruse, H., Schroeder, M., Kuever, M., Upmeier, B., Quast, U., *Theoretical and Experimental Investigations of Advantageous Refrigerant Mixture Applications,* ASHRAE Transactions , Vol. 91, Pt. 2, Paper No. HI-85-27 No.4, 1985

14. Domanski, P.A. , McLinden, M.O., *A Simplified Cycle Simulation Model for the Performance Rating of Refrigerants and Refrigerant Mixtures*, International Journal of Refrigeration, Vol. 15, No. 2, pp. 81-88, 1991

15. McLinden, M.O. and Rademacher, R., *Methods for Comparing the Performance of Pure and Mixed Refrigerants in the Vapor Compression Cycle*, International Journal of Refrigeration, Vol. 10, pp. 318-326, November 1987

16 Morrison, G., McLinden M., *Two Refrigerant Mixtures and the Hard Sphere Fluid,* ASHRAE Transactions, Vol. 91, Pt. 2, Paper HI-85-18 No. 3, 1985

17. Morrison, G., McLinden M., *Azeotropy in Refrigerant Mixtures,* NBS Technical Note, National Bureau of Standards and Technology, Gaithersburg, Md 20899, USA

18. Morrison, G. , Gallagher, J.S., *REPROP: A Thermodynamic Properties Software Program for Refrigerants and their Mixtures,* Thermophysic Division at the National Institute of Standards and Technology, Gaithersburg, Md. 20899, USA

19. Jung, D.S., Rademacher, R., *Performance simulation of single-evaporator domestic refrigerators charged with pure and mixed refrigerants,* International Journal of Refrigeration, Vol.14, pp. 223-232, July 1991

20. Herold, H. E., *Performance Limits for Thermodynamic Cycles*, ASME Winter Annual Meeting, San Francisco, December 1989

21. Ibrahim, O.M., Klein, S. A., and Mitchell, J.M., *Optimum Heat Power Cycles for Specified Boundary Conditions*, ASME Journal for Gas Turbines and Power, Vol 113, No. 4, pp. 514-521, 1991

22. Thornton, J.W., *Supermarket Refrigeration Options*, MS Thesis, Solar Energy Laboratory, Dept. of Mechanical Engineering, University of Wisconsin - Madison, 1991

23. Montreal Protocol on Substances that Deplete the Ozone Layer, Final Act, United Nations Environment Program, Nairobi (1987)

24. Morrison, G., McLinden M.O., *Application of a Hard Sphere Equation of State to Refrigerants and Refrigerant Mixtures*, NBS Technical Note 1226, National Bureau of Standards, Gaithersburg, Md 20899, USA